Dark Matter Search with a Mono-Z' Pencil Jet with the Compact Muon Solenoid Detector at the Large Hadron Collider

Usama Hussain

University of Wisconsin Madison

Preliminary Examination

Overview

- Theoretical and Experimental Motivation
- Large Hadron Collider
- Compact Muon Solenoid
- Event Reconstruction
- Background Sources
- Analysis Strategy and Cut Flow
- Results
- Conclusion and Future Plans

The Standard Model

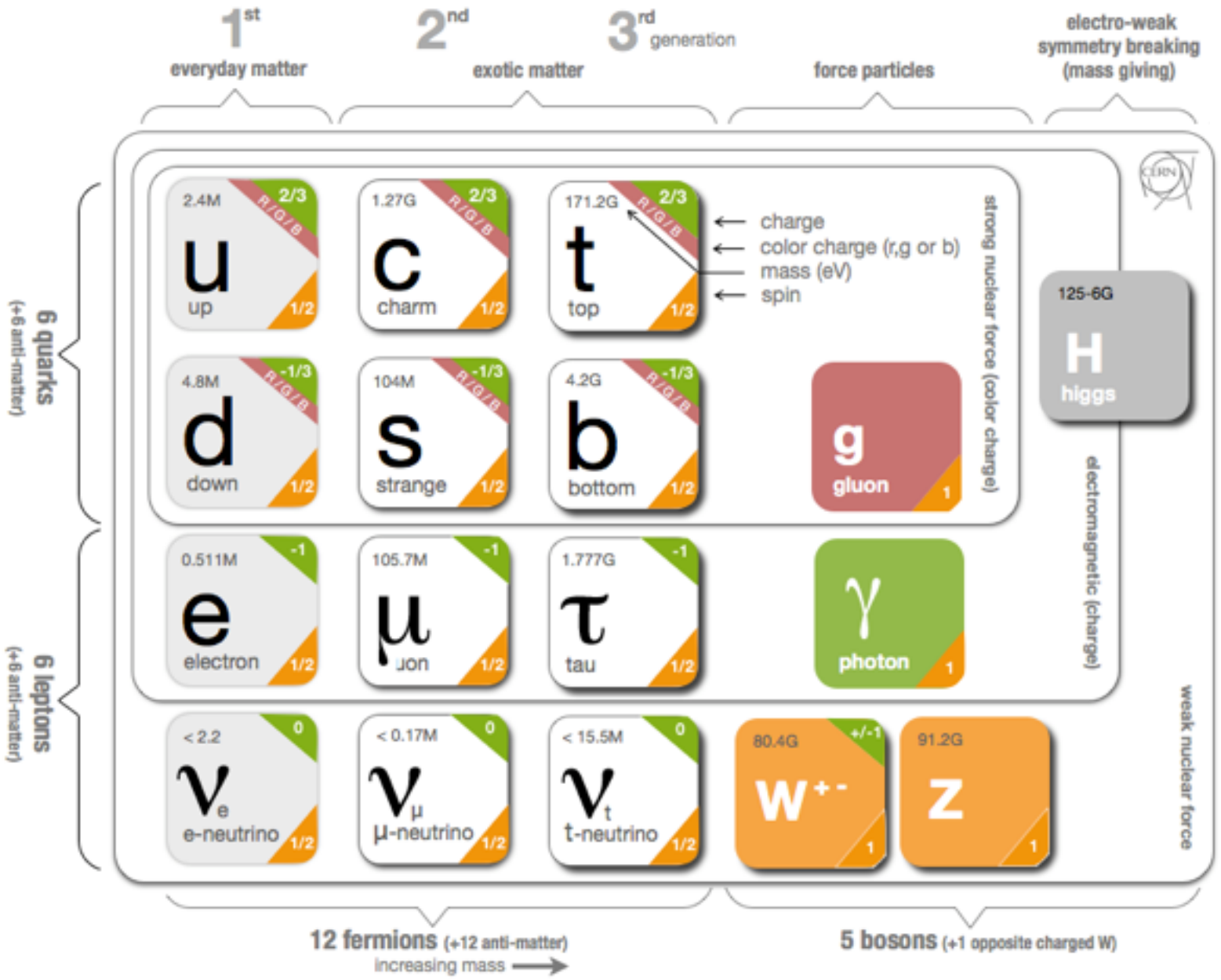

Standard Model Interactions

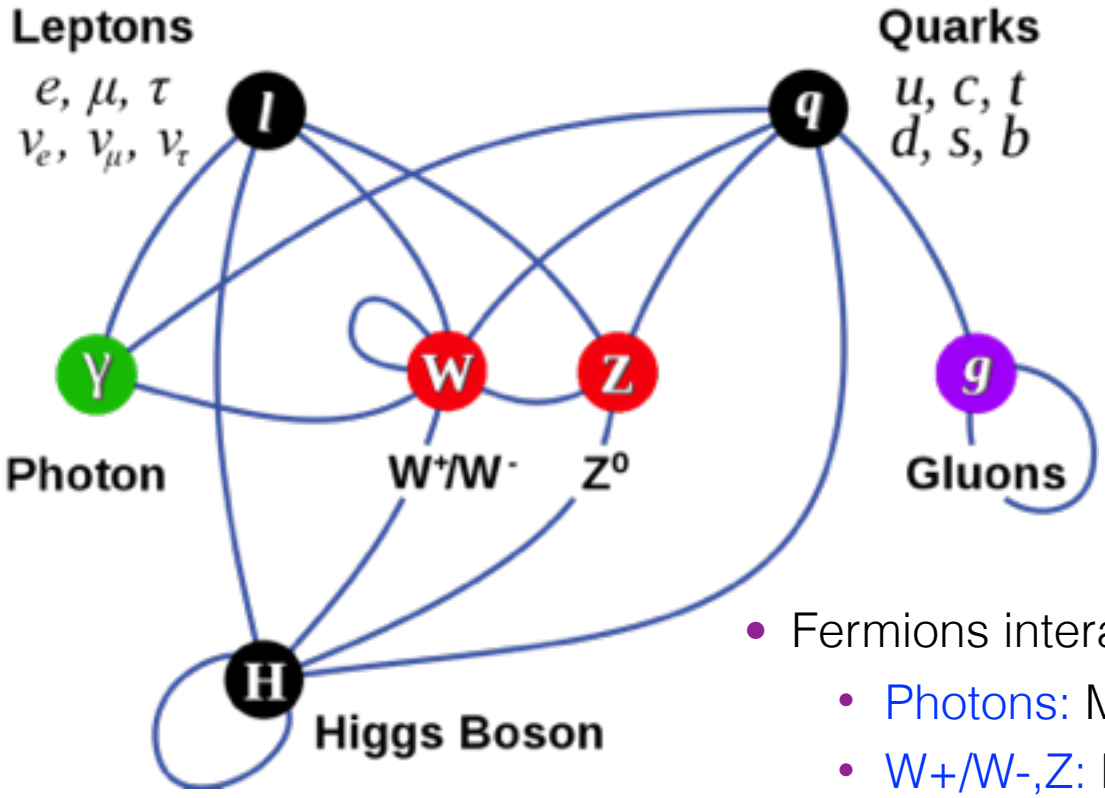

- Fermions interact through gauge bosons
  - Photons: Mediate Electromagnetic Force
  - W+/W-,Z: Mediate the Weak Force
  - Gluons: Mediate the Strong Force
- Higgs field provides mass for:
  - Weak bosons
  - Massive fermions

Motivation for Dark Matter

Composition of Matter:

- Majority of matter content in the universe is of unknown nature.
- We know it is out there but we do not know what it is.

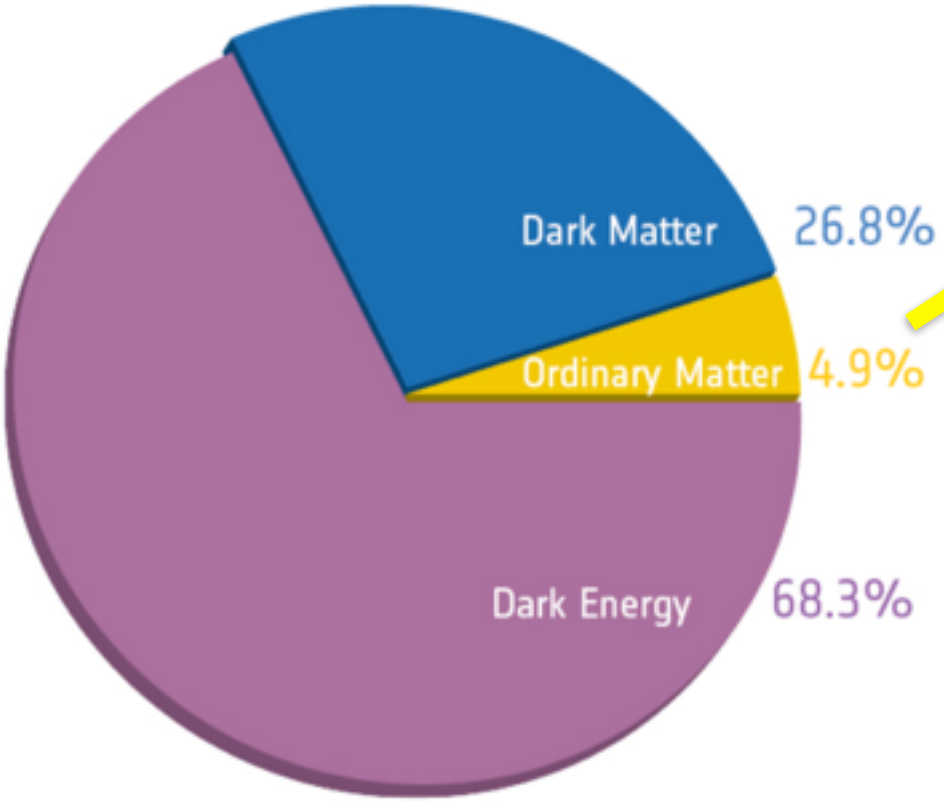

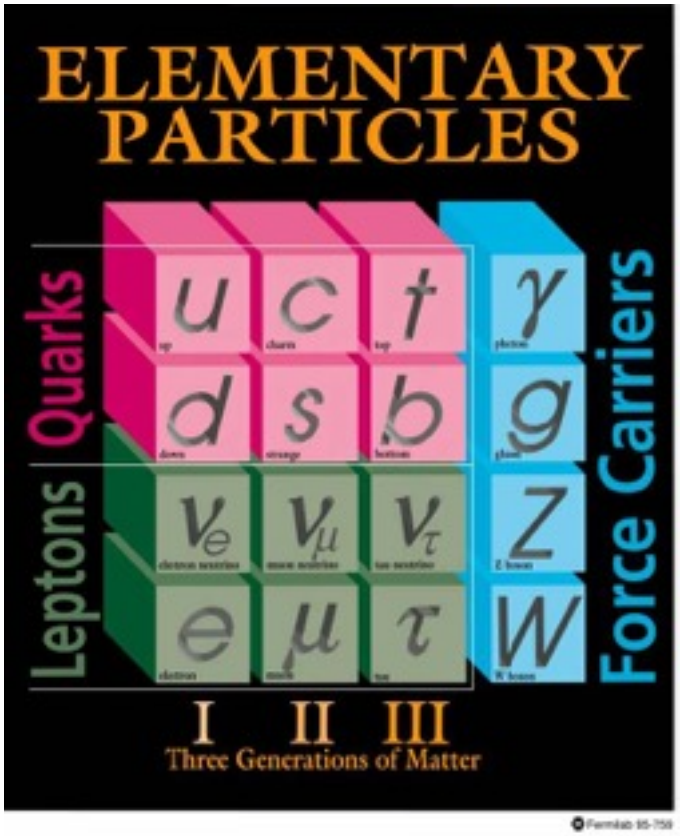

Evidence for Dark Matter

- **Galactic rotation curves** characteristically exhibit flat behavior at large distances i.e. far beyond the edge of visible disks
  - Behavior proves the existence of a dark matter "halo"

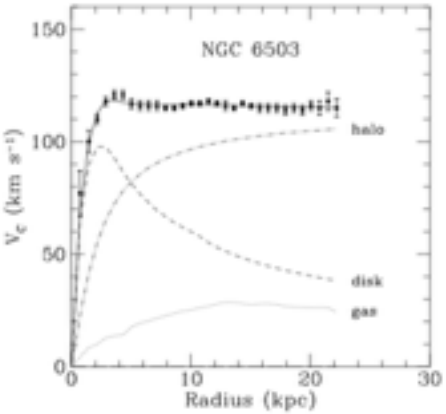

Evidence for Dark Matter

- **Galactic rotation curves** characteristically exhibit flat behavior at large distances i.e. far beyond the edge of visible disks
  - Behavior proves the existence of a dark matter "halo"
- **Cluster Collisons (missing mass / collisionless matter)**
  - Separation of dark and normal matter seen in the data
  - Gravitational potential (via **lensing**) consistent with DM distribution (blue) centered in galaxies
  - X-ray emitting (red) is visible matter

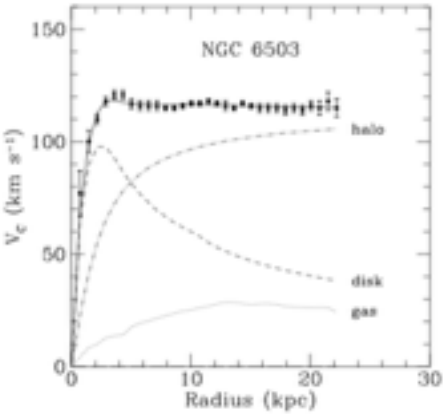

Evidence for Dark Matter

- **Galactic rotation curves** characteristically exhibit flat behavior at large distances i.e. far beyond the edge of visible disks
  - Behavior proves the existence of a dark matter "halo"
- **Cluster Collisons (missing mass / collisionless matter)**
  - Separation of dark and normal matter seen in the data
  - Gravitational potential (via **lensing**) consistent with DM distribution (blue) centered in galaxies
  - X-ray emitting (red) is visible matter
- **Cosmic microwave background**
  - Planck 2015 cosmic microwave background (CMB) temperature anisotropy power spectrum encodes information about cosmological parameters
  - First acoustic peak: Universe is spatially flat overall
  - Second peak: $\Omega_b \sim 0.05$.
  - Third peak: Overall nonrelativistic matter density $\Omega_M \sim 0.3$
    Therefore, $\Omega_{DM} = \Omega_M - \Omega_b = 0.25$

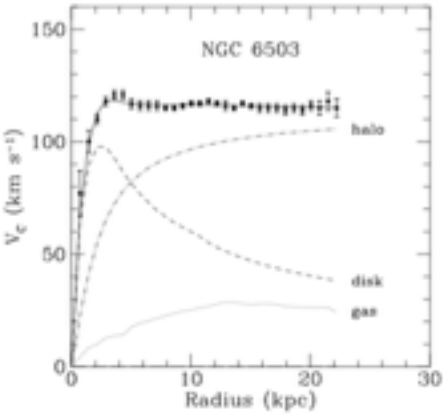

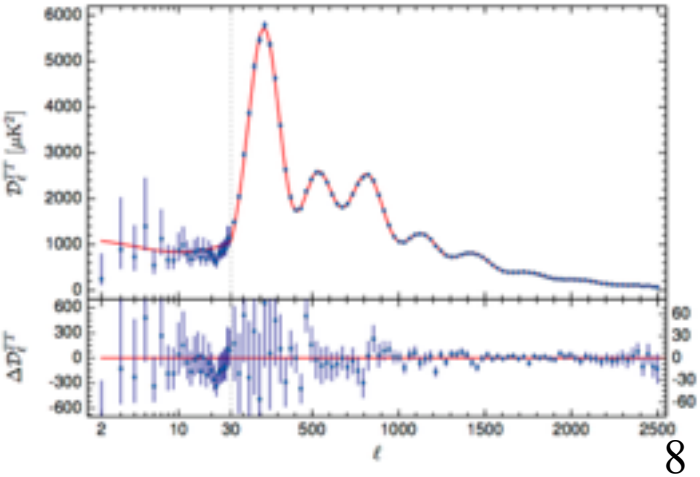

Dark Matter Detection techniques

- **Indirect detection (ID)** involves looking for Standard Model particles produced by astrophysical sources of Dark Matter.

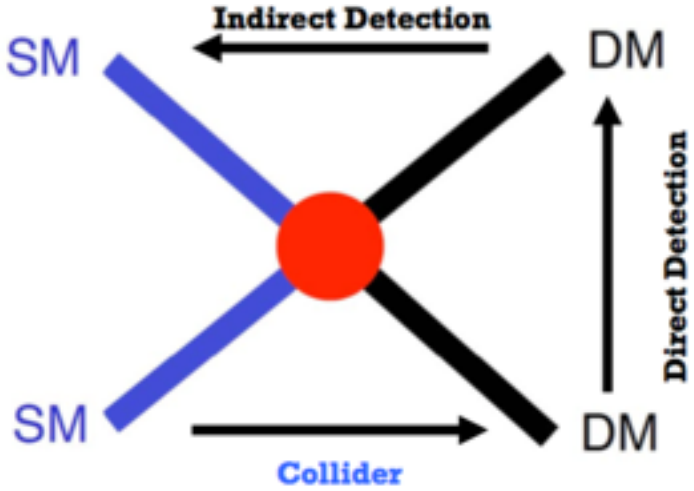

Dark Matter Detection techniques

- **Indirect detection (ID)** involves looking for Standard Model particles produced by astrophysical sources of Dark Matter.

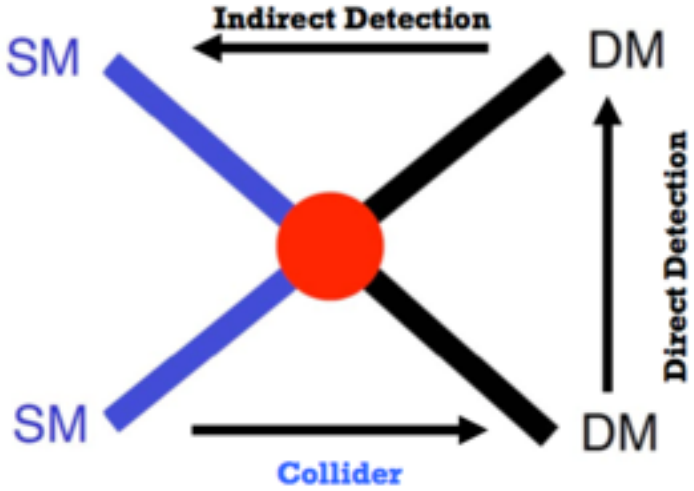

- **Direct Detection (DD)** involves detecting recoil due to scattering of DM particles off target nuclei

Dark Matter Detection techniques

- **Indirect detection (ID)** involves looking for Standard Model particles produced by astrophysical sources of Dark Matter.

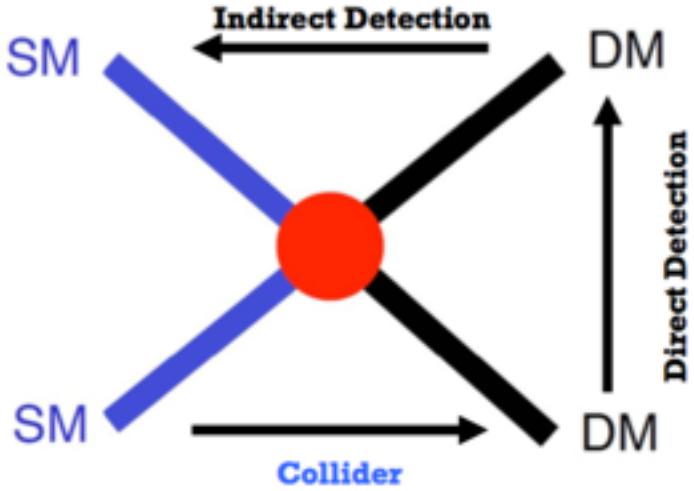

- **Direct Detection (DD)** involves detecting recoil due to scattering of DM particles off target nuclei

- **Collider Searches** are an effort to produce DM via collisions of SM particles
  - Dark Matter interaction with SM particles has low cross-section so difficult to observe

Dark Matter EFT

- **Effective Field Theory (EFT)** with a contact interaction between DM and SM particles.
- EFT depends on two parameters:
  - DM mass: m_χ
  - Interaction scale: Λ

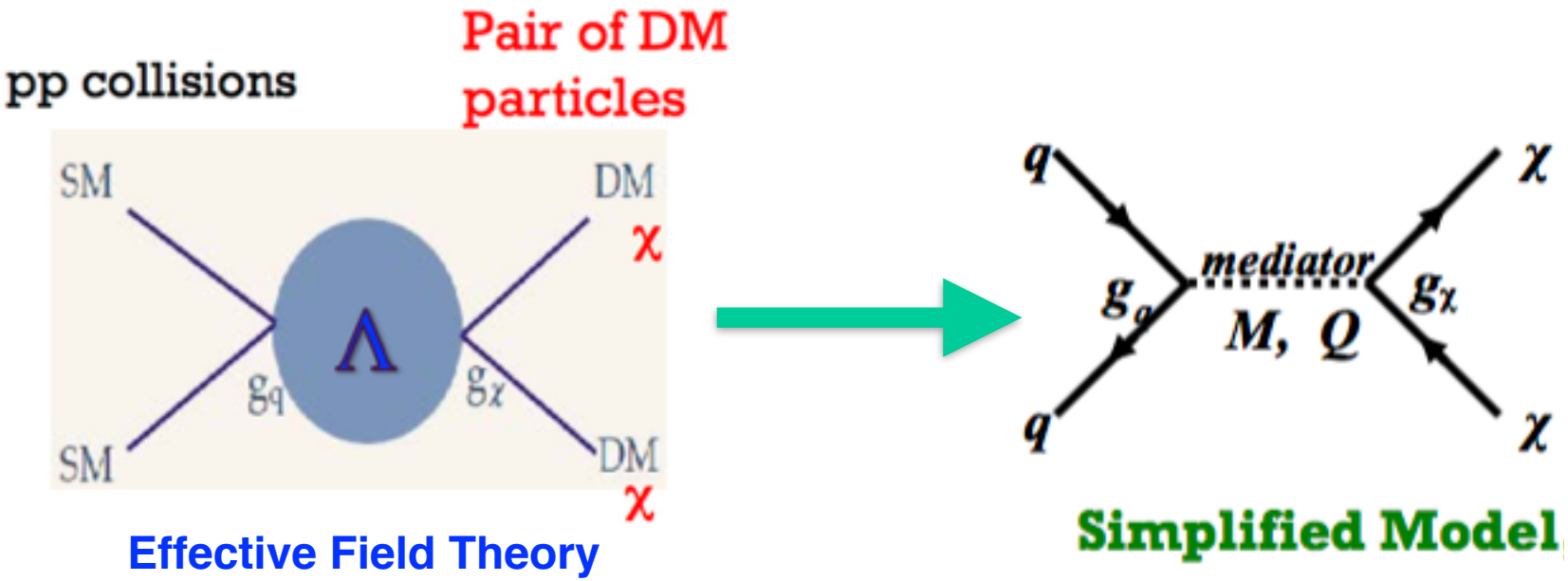

- **EFT** are reliable only if $M^2 >> \langle Q^2 \rangle$ which is not always true at LHC energies.

Dark Matter Simplified Models

- Search for visible (SM) particles (Gluon/photon/boson) recoiling against MET
- Photons/gluons/bosons emitted as ISR, DM escapes undetected as MET

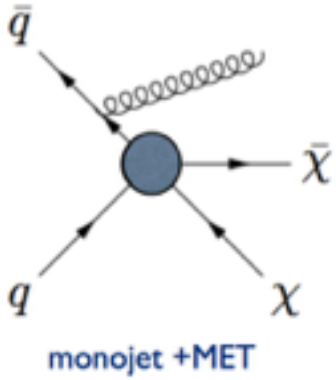

monojet +MET

- **Mono-Z' Simplified Model:**
  - DM particle is a Dirac fermion
  - DM particles are pair-produced
  - A new massive particle mediates the DM-SM interaction
  - There is an additional Z' emitted as FSR in this model
  - Mediator has minimal decay width

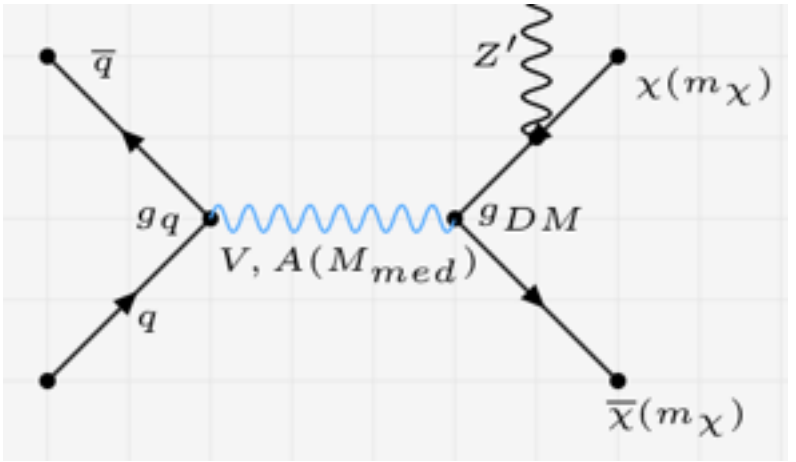

- **Minimal set of parameters**
  - M_{MED}, M_{DM}, g_{SM} (0.25), g_{DM} (1)
- Reduce to EFT in **high-M_{med}** limit:

$$\Lambda = M_{med}/\sqrt{g_q g_{DM}}$$

Mono-Z' Model

- Final State radiation of dark matter can generate the signature of a mono-Z' jet plus missing transverse energy.
- We study dominant decay of Z' into quarks.
- For GeV-scale Z' , there are 2 important effects :
  - The boosted Z' appears as a jet with a very narrow cone of radiation and a small multiplicity of charged particles.
  - The rate for dark matter FSR of Z' jets can be larger than the rate for ISR jets
- For a GeV-scale Z' (produced in association with large E_T^{miss}) decaying to hadrons, the boosted Z' gives a new collider signature.

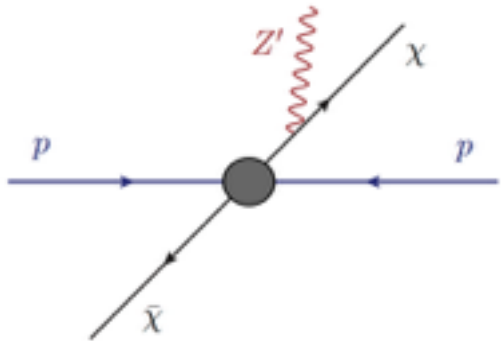

arXiv:1504.01395v2

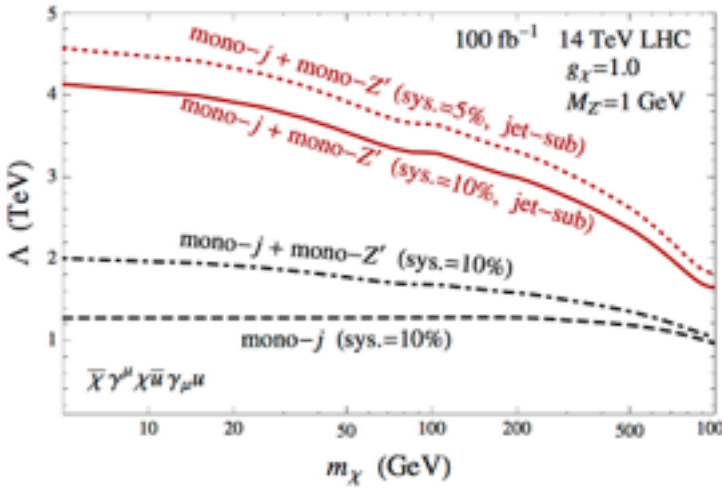

- Mono-Z' model depends on the following parameters (initial values provided)
  - $M_{Z'}$ = 1 GeV
  - DM Mass, m_χ = 5 GeV
  - g_{SM} = 0.25 , g_{DM} = 1.0
  - M_{MED} = 1000 GeV

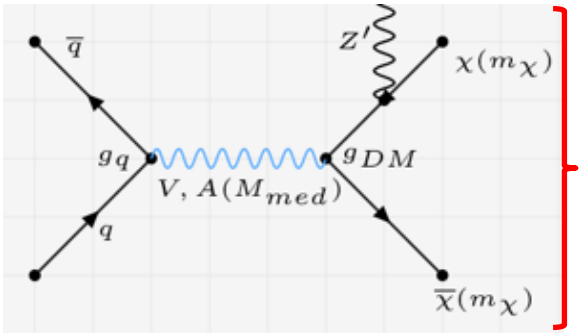

E_T^{miss} > 300 GeV

The Large Hadron Collider

CMS experiment

Large Hadron Collider

- 27 km circumference
- Depth 100m; tilt 1.4º.
- 1600 superconducting magnets at 1.9° K (-271.3° C or –459.7° F)
- Accelerates beams of protons to 99.9999991% the speed of light

The Large Hadron Collider

- **LHC is capable of colliding protons and heavy ions**
- **Serves four primary experiments**
  - CMS and ATLAS: general purpose
  - LHCb: forward hadronic physics
  - ALICE: heavy ion collisions
- **Designed for 14TeV center of mass energy**
  - Achieved 8TeV in 2012
  - Achieved 13 TeV in 2015-2016

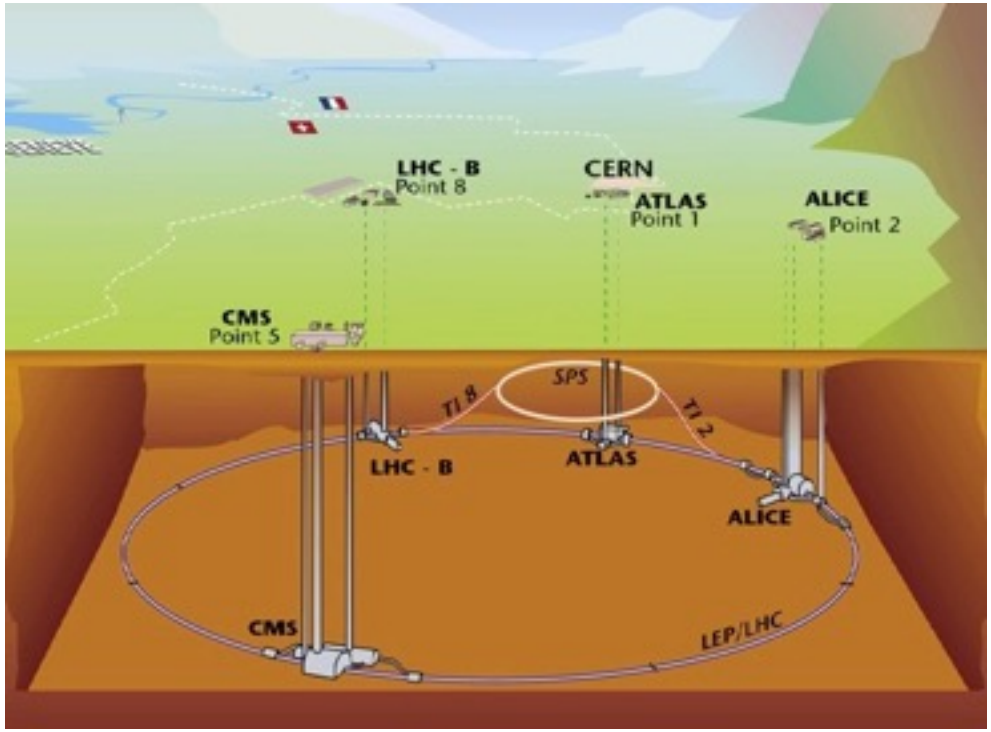

Year	LHC center of mass energy
2010-2011	7 TeV
2012	8 TeV
2015-2017	13 TeV
Design	14 TeV

Proton Beam and Luminosity

- Number of events for a given process:

$$N = \sigma \int L \, dt$$

  - σ = cross section of process
  - L = Instantaneous luminosity of collider

	Design	2012	2015	2016	2017
Beam Energy (TeV)	7	4	6.5	6.5	6.5
Bunches per beam	2808	1368	2232	2208	2448
Bunch Spacing (ns)	25	50	50/25	25	25
Integrated Luminosity (fb^{-1})		23.3	4.2	40.8	51.0

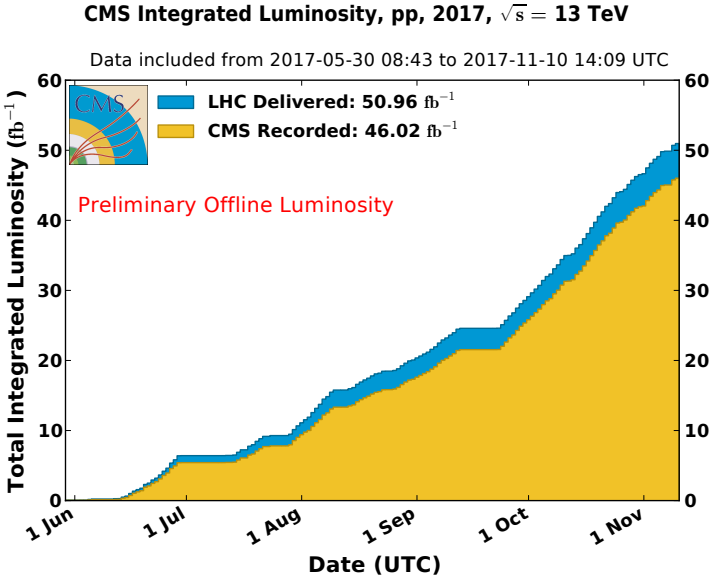

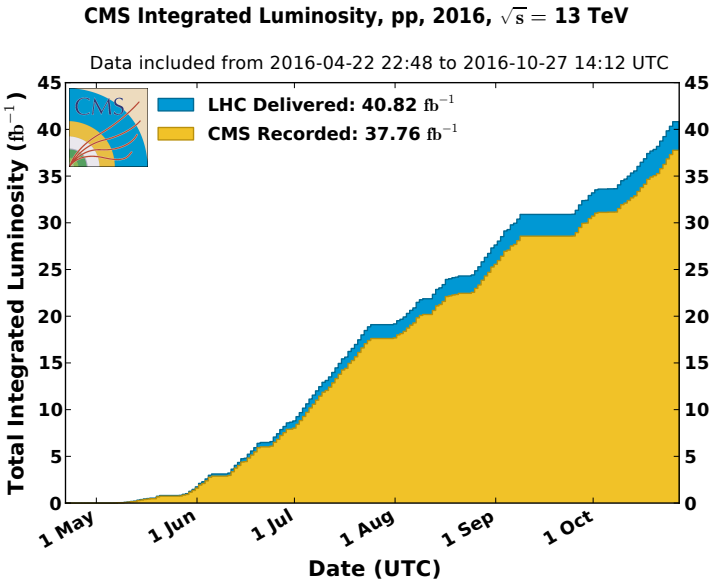

- Present analysis uses part of 2016 data: 1.89 fb^{-1}
- 2018: Reach ~150 fb^{-1}

The Compact Muon Solenoid

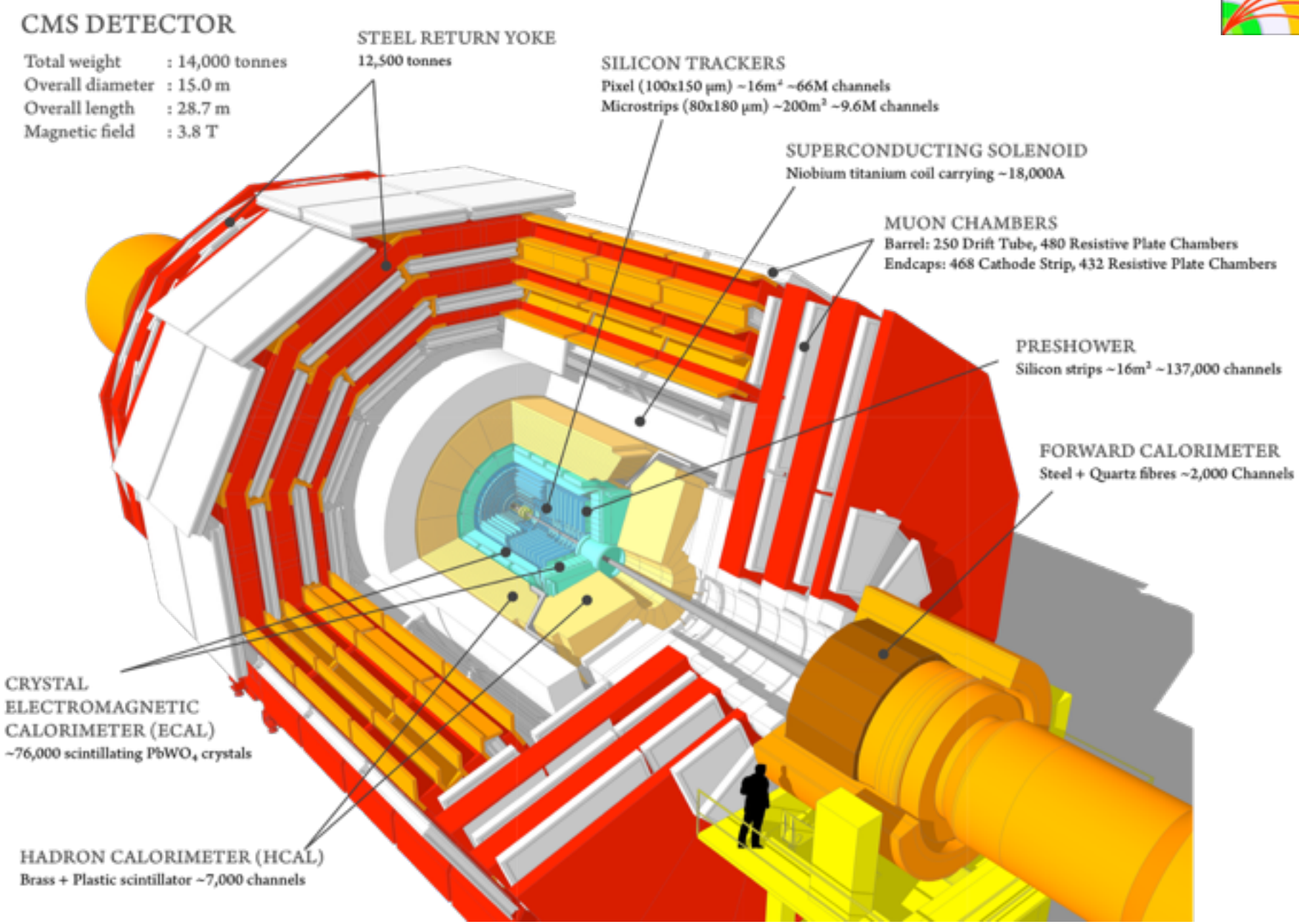

CMS Magnet

- **Purpose:** Strong magnetic field to bend path of charged particles
  - Allows momentum calculation
- 12.5 m length x 6.3 m diameter, cooled to 4.7 K by liquid Helium
- Superconducting high field (3.8T) solenoid coil inside central barrel
- Iron return yoke provides ~2T field outside solenoid
- Largest magnet in the world by measure of stored energy

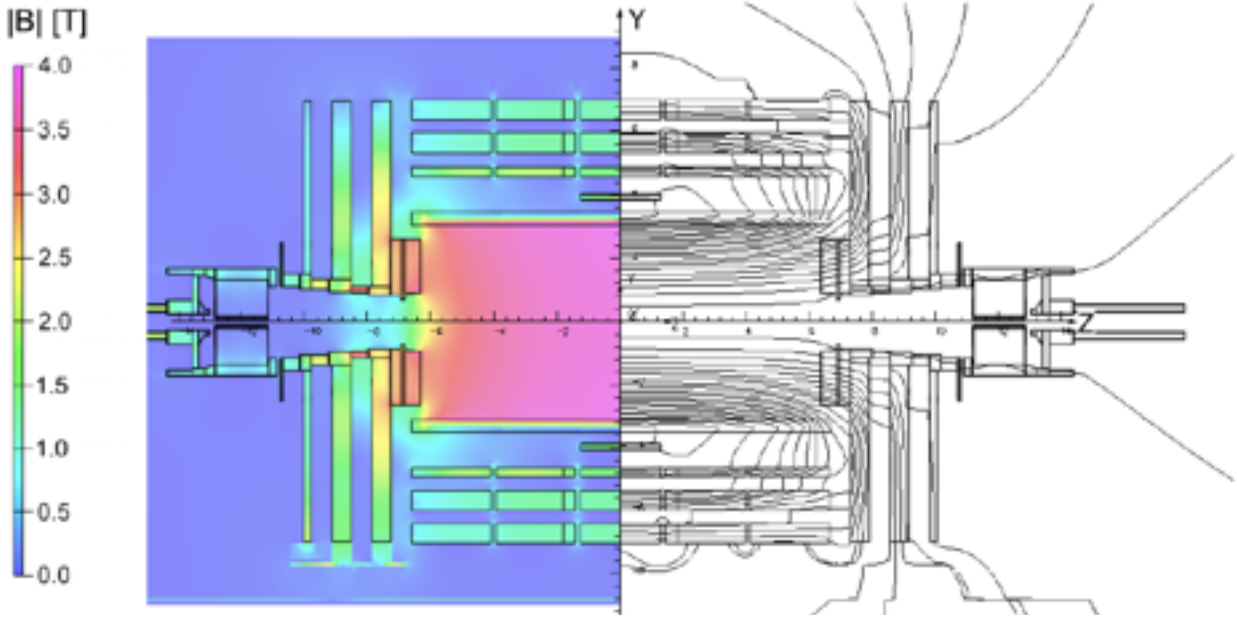

Silicon Tracker

- **Purpose:** High resolution tracks for p_T and vertex measurement & matching
- Over 200m² Silicon cooled to below -10°C
- **Pixel detector** on the inside r<15 cm
  - 66 million channels
  - 3 layers, now upgraded to a new 4-layer detector
- **Silicon strip detector** outside to radius 1.1 m
  - 9.6 million channels

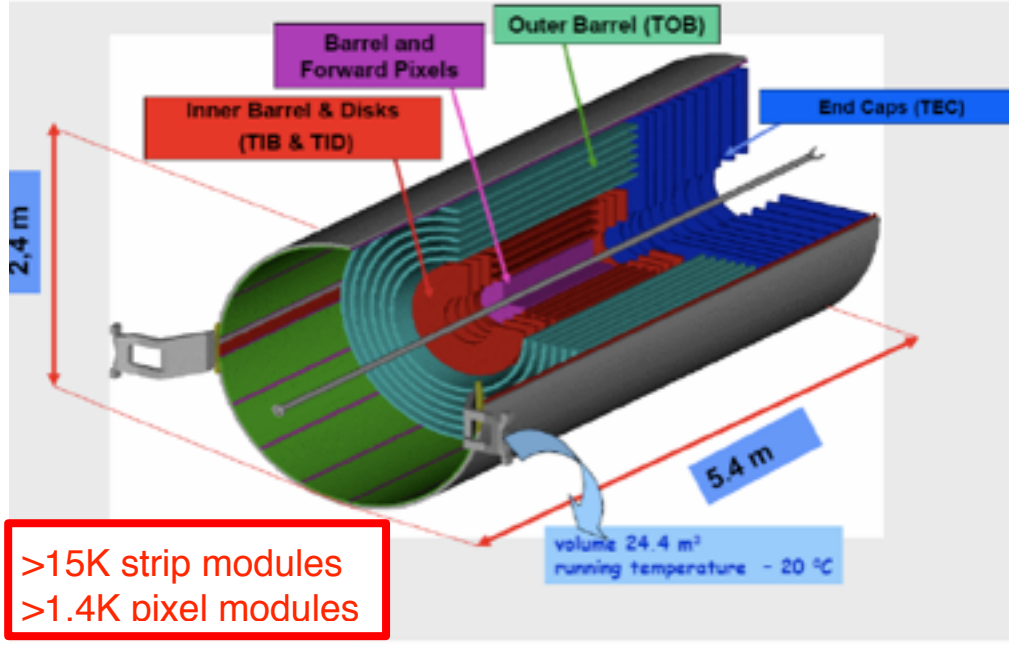

>15K strip modules
>1.4K pixel modules

p_T Resolution (barrel):

$$\frac{\delta p_T}{p_T} = \left(15 \frac{p_T}{TeV} \oplus 0.5\right) \%$$

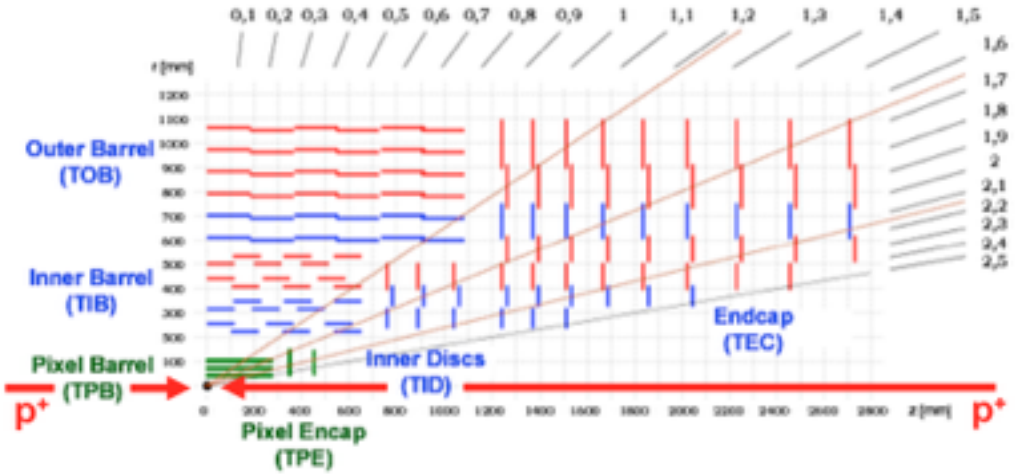

The track pT resolution is roughly 0.5–2% for most of the relevant kinematic range, with less good track pT resolution (up to 5%) for low pT tracks (less than 1 GeV) at high pseudorapidities

$$\eta \equiv -\ln\left[\tan\left(\frac{\theta}{2}\right)\right]$$

Electromagnetic Calorimeter

- **Purpose:** High resolution position and energy measurements for electrons and photons
- Over 75k Lead Tungstate crystals with Photodetectors
  - 61200 in Barrel region (**EB, |η| < 1.48**)
  - 14648 in Endcap (**EE, 1.48 < |η| < 3.0**)

	Lead Tungstate ($PbWO_4$)
Density	8.28 g/cm^3
Radiation Length	0.89cm
Molière radius	2.19cm

Barrel: Avalanche PhotoDiodes (APD)
Endcap: Vacuum PhotoTriodes (VPT)

- **Resolution in Barrel:**

$$\frac{\sigma}{E} = \frac{2.8\%}{\sqrt{E}} \oplus \frac{0.128}{E} \oplus 0.3\%$$

e.g. a 50 GeV photon has energy resolution of 0.55% in the barrel.

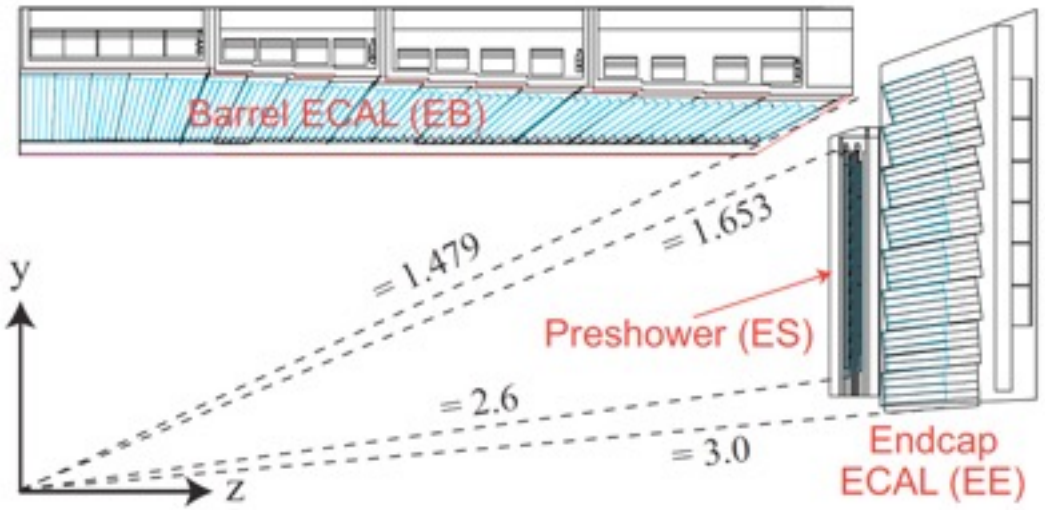

The ECAL energy resolution for electrons and photons is roughly 0.5–3%, depending on both pseudorapidity and energy, for electron/photon energies greater than 10 GeV.

Hadronic Calorimeter

- **Purpose**: Long lived hadrons (Jets) and missing energy (MET) measured and triggered by compact (inside solenoid), hermetic ($|\eta| < 5$) sampling hadronic calorimeter (HCal)
- The CMS HCal:
  - **HCAL Barrel (HB)**
    - 5.8-10.6 λ (+1.1 λ from ECAL)
  - **HCAL Endcap (HE)**
    - ~10 λ (including ECAL)
  - Over 1000 tons of brass plates interleaved with scintillator tiles
  - Resolution (HB/HE):

$$\frac{\sigma}{E} = \frac{115\%}{\sqrt{E}} \oplus 5.5\%$$

  - **HCAL Forward (HF)**
    - Steel plates embedded with quartz fibers
    - Cherenkov-based detector
    - Measures EM rich jets outside of ECal acceptance.
    - Resolution: $\frac{\sigma}{E} = \frac{280\%}{\sqrt{E}} \oplus 11\%$

Barrel (HB)
36 brass/scintillator wedges
17 longitudinal layers
5cm brass + 3.7mm scint
coverage: $|\eta|<1.3$

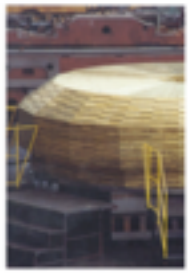

Endcap (HE)
Two brass endcap discs
19 longitudinal layers
8cm brass + 3.7mm scint
coverage: $1.3<|\eta|<3.0$

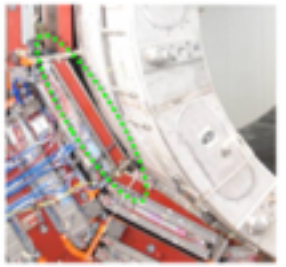

Outer (HO)
scintillator tiles outside yoke
1 or 2 longitudinal layers
10mm scint
coverage: $|\eta|<1.3$

Forward (HF)
Steel absorber, in 20 deg wedges
Quartz fibre active element (~1000km)
coverage: $3<|\eta|<5.0$

Muon System

- **Purpose**: triggering, identification, and assisting inner tracker in measuring high-p_T muons
- ~14000 tonnes of iron absorber and solenoid flux return
- Three types of gas detectors
  - Cover very large ~40K m^2 area at low cost

1. Drift Tubes (DT) in the barrel $|\eta| < 1.2$
2. Cathode Strip Chambers (CSC) in the endcap $0.9 < |\eta| < 2.4$
3. Resistive Plate Chambers (RPC) in both: $|\eta| < 1.6$

Momentum measurement below about 200 GeV is tracker dominated, but above that the full system has better resolution

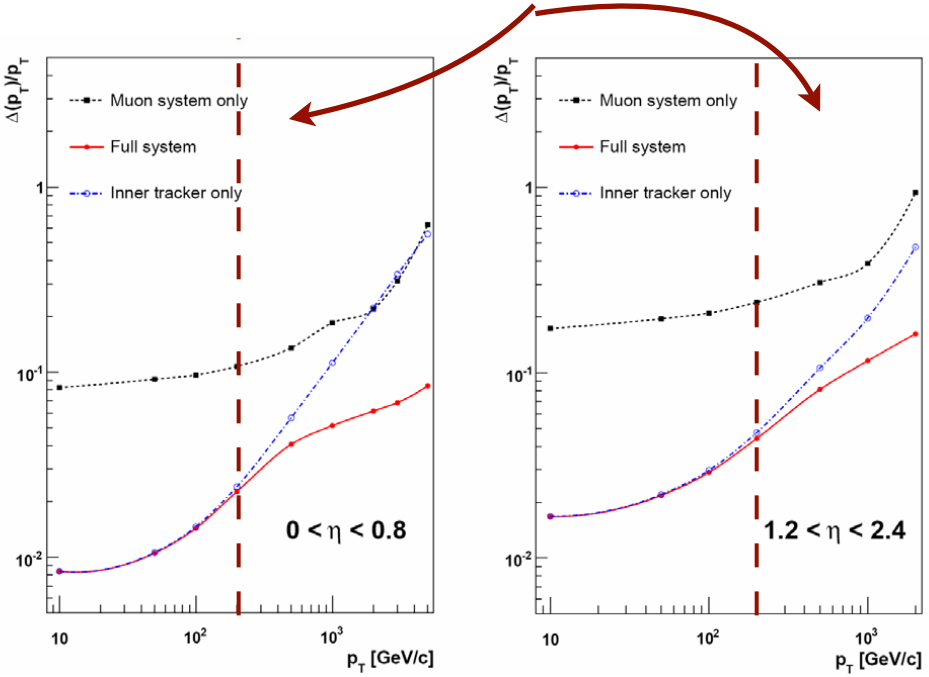

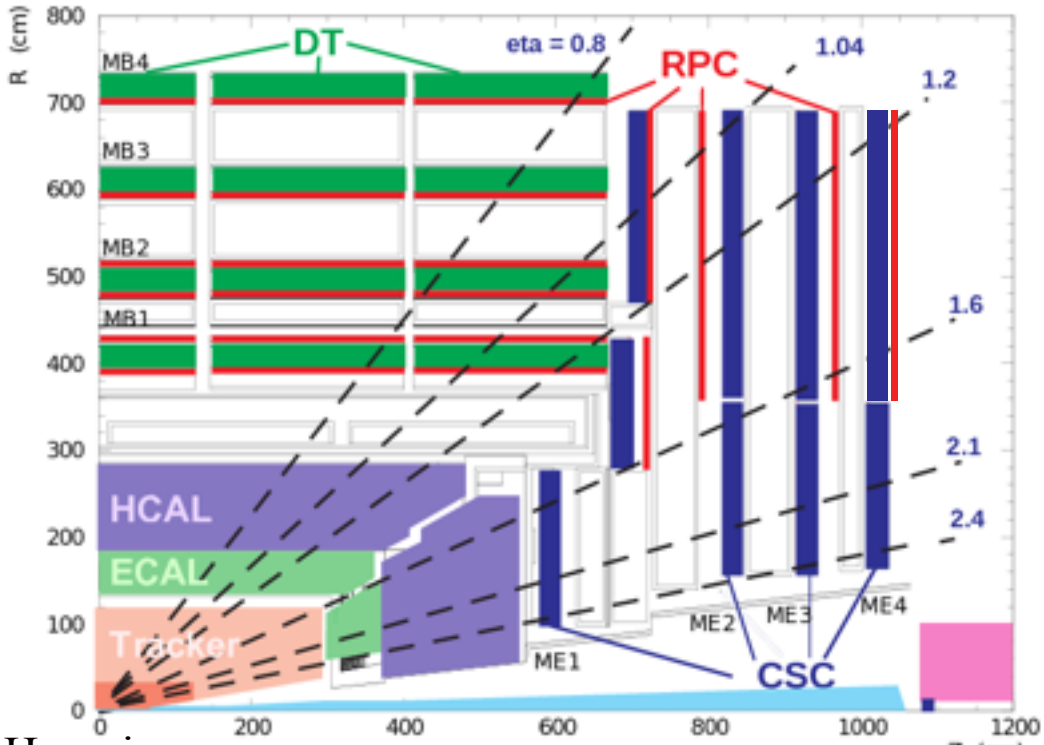

Trigger System

- 40 MHz of beam crossings, with a average of ~25 interactions/crossing means that there are nearly 1 billion interactions/ second
- Beam crossings generate ~1 MB of data per event or 40 Terabytes/s
- CMS can record ~1kHz at a MB per event
- Need to reject 99.9998% of events in quasi real time

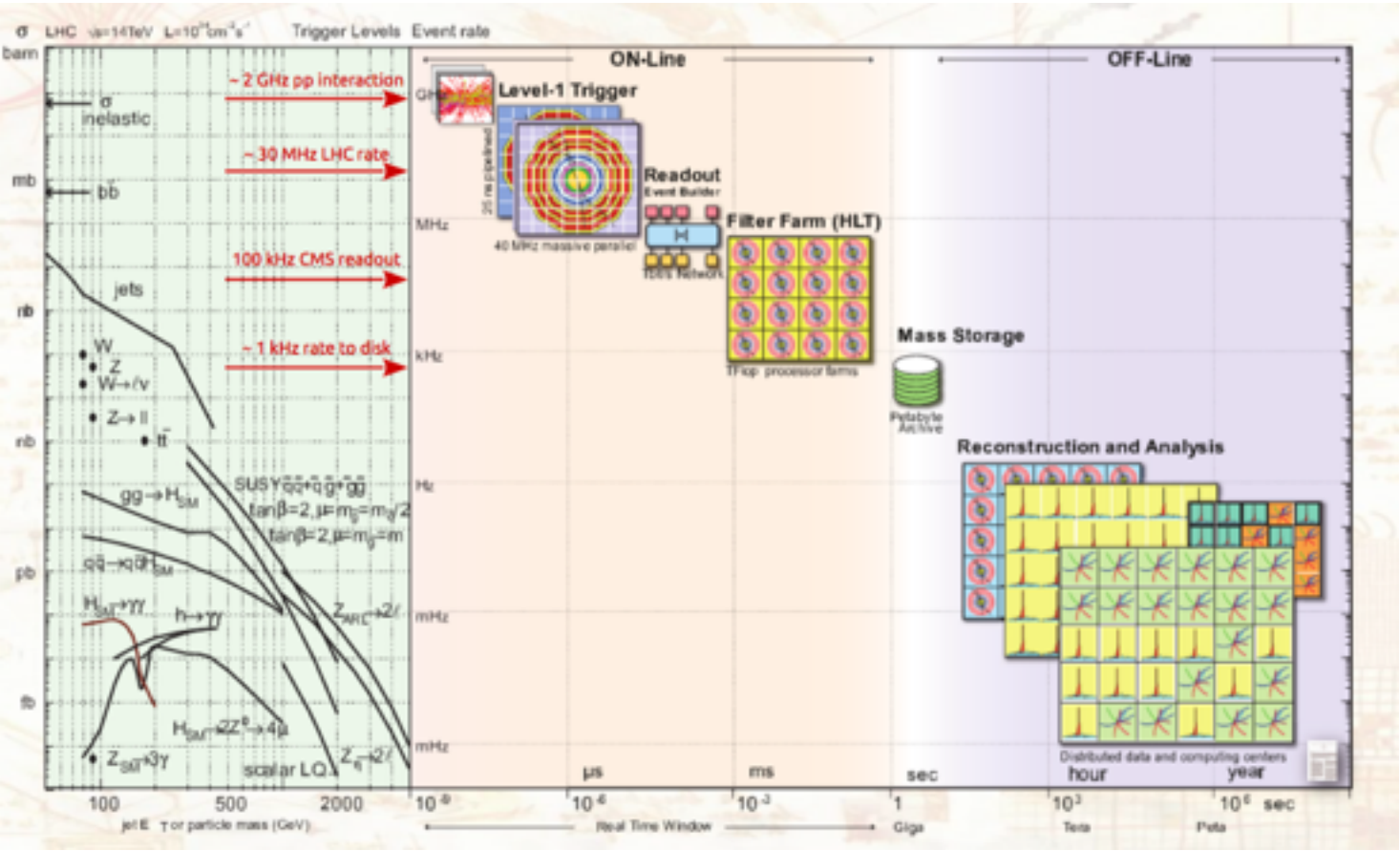

Rate reduction in two steps:

- **Level-1 Trigger**
  - Custom hardware
  - Subset of detector information
  - Reduces rate to ~100kHz
- **High-Level Trigger**
  - Software, CPU-limited
  - Full detector information
  - Reduces rate to ~1kHz

Level 1 Trigger

- Using only calorimeters and muon systems, Level 1 (L1) Hardware trigger finds
  - EG Candidates (electrons/photons)
  - Jet Candidates
  - Missing Energy estimate
  - Muon Candidates

- Constraints from the detectors readout
  - pipeline: ~ 4 μs long
  - 100 kHz maximum output rate

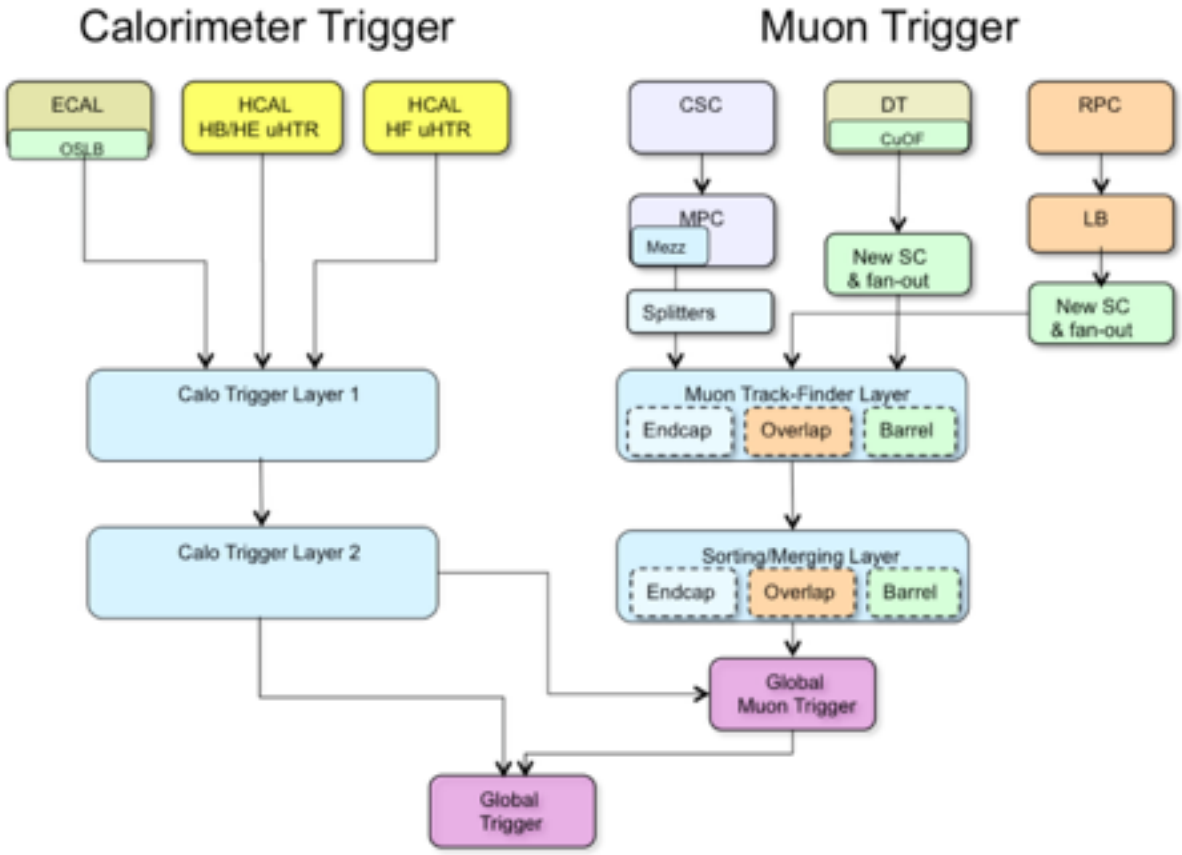

High Level Trigger

- Full detector readout, full granularity
  - 100 kHz input rate
- Implementation
  - Subset of reconstruction algorithms used for simulation and offline analyses
  - running on a cluster of commercial PCs (filter farm)
  - Over 450 trigger paths in HLT menu
- Constraints
  - ~220 ms *average* processing time to take a decision
  - 1 kHz *average* output rate (limited by offline resources)

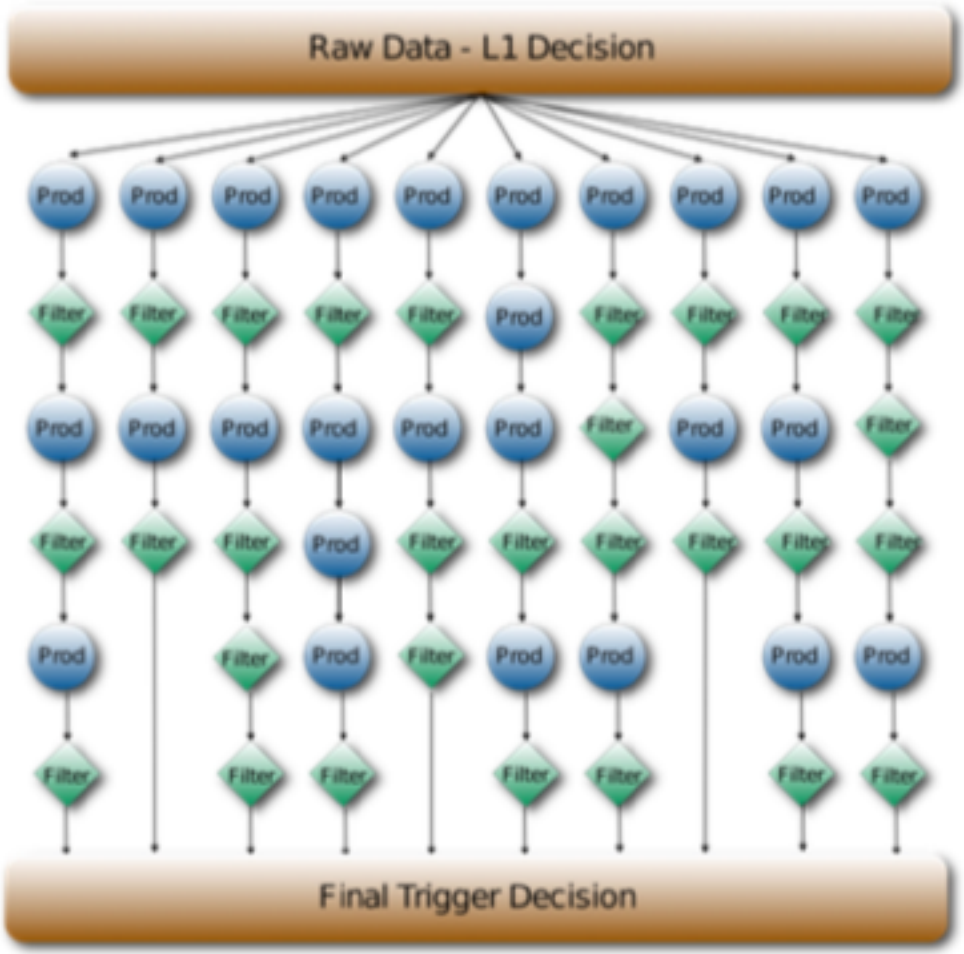

Schematic representation of a HLT menu in CMS and of the HLT paths in it. The final trigger decision is the logical OR of the decisions of the single paths.

Particle Flow Reconstruction

Particle Flow Reconstruction combines information from sub-detectors in the best possible way to reconstruct all stable particles in an event

- Muon system tracks are matched to tracks in inner tracker - **Muons**
- Remaining tracks are then associated with energy deposits in ECAL (**electrons**) and HCAL (**charged hadrons**)
- Remaining energy deposits are clustered to form **photon candidates** (ECAL) and **neutral hadron candidates** (HCAL)

Higher level physics objects such as hadronic taus, jets, missing transverse energy can be built from these objects

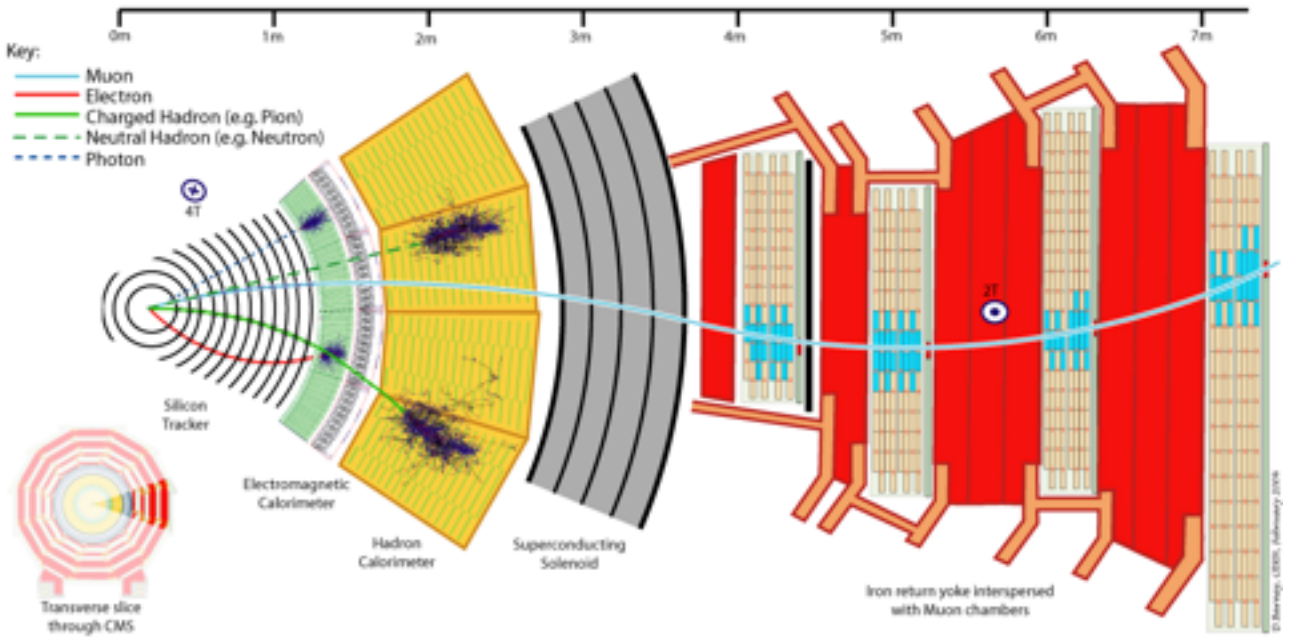

type	tracking	ECAL	HCAL	MUON
γ				
e				
μ				
Jet				
Et miss				

Jet Reconstruction

Most physics channels of interest at the LHC require good understanding of jet reconstruction.

- Collimated bunches of stable hadrons, originating from partons (quarks and gluons) after fragmentation and hadronization
- Jets are the observable objects to relate experimental observations to theory predictions.

- Jet reconstruction algorithms
  - Iteratively cluster nearby particles into jet objects

In this analysis,

- Use **AK4PFCHS** jets (charged particles from non-primary vertices (pileup) are removed before clustering).
- Anti-k_T jet algorithm distance metric with R = 0.4: $d_{ij} = \min(\frac{1}{k_{ti}^2}, \frac{1}{k_{tj}^2})\frac{\Delta_{ij}^2}{R^2} \qquad \Delta_{ij}^2 = (\eta_i - \eta_j)^2 + (\phi_i - \phi_j)^2$
- distance $\mathbf{d_{ij}}$ between two particles i and j

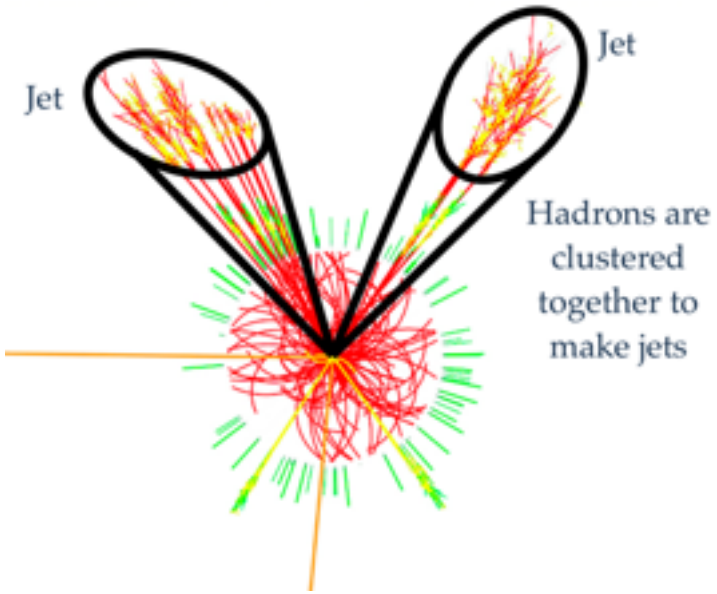

Pencil Jet Reconstruction

- Compute energy weighted η width and ϕ width by looping over all Particle Flow Constituents of the jet

- η Width = $\sqrt{\frac{\sum(\eta_i^2 E_i)}{\sum E_i} - \left(\frac{\sum(\eta_i E_i)}{\sum E_i}\right)^2}$

- ϕ Width = $\sqrt{\frac{\sum(\phi_i^2 E_i)}{\sum E_i} - \left(\frac{\sum(\phi_i E_i)}{\sum E_i}\right)^2}$

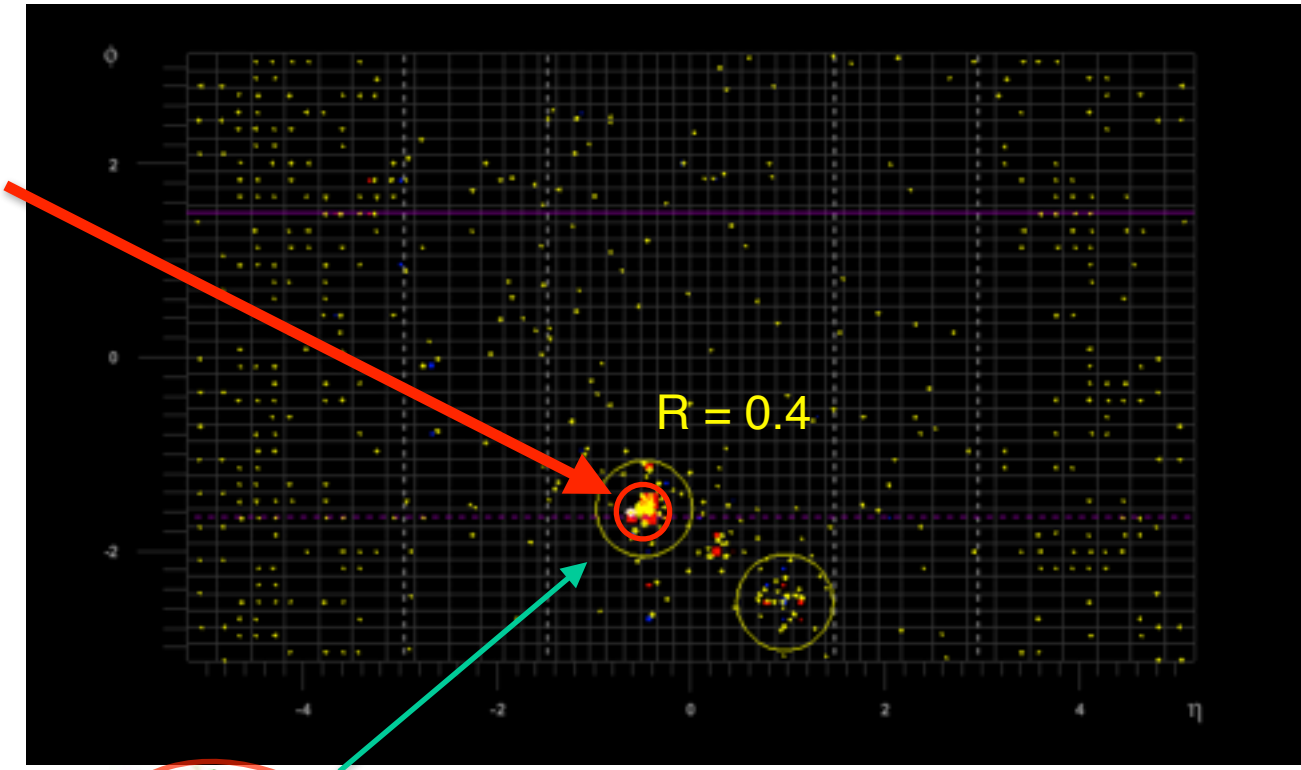

- Z' → two quarks → hadronize

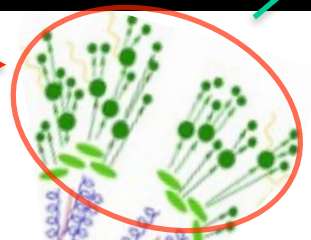

CMS event display with η-ϕ view

R = 0.4

- Boosted Z' is highly collimated and energy deposits from its constituents are concentrated in η and ϕ

- See event display

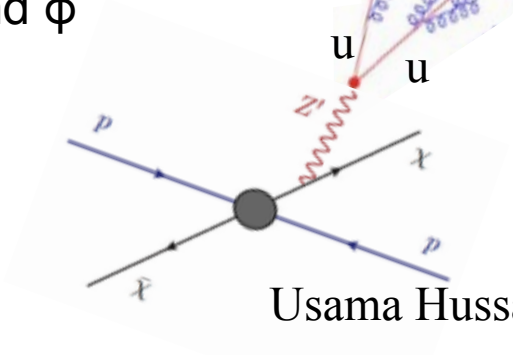

Missing Transverse Energy

Missing Transverse Energy (MET)

- Negative vector sum of transverse momentum from all reconstructed particles (PF objects). $\vec{\not{E}}_{\mathrm{T}} = -\sum_{i \in \mathrm{vis.}} \vec{p}_{\mathrm{T}i}$
- Neutrinos and potentially beyond the standard model particles will not deposit energy in the CMS detector resulting in MET.

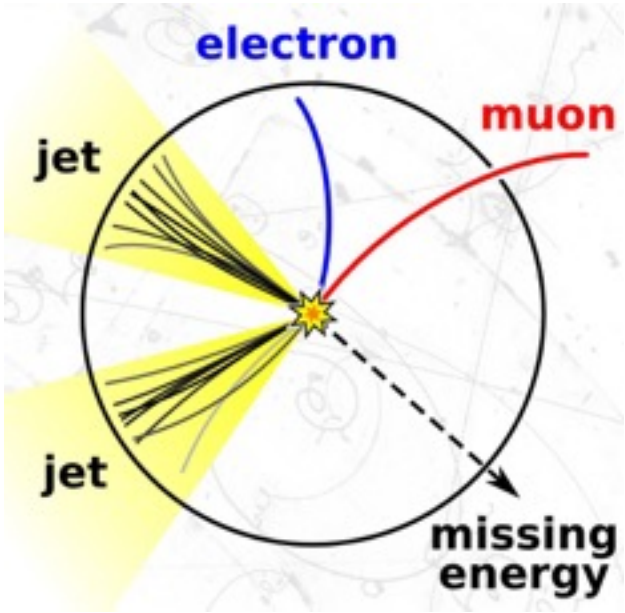

In this analysis,

- Use pfMET (all particle flow candidates are summed)
- pfMET measurement sensitive to:
  - detector effects: noise, dead/hot cells
  - beam halo, cosmics, pile-up
- MET Filters are applied to account for some of these effects
- Jet energy corrections are applied to particles associated with a jet $\vec{\not{E}}_{\mathrm{T}}^{\mathrm{corr}} = \vec{\not{E}}_{\mathrm{T}} - \sum_{\mathrm{jets}} (\vec{p}_{\mathrm{T,jet}}^{\mathrm{corr}} - \vec{p}_{\mathrm{T,jet}})$

Event Simulation

Full data taking process is simulated, from hard scatter process through event reconstruction: "Monte Carlo" (MC)

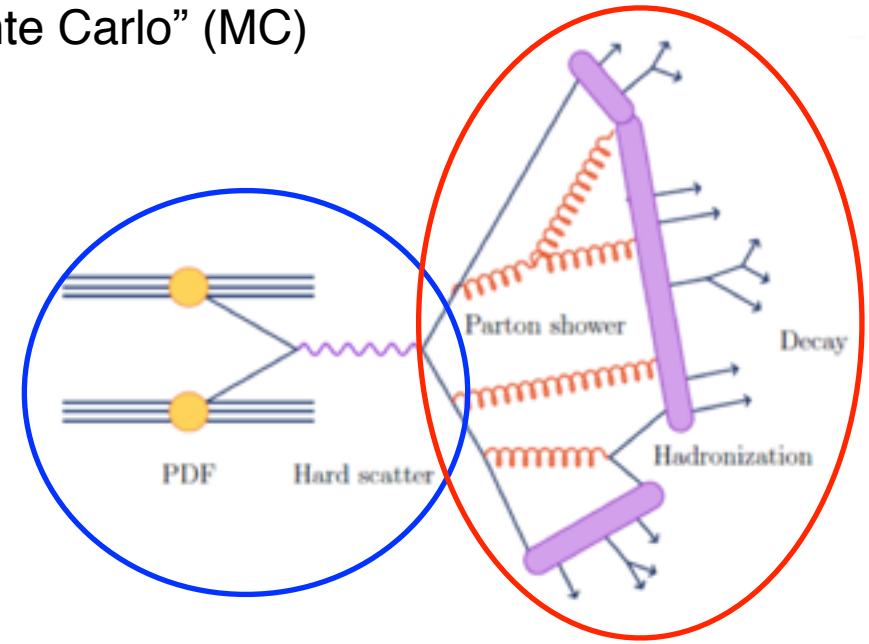

Modeled in GEANT4:

- Particle Interactions with matter
- Simulate detector response

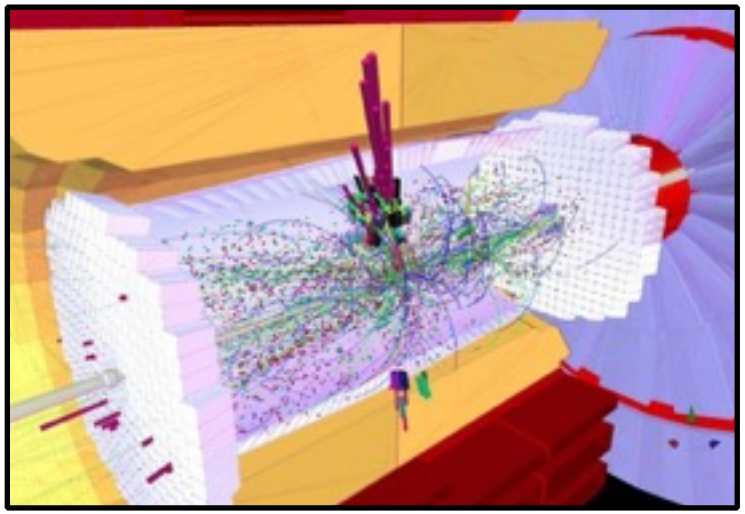

Event Reconstruction

Common programs for hard scatter simulation at CMS:

- MadGraph5_aMC@NLO
- POWHEG
- PYTHIA

Pythia simulates:

- Parton Shower
- Hadronization
- Decay

Analysis Strategy

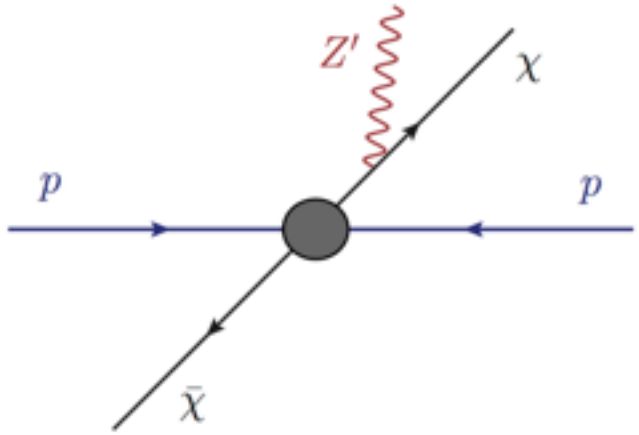

- Use the topology of the signal where the Z' appears as a narrow “Pencil” Jet to improve the limits obtained by Mono-Jet Analysis.
- Find a set of selection criteria that would optimally identify this unique signature.
- The more sophisticated selection criteria can then be better optimized to reduce background that is more likely to be faking signal.

Backgrounds

- Jet+MET final state can be mimicked by a variety of non-signal processes
- All significant background MC processes used in this analysis are summarized:

Data	
ZprimeSignal	Signal Simulation, produced with Madgraph
Z→νν	Main irreducible background in this analysis
W→lν	Second largest background in this analysis
WW/WZ/ZZ	One weak boson decays leptonically (*W ->lν, Z -> νν*) while the other decays hadronically producing jets and E_T^{miss}
Top Quark	W produced from top decay, W decays leptonically producing genuine E_T^{miss} in the event
γ+jets	Fake MET due to events in which the photon goes undetected
DYJets→LL	Fake MET
QCD	Mismeasured or undetected jet events can serve as background events

Cut Flow Overview

Preselection reduces ~6.4 million events from the MET primary dataset to ~2.2 million events.

Preselection:

- Require MET filters to reduce fake MET from detector effects, beam halo, cosmics etc.
- Require HLT path with
  - PFMET > 170 GeV

Selection Cuts:

- Cuts motivated in following slides

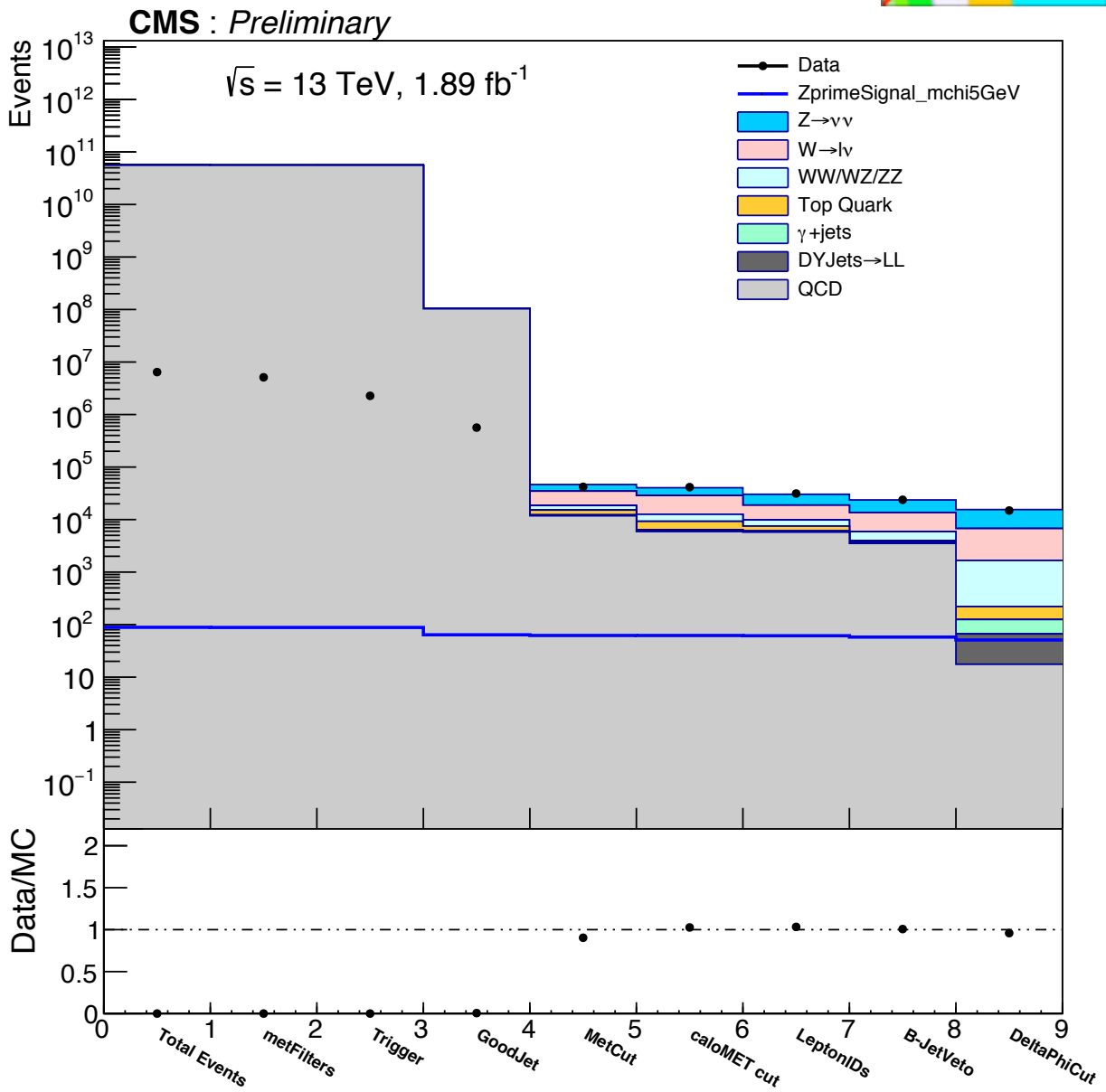

Triggers

HLT path	L1 seed	Primary dataset
HLT_PFMET170_*	L1_ETM70	MET
HLT_PFMETNoMu[X]_PFMHTNoMu[X]_IDTight	L1_ETM70 L1_ETM60_NotJet52WdPhi2	MET

MET Cleaning and Trigger

- Data Events pass the E_T^{miss} triggers described in previous slide.
- Reject fake MET caused by detector noise, cosmic rays and beam-halo particles which improves the agreement of the MET spectrum with Monte Carlo, in which causes of false MET are not explicitly simulated.

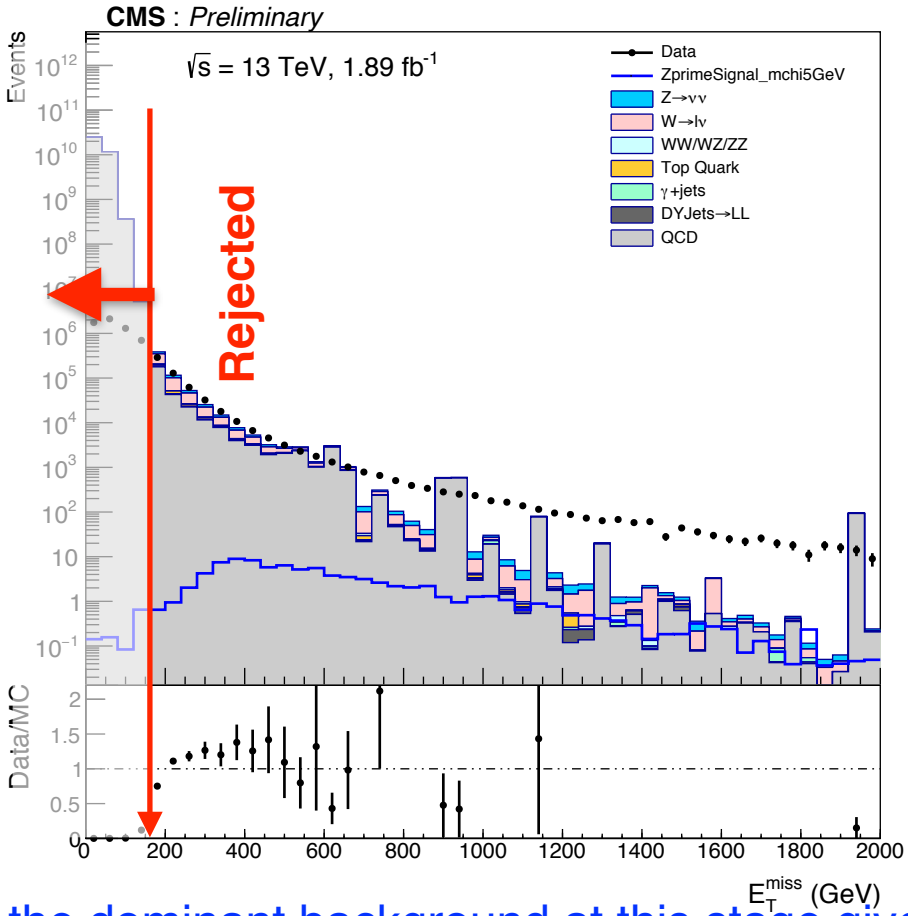

	Before Cut	After Cut
Data	6.4E+06	2.3E+06
QCD	3.65E+10	3.6E+10
Signal	88.3	87.7
S/√B	0.000462	0.000458

QCD is the dominant background at this stage given the large cross-section with which these events are produced

Jet Cleaning

- A good jet candidate passes:
  - Loose Particle Flow JetID
    - Reject fake, badly reconstructed and noise jets
- Kinematic cuts
  - jet momentum is greater than 200 GeV
  - Neutral Hadron Fraction of the Jet < 0.8
  - Charged Hadron Fraction of the Jet > 0.1
  - |jetEta| < 2.4
- MET filters remove a lot of fake MET events from detector noise and beam halo
- Additional Cleaning of Jets required to suppress backgrounds due to detector noise and beam backgrounds

	Before Cut	After Cut
Data	2.3E+06	563938
W+Jets	1.1E+08	193971
Z+Jets	868754	45562
QCD	3.6E+10	1.0E+08
Signal	87.7	63.7
S/√B	0.000458	0.00637

Cut Flow - MET Cut

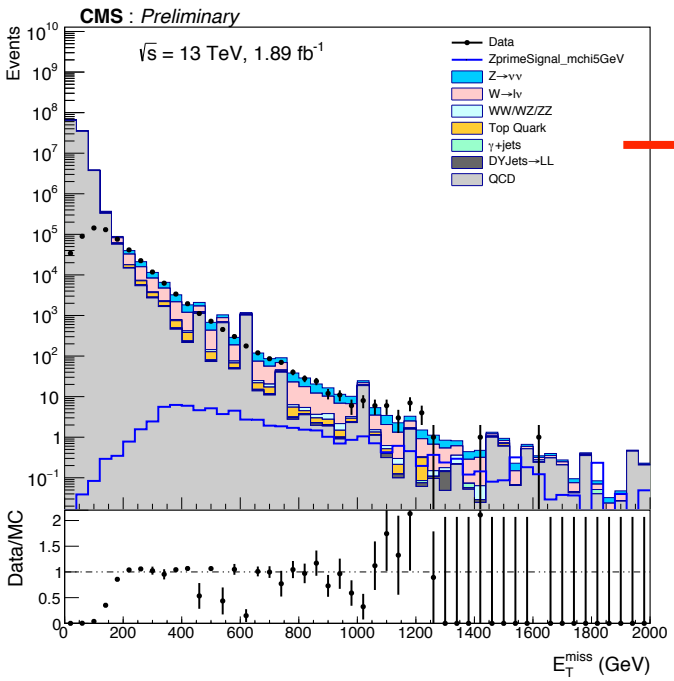

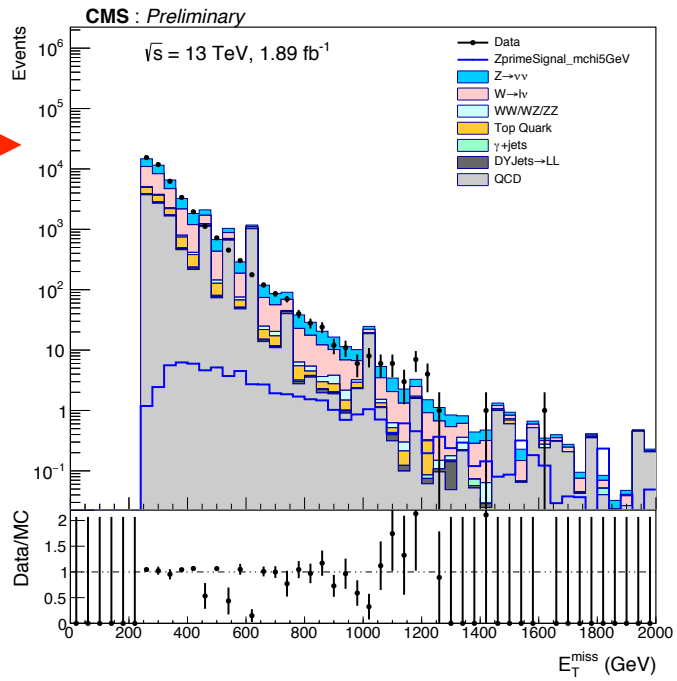

	Before Cut	After Cut
Data	563938	41985
W+Jets	193971	16283
Z+Jets	45562	11629
QCD	1.0E+08	11799
Signal	63.7	61.7
S/√B	0.00637	0.295

- Expect significant amount of missing energy (MET) in our signal
- Cut MET > 250 GeV

Cut Flow - CaloMET based Cut

- **CaloMET**: MET of all energy deposits in calorimeter towers in EB, EE, HB, HE, and HF
- Badly measured tracks/muons reconstructed as high momentum Particle Flow candidates
- Particle Flow MET is mismeasured
- CaloMET is not affected
- (caloMET-pfMET)/pfMET variable typically has a large value for events in which PF MET is mismeasured.

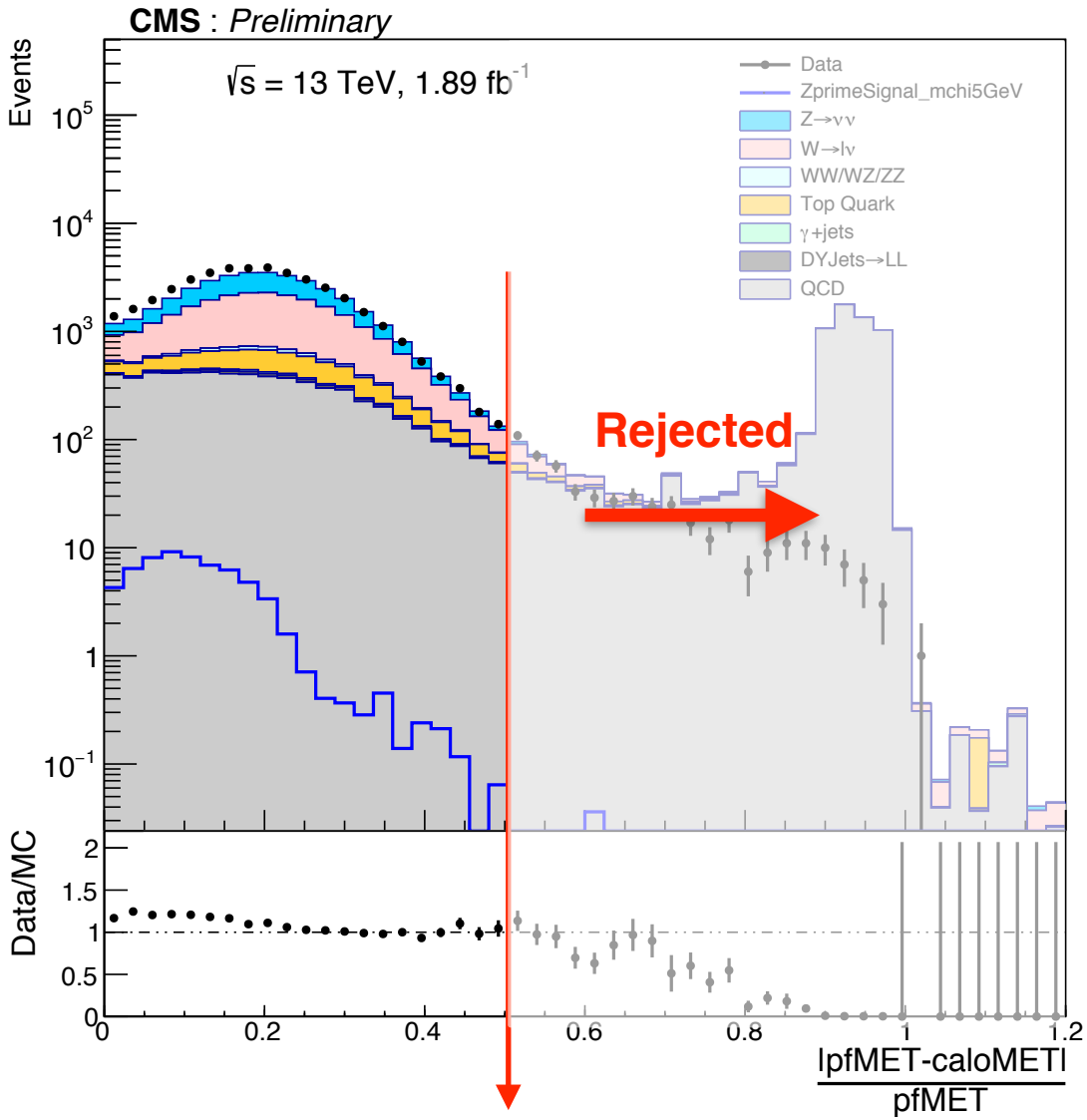

Cut applied here at 0.5 to suppress bad/ mismeasured muons faking MET

Cut Flow - CaloMET based Cut

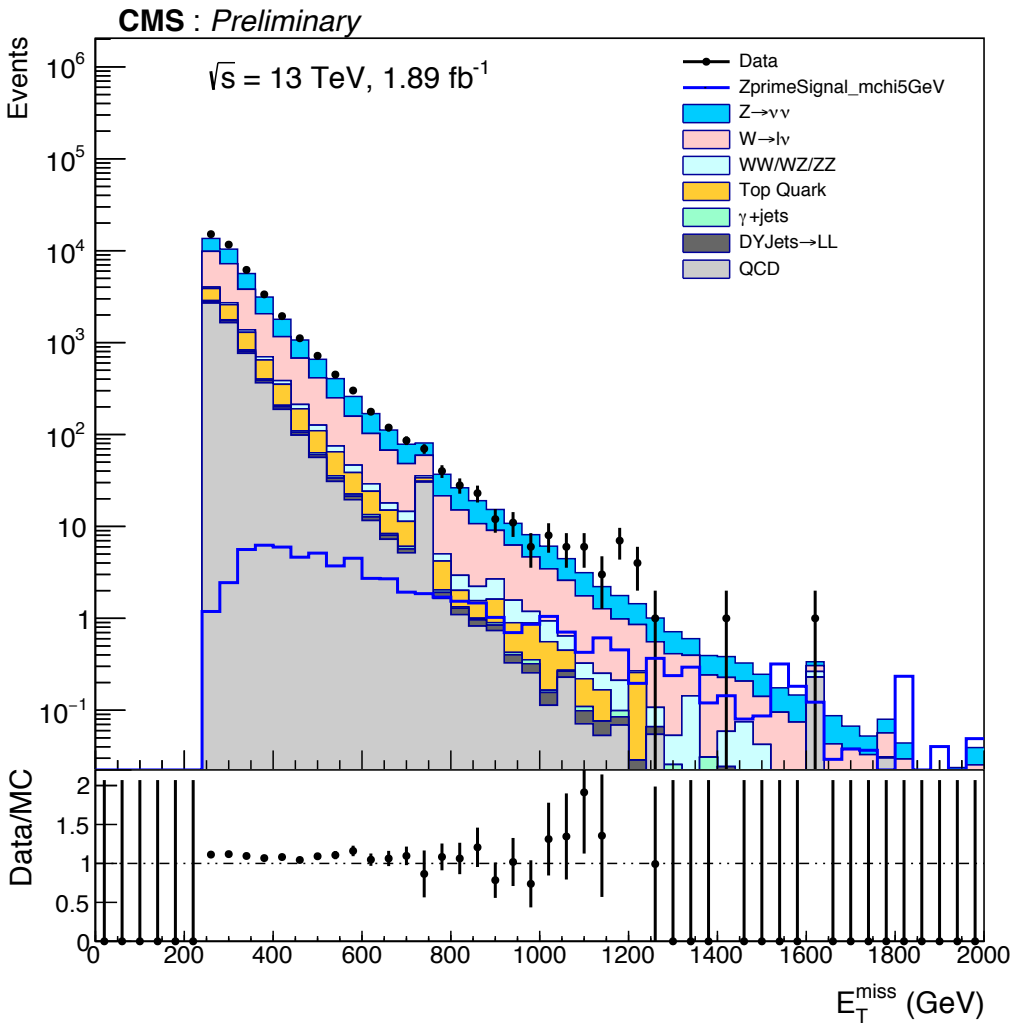

	Before Cut	After Cut
Data	41985	41452
W+Jets	16283	16162
Z+Jets	11629	11613
QCD	11799	5919
Signal	61.7	61.7
S/√B	0.295	0.318

No significant change in the main backgrounds as expected and a large reduction in QCD events.

Cut Flow - Lepton Veto

- Electron Veto
  - Electron with transverse momentum greater than 10 GeV
  - Electron does not overlap with jet (deltaR > 0.5)
- Muon Veto
  - Muon with transverse momentum greater than 10 GeV
  - Muon does not overlap with jet (deltaR > 0.5)
- Lepton veto reduces the W+Jets reducible background
- Z+Jets is the irreducible background in this analysis

	Before Cut	After Cut
Data	41452	31318
Z+Jets	16162	11506
W+Jets	11613	8965
QCD	5919	5769
Signal	61.7	61.1
S/√B	0.318	0.363

B-Jet Cleaning

- Top quarks predominantly decay to a W boson + b quark.
- Veto of b-tagged jets lowers top background

	Before Cut	After Cut
Data	31318	23822
Z+Jets	11506	10064
W+Jets	8965	7688
Top Quark	1447	225.4
Signal	61.1	57.5
S/√B	0.363	0.388

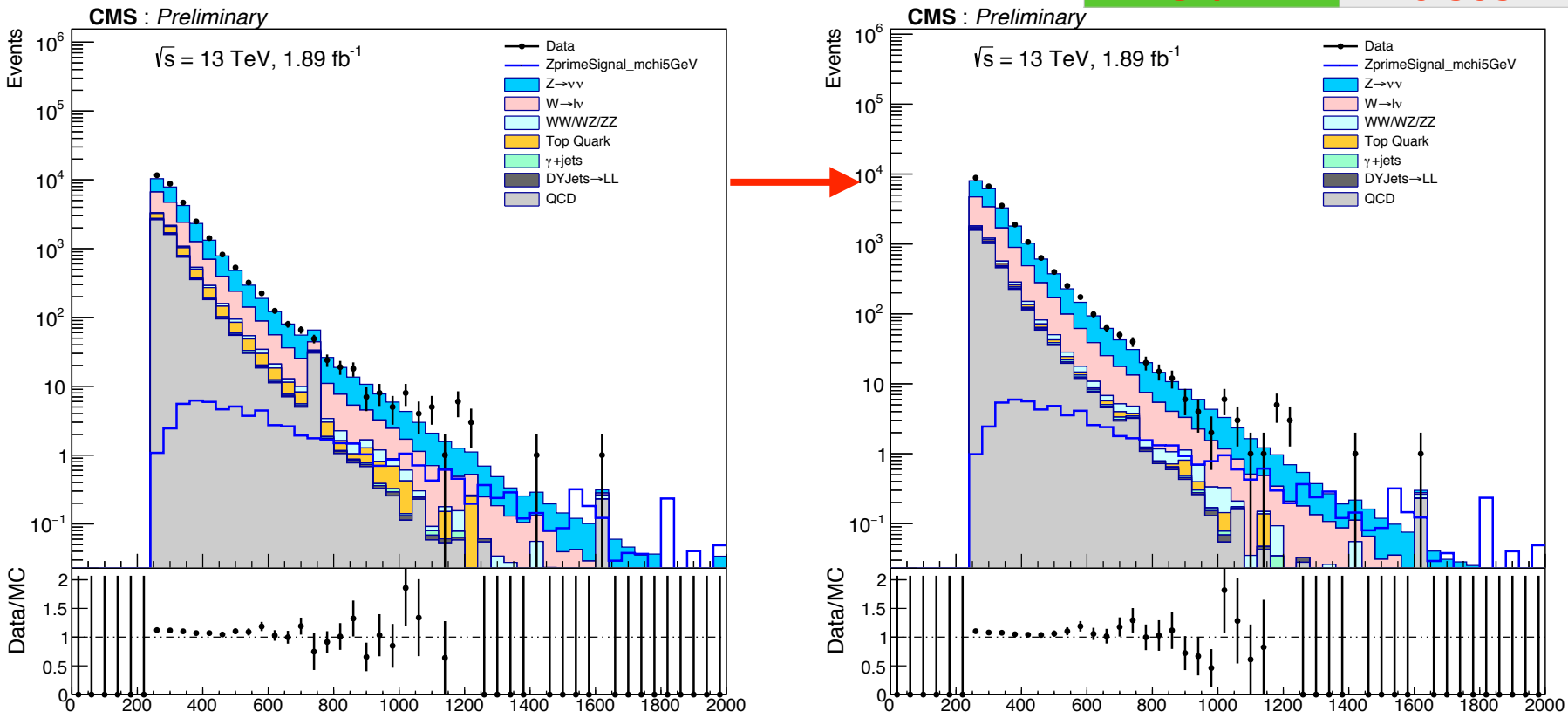

Cut Flow - Delta Phi

- Kinematics of the Z' jet and MET considered together
- Most events ‘back-to-back’ except QCD events
- Azimuthal separation between closest jet and MET $\Delta\Phi$ (Jet, MET) > 0.5

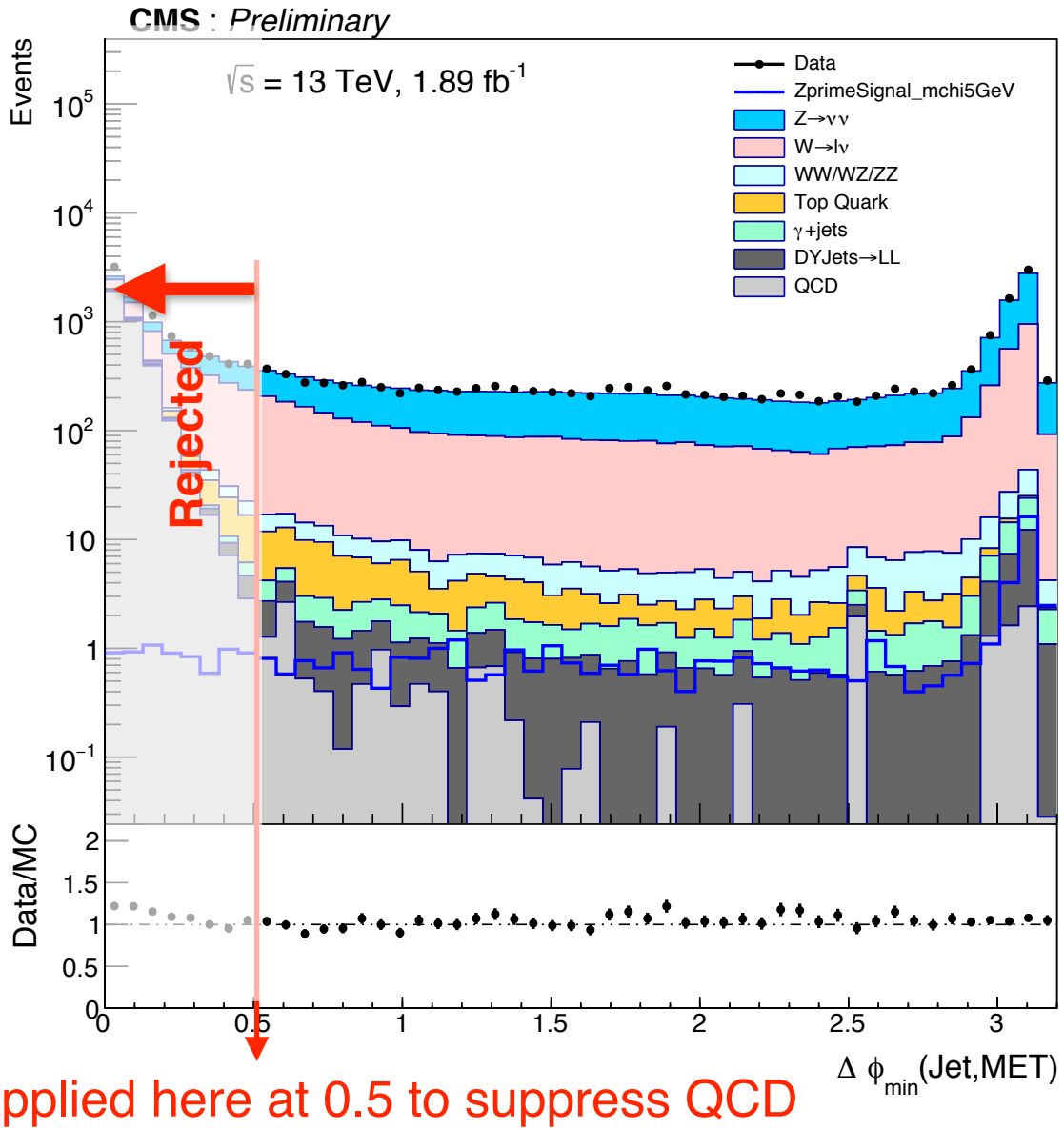

Cut applied here at 0.5 to suppress QCD

Delta Phi Cut

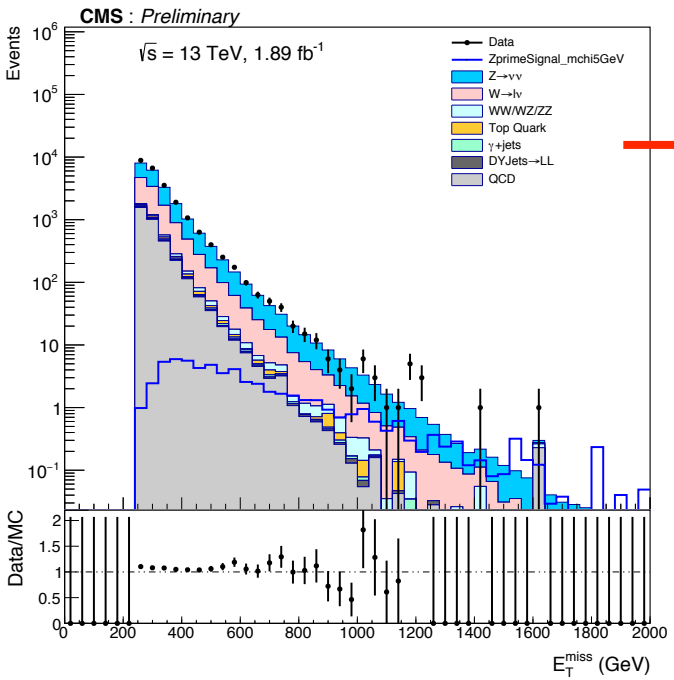

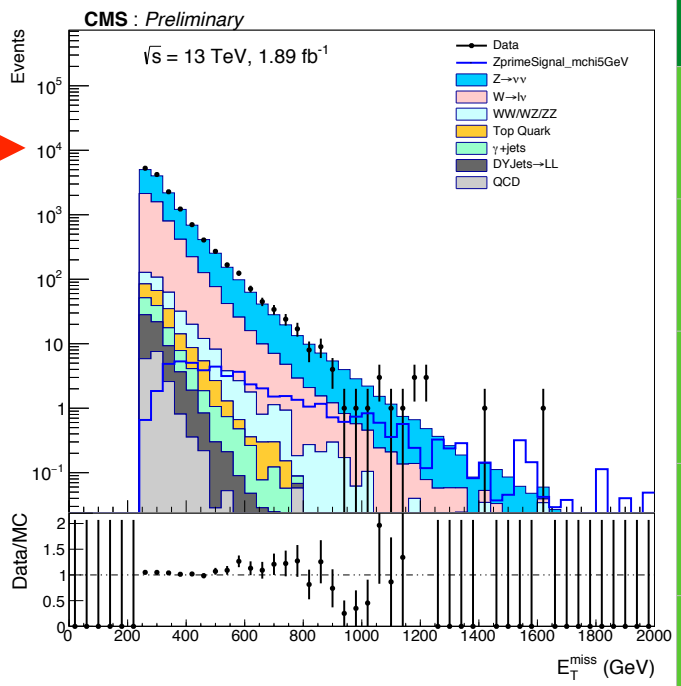

	Before Cut	After Cut
Data	23882	14874
W+Jets	7688	5093
Z+Jets	10064	8758
QCD	3523	17.6
Signal	57.5	50.9
S/√B	0.38	0.43

As expected, this cut gets rid of essentially all of the QCD background and it also reduces the W+ Jets background significantly making Z+Jets as the dominant irreducible background in this analysis.

Analysis Strategy

- First, identified our signal using the “Jet η width” variable as shown in the next few slides

Pencil Jet η width Cut

- Compute energy weighted η width by looping over all Particle Flow Constituents of the jet
- η Width = $$\sqrt{\frac{\sum(\eta_i^2 E_i)}{\sum E_i} - \left(\frac{\sum(\eta_i E_i)}{\sum E_i}\right)^2}$$
- Leading Jet η Width < 0.04

Expected Counts

	Before Cut	After Cut
Signal	50.9	40
Z+Jets	8758	1080
W + Jets	5093	639

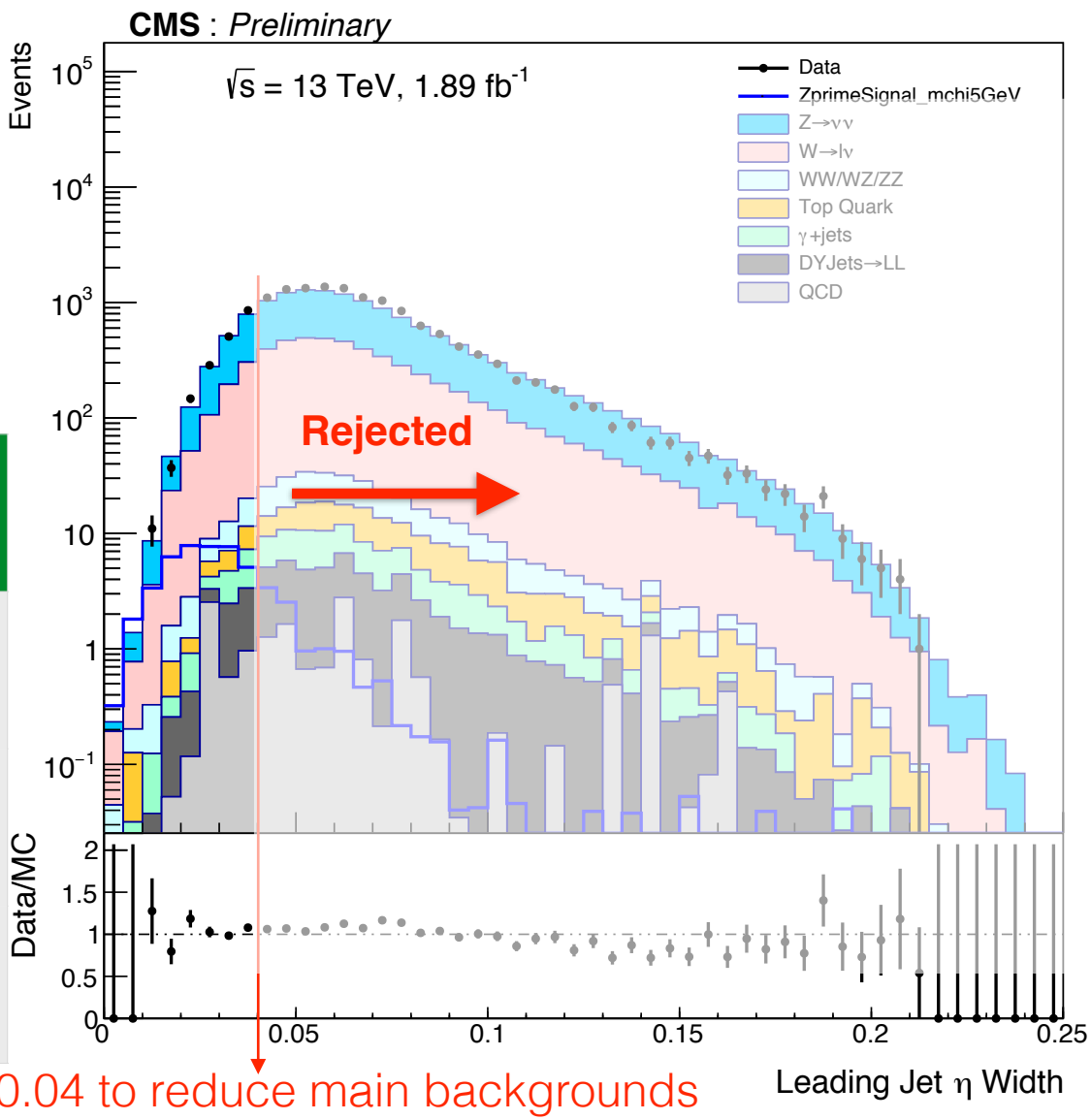

Cut applied here at 0.04 to reduce main backgrounds

Expected Counts

	Baseline Selection Cuts	Baseline + Leading Jet η Width Cut
Data (1.89 fb^{-1})	14,874	1842
Signal	**50.9**	**40**
Z⟶νν	8758	1080
W ⟶ lν	5093	639
Top Quark	95.7	9
QCD	17.6	4.3
γ+Jets	58.5	7.8
WZ/WW/ZZ	161.8	20
DYJets⟶ LL	49	5.5
Total Background	**14,234**	**1766**
Data/MC	1.04	1.04
S/√B	**0.43**	**0.95**

Results: Leading Jet P_T

Before Leading Jet η Width Cut

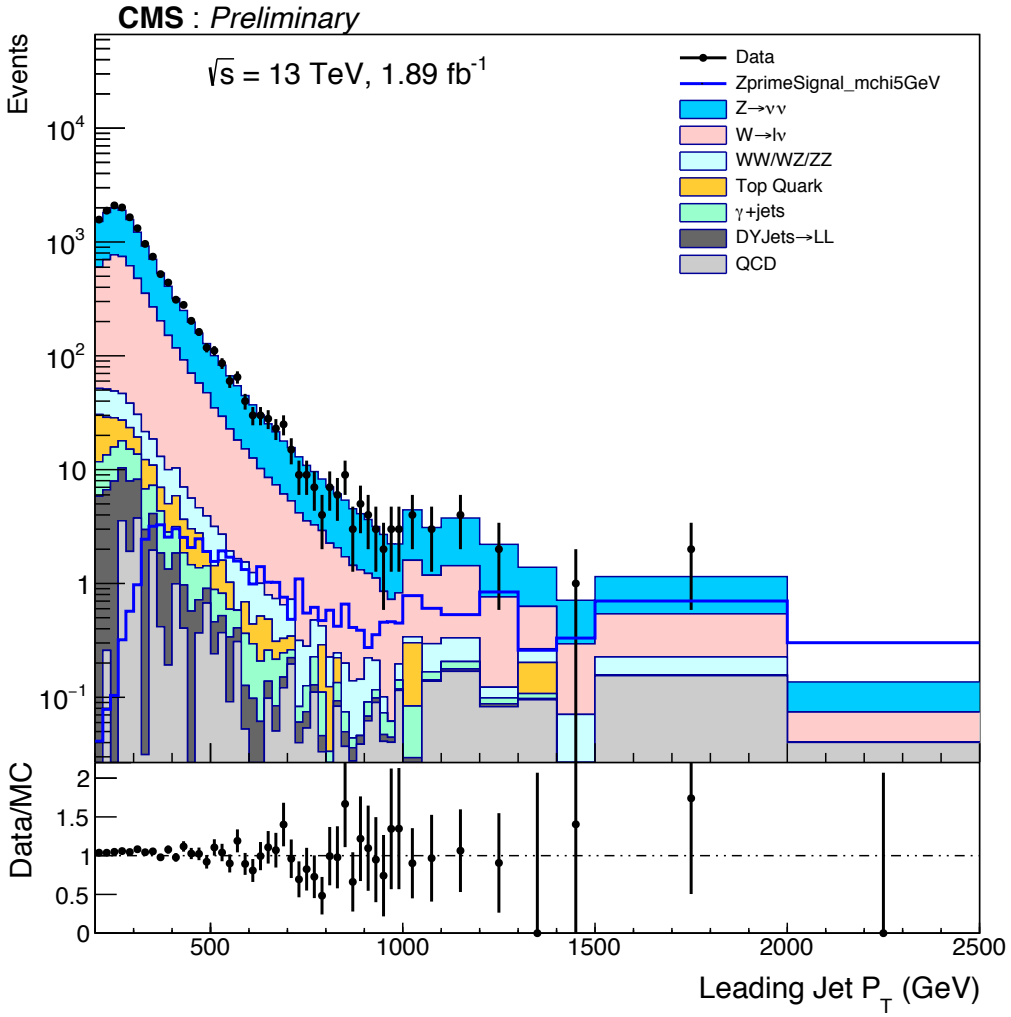

After Leading Jet η Width Cut

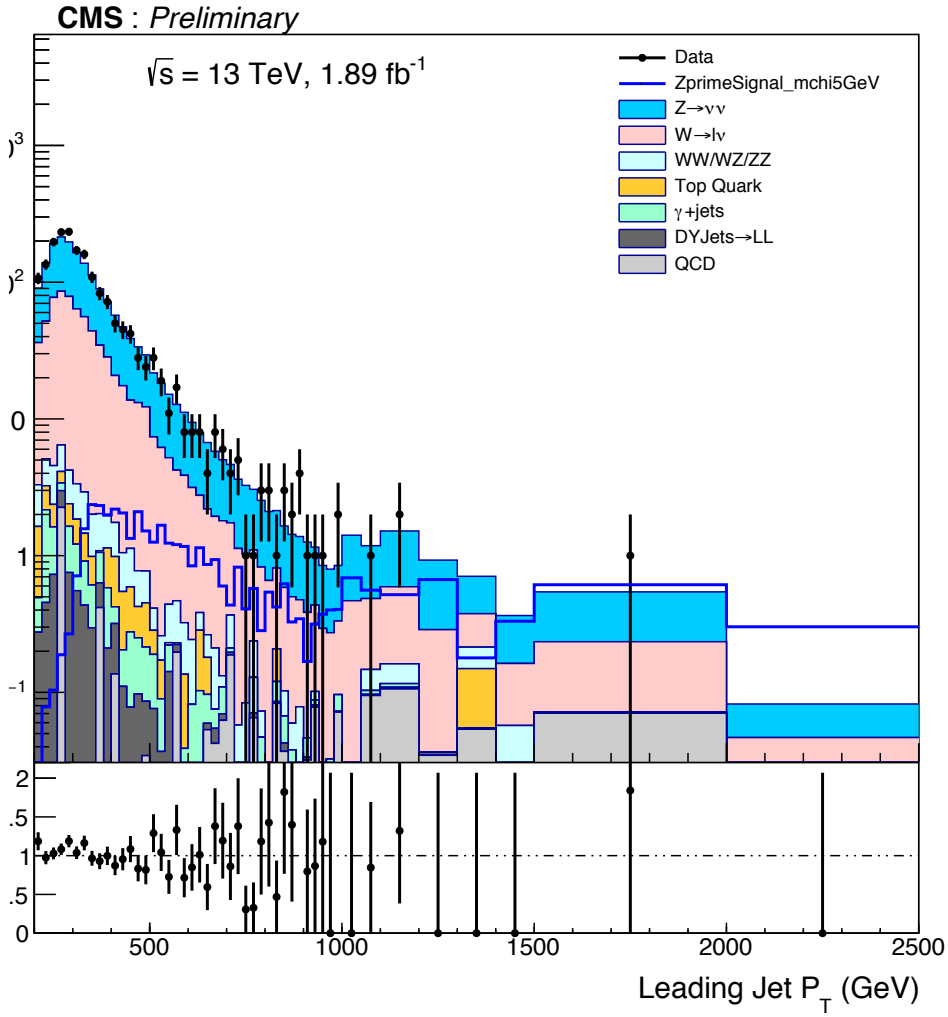

Analysis Strategy

- First, identified our signal using the “Jet η width” variable as shown in the last few slides
- Now, I will show some more techniques for signal extraction
  - Basically, we split up our signal region into **<u>Three Categories</u>** and present results in each category separately.
    - **Category 1**: $\pi^+ \pi^-$
    - **Category 2**: $\pi^+ \pi^-$ + 1 boosted π^0 (Photon)
    - **Category 3**: Remaining Events < 2 Charged Hadrons

Category 1: $\pi^+ \pi^-$

(24.1 % of the Signal)

P_T Fraction carried by π^+ π^- in the Leading Jet

- We sum the P_T of the two leading oppositely charged hadron constituents of the Leading Jet and calculate the fraction with respect to the overall jet transverse momentum.
- P_T^{12} Fraction = $(P_T^1 + P_T^2)/j1PT$
- P_T^{12} Fraction > 0.7

Expected Counts

	Before Cut	After Cut
Signal	13.6	12.8
Z+Jets	1595	98
W + Jets	934	57.7

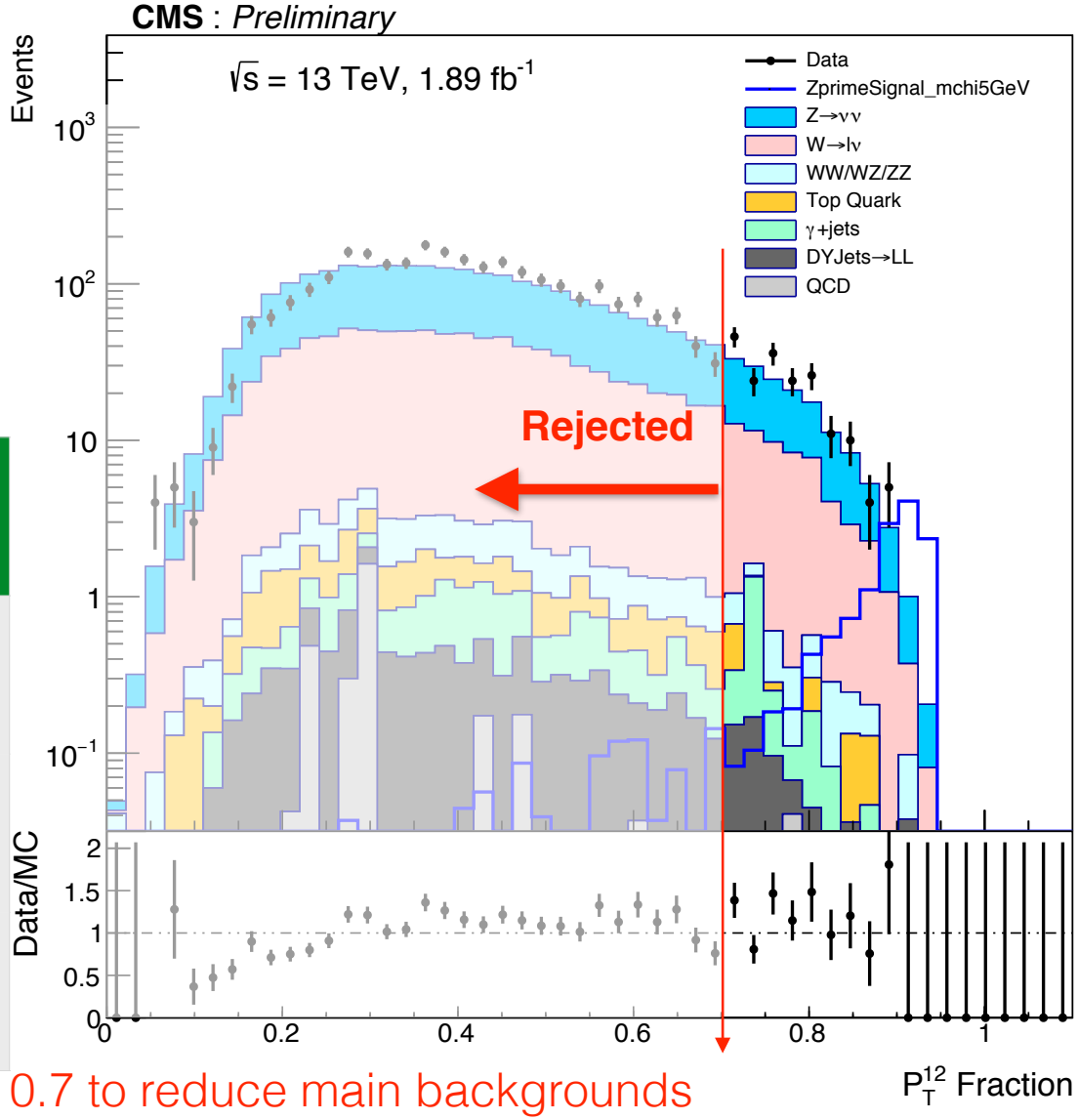

Cut applied here at 0.7 to reduce main backgrounds

Expected Counts

	Baseline Selection Cuts	Baseline + $P_T PF^{12}$ Frac > 0.7
Data (1.89 fb^{-1})	2802	189
Signal	**13.6**	**12.8**
Z ⟶ νν	1595	98
W ⟶ lν	934	57.7
Top Quark	16.5	0.68
QCD	3.0	0.07
γ+Jets	12.3	1.8
WZ/WW/ZZ	28.3	2.1
DYJets ⟶ LL	9	0.6
Total Background	**2598**	**161**
Data/MC	1.08	1.17
S/√B	**0.27**	**1.01**

Results: Leading Jet P_T

Before P_T^{12} Fraction Cut

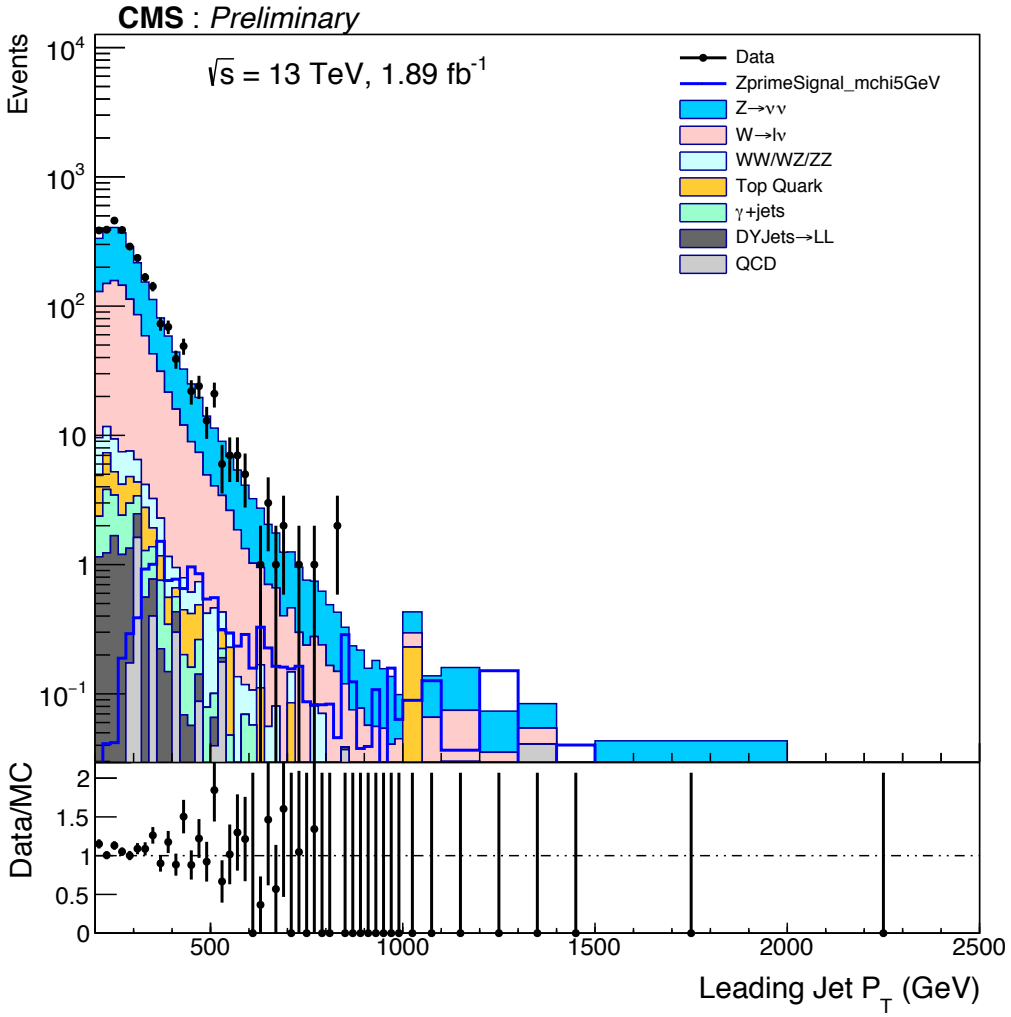

After P_T^{12} Fraction Cut

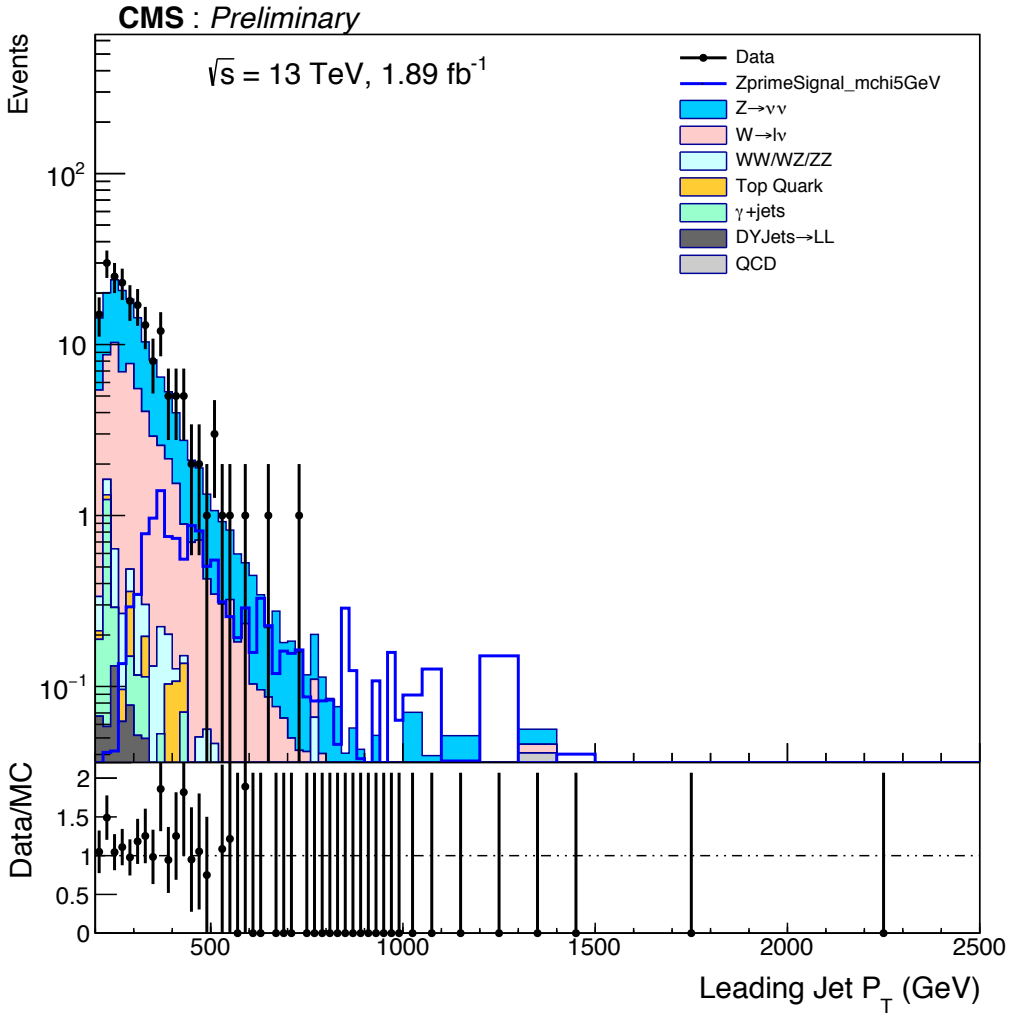

Category 2: $\pi^+ \pi^-$ + 1 boosted π^0 (Photon)

(30.4% of the Signal)

P_T Fraction carried by $\pi^+ \pi^- + \gamma$ in the Leading Jet

- We sum the P_T of the two leading oppositely charged hadron constituents and the high P_T photon in the Leading Jet and calculate the fraction with respect to the overall jet transverse momentum.
- P_T^{123} Fraction = $(P_T^1 + P_T^2 + P_T^3)/j1PT$
- P_T^{123} Fraction > 0.7

Expected Counts

	Before Cut	After Cut
Signal	16.5	16.0
Z+Jets	2879	652
W + Jets	1678	381.5

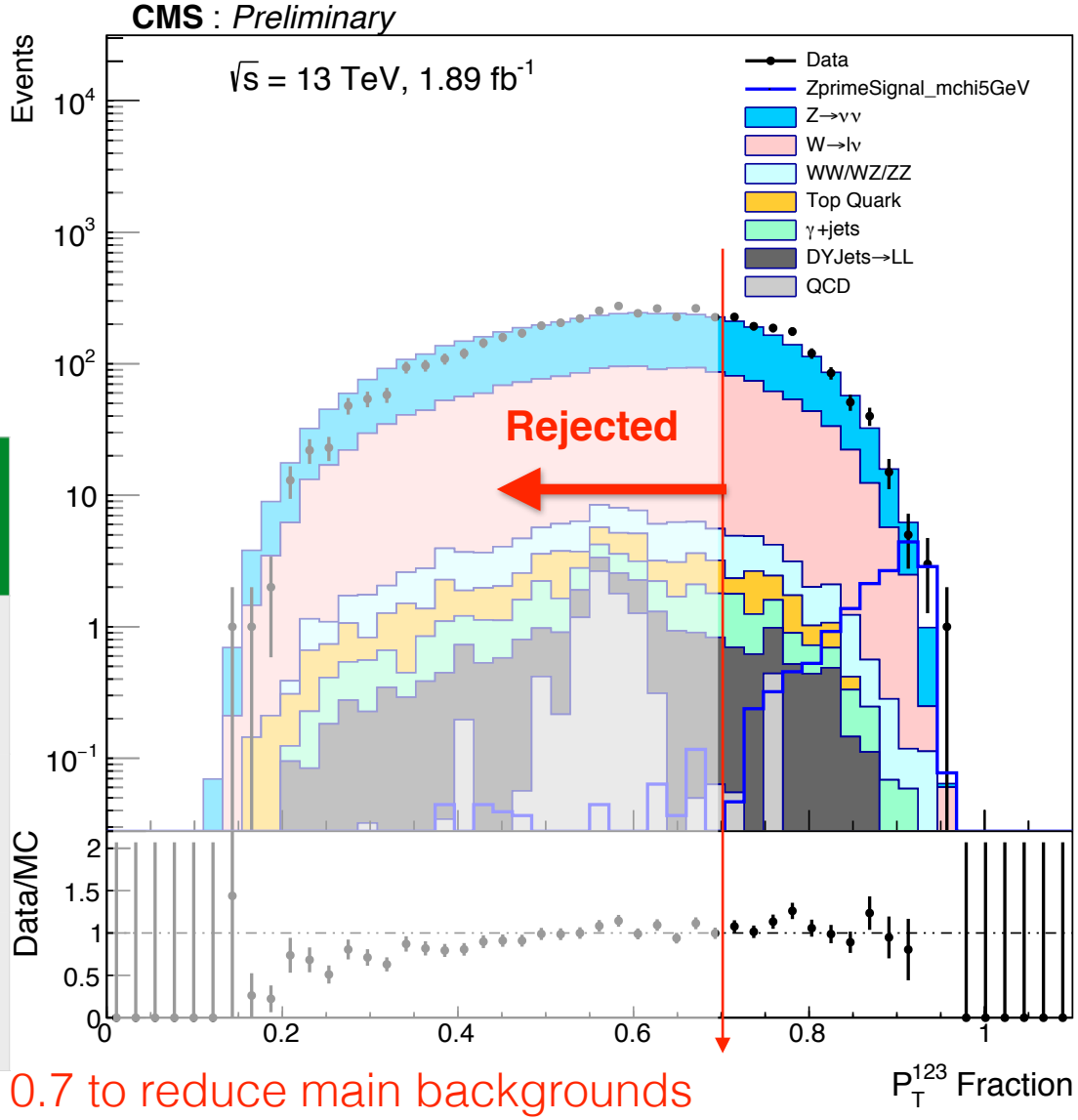

Cut applied here at 0.7 to reduce main backgrounds

Expected Counts

	Baseline Selection Cuts	Baseline + $P_T PF^{123}$ Frac > 0.7
Data (1.89 fb^{-1})	4590	1145
Signal	**16.5**	**16.0**
$Z \longrightarrow \nu\nu$	2879	652
$W \longrightarrow l\nu$	1678	381.5
Top Quark	7	4.6
QCD	8.8	0.5
γ+Jets	18.1	3.8
WZ/WW/ZZ	52.7	12.0
DYJets $\longrightarrow$ LL	16.1	3.6
Total Background	**4660**	**1058**
Data/MC	0.98	1.08
$S/\sqrt{B}$	**0.24**	**0.49**

Results: Leading Jet P_T

Before P_T^{123} Fraction Cut

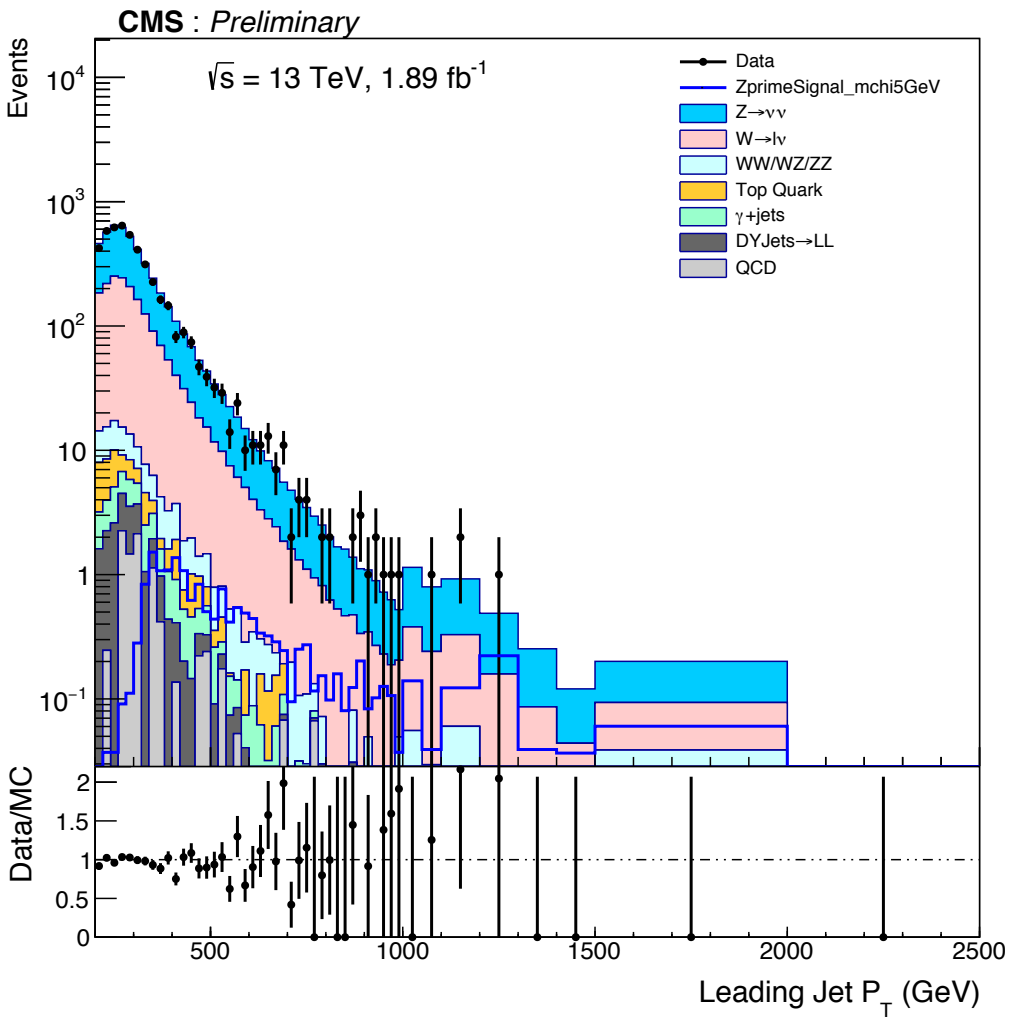

After P_T^{123} Fraction Cut

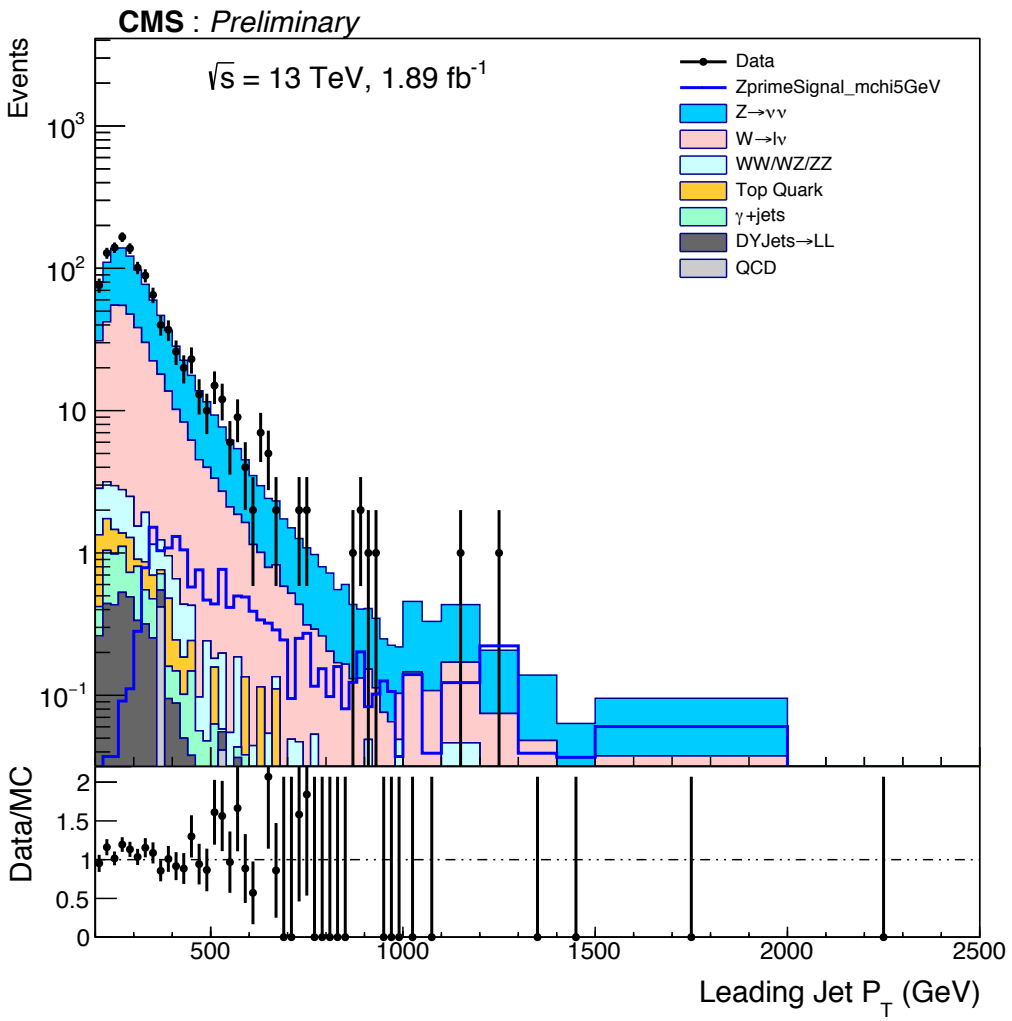

Category 3: Remaining Events < 2 Charged Hadrons

(45.5% of the Signal)

Pencil Jet η width Cut

- Compute energy weighted η width by looping over all Particle Flow Constituents of the jet
- η Width = $$\sqrt{\frac{\sum(\eta_i^2 E_i)}{\sum E_i} - \left(\frac{\sum(\eta_i E_i)}{\sum E_i}\right)^2}$$
- Leading Jet η Width < 0.04

Expected Counts

	Before Cut	After Cut
Signal	20.8	16.0
Z+Jets	4283	490.8
W + Jets	2481	298.5

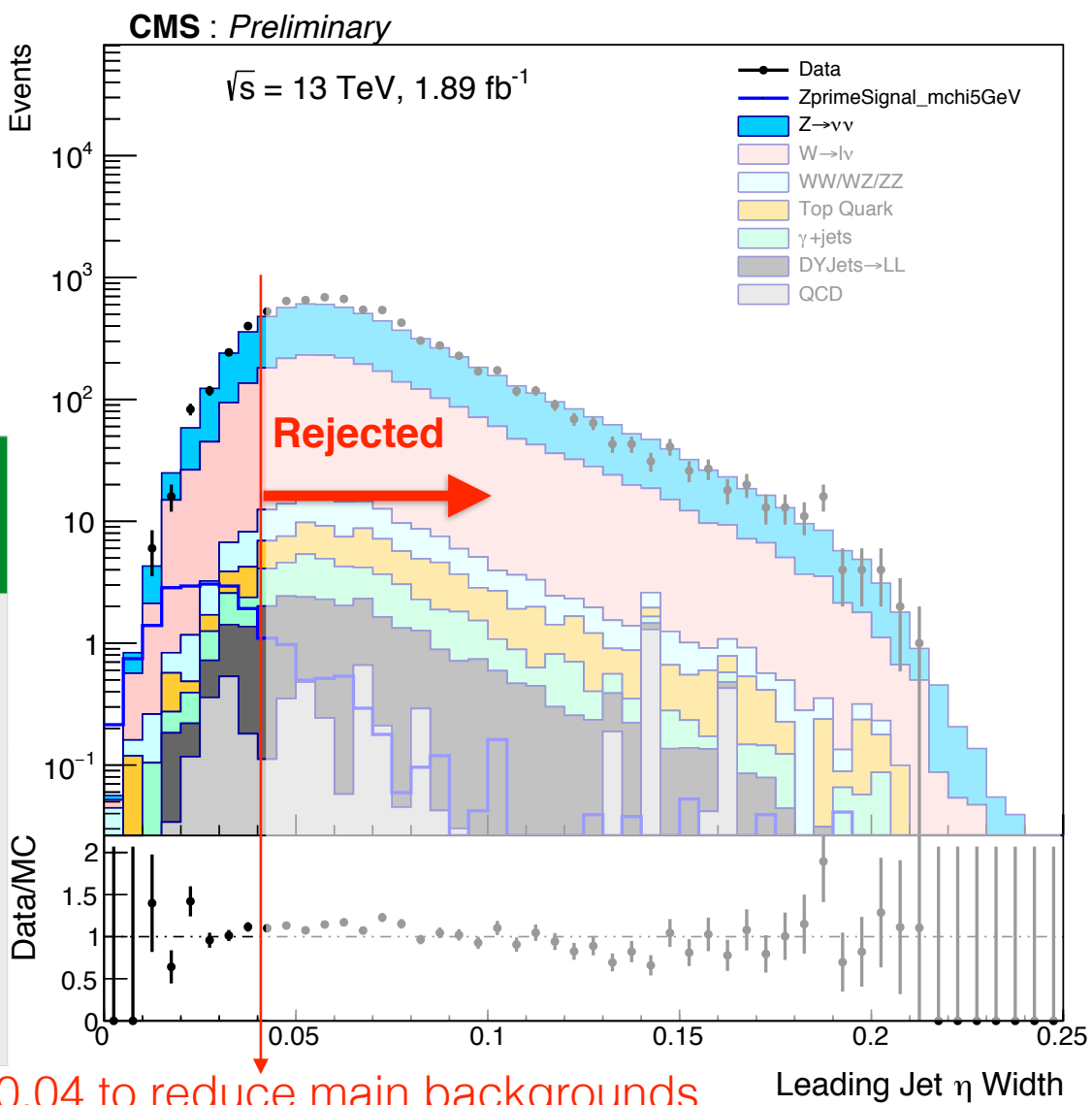

Cut applied here at 0.04 to reduce main backgrounds

Expected Counts

	Baseline Selection Cuts	Baseline + Leading Jet η Width Cut
Data (1.89 fb^{-1})	7482	866
Signal	**20.8**	**16.0**
Z → νν	4283	490.8
W → lν	2481	298.5
Top Quark	51.2	4.1
QCD	5.8	1.2
γ+Jets	28.2	3.1
WZ/WW/ZZ	80.7	9.5
DYJets → LL	23.8	2.7
Total Background	**6954**	**810**
Data/MC	1.08	1.07
S/√B	**0.25**	**0.56**

Results: Leading Jet P_T

Before Leading Jet η Width Cut

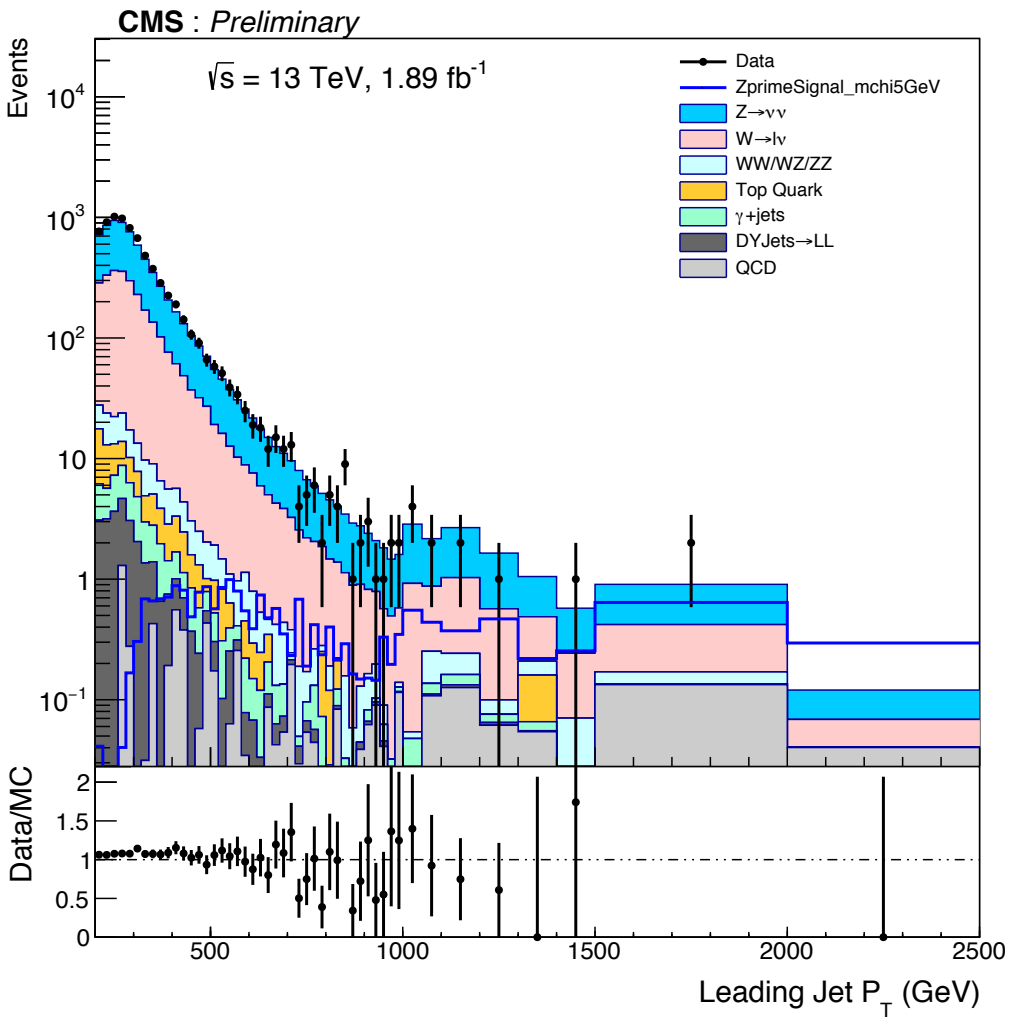

After Leading Jet η Width Cut

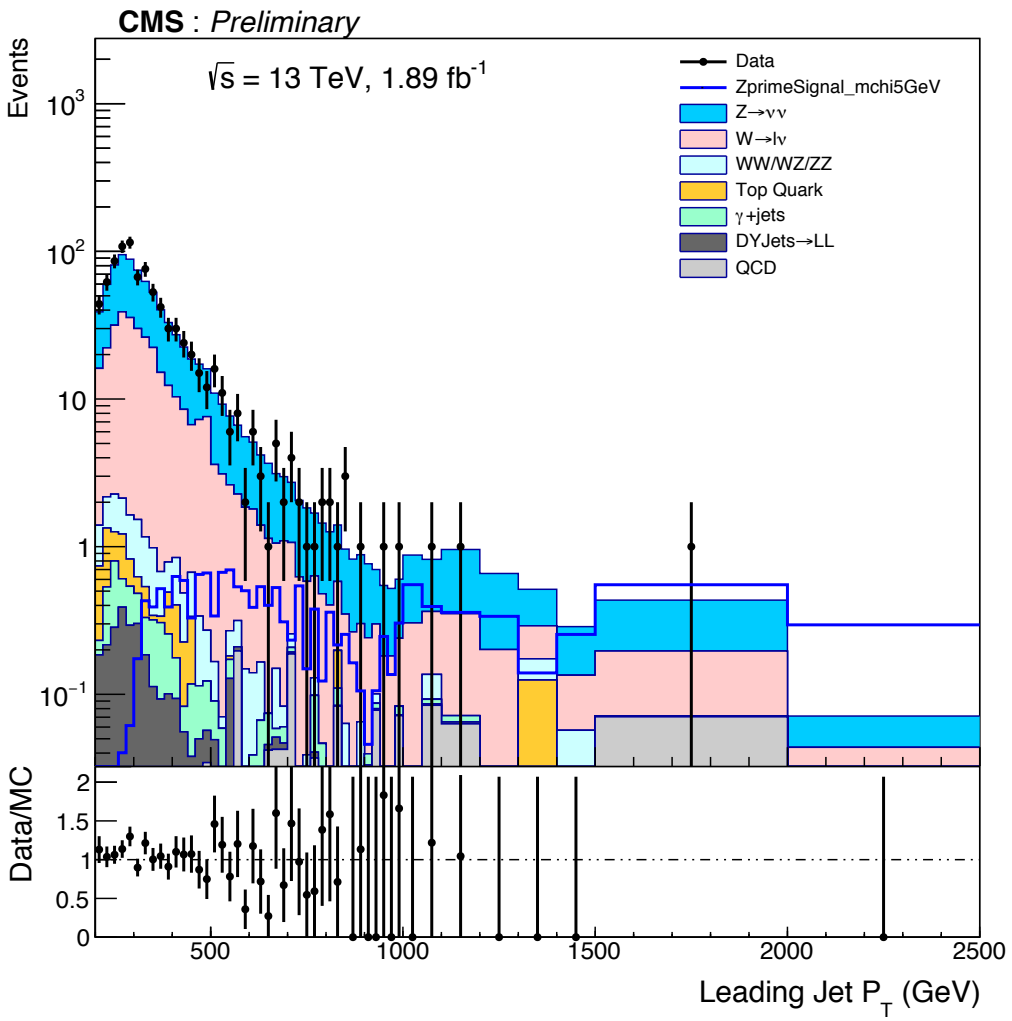

Limit Descriptions

- Limits are computed using Cut and Count Approach
- Following Systematics are considered
  - Luminosity: 6%
  - EWK Uncertainty for Z+Jets and W+Jets
    - Following Monojet procedure (Full correction applied for nominal estimate)
  - MET energy scale : 5%
  - B-jet veto : 2%
  - Trigger : 1%

NoCategories vs 3 Categories Expected Limits

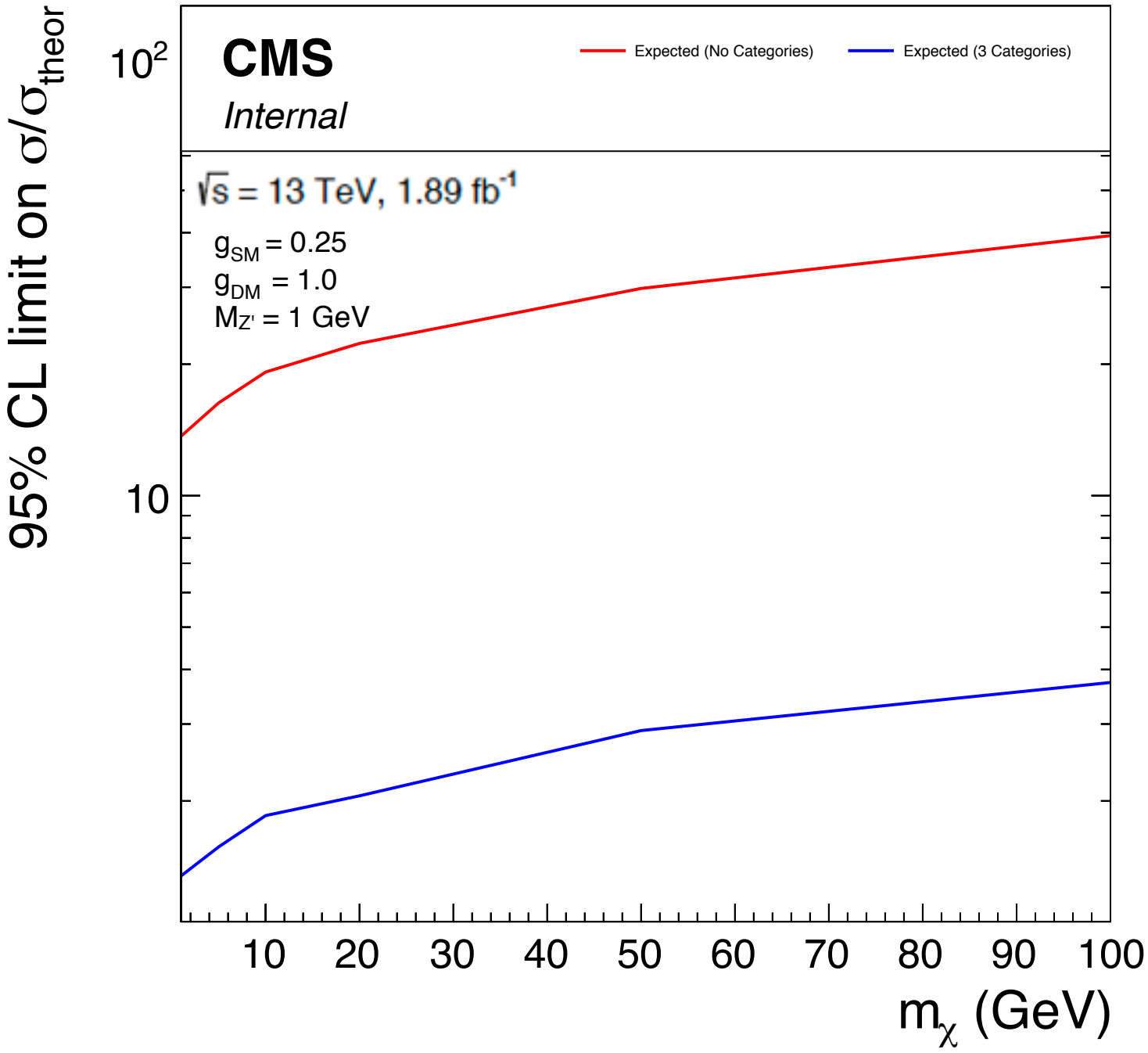

Summary & Outlook

- Summary:
  - Studied the Mono-Z' model with 1.89 fb^{-1} of p-p collisions data using the PencilJet analysis.
  - No significant excess above the SM prediction is observed
- Ongoing:
  - Extension of analysis to full 2016 + 2017 dataset (36 + 41 fb^{-1})
  - Make an effective comparison with results from Direct Detection Searches.
- Outlook:
  - Transition from “cut-and-count” to shape-based approach.
  - Data-driven approach to Z + Jets and W + Jets background estimates
  - Thesis work with ~ 150 fb^{-1} data

Backup Slides

Signal Efficiency

$$Signal\ Efficiency = \frac{events\ passing\ selection}{Total\ no.\ of\ events}$$

m_X [GeV]	σ [pb]	Signal Efficiency Baseline Selection Cuts	Signal Efficiency After Leading Jet η Width Cut
1	0.056	0.547	0.434
5	0.047	0.565	0.452
10	0.040	0.564	0.455
20	0.034	0.575	0.459
50	0.025	0.572	0.463
100	0.019	0.579	0.469

Limits: Mono-Z' EFT Model

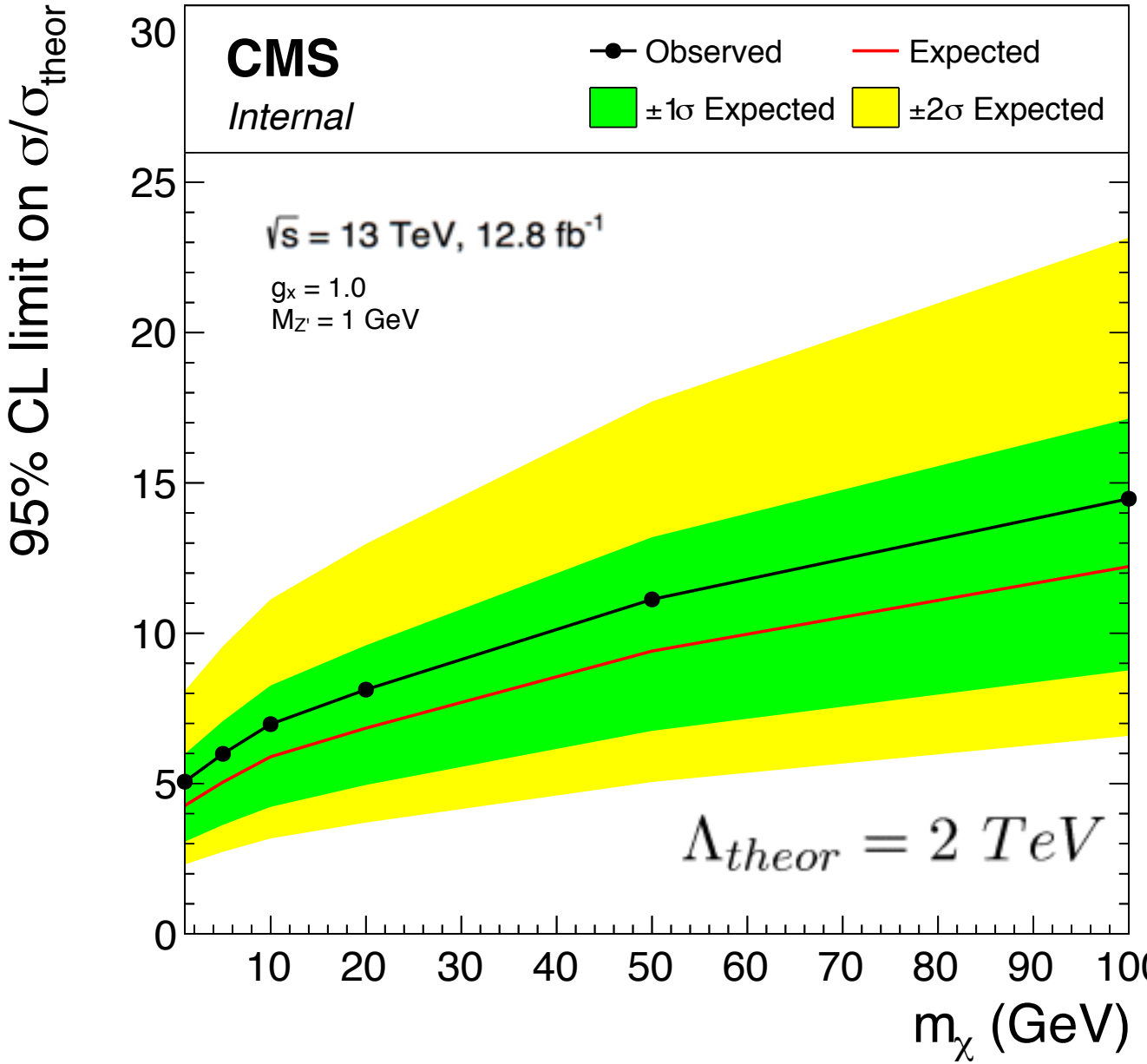

- Upper limit on signal production cross section as a function of dark matter mass

Limits on Interaction Scale Λ

- Excluded Λ up to 1.3 TeV for dark matter masses ~1 GeV

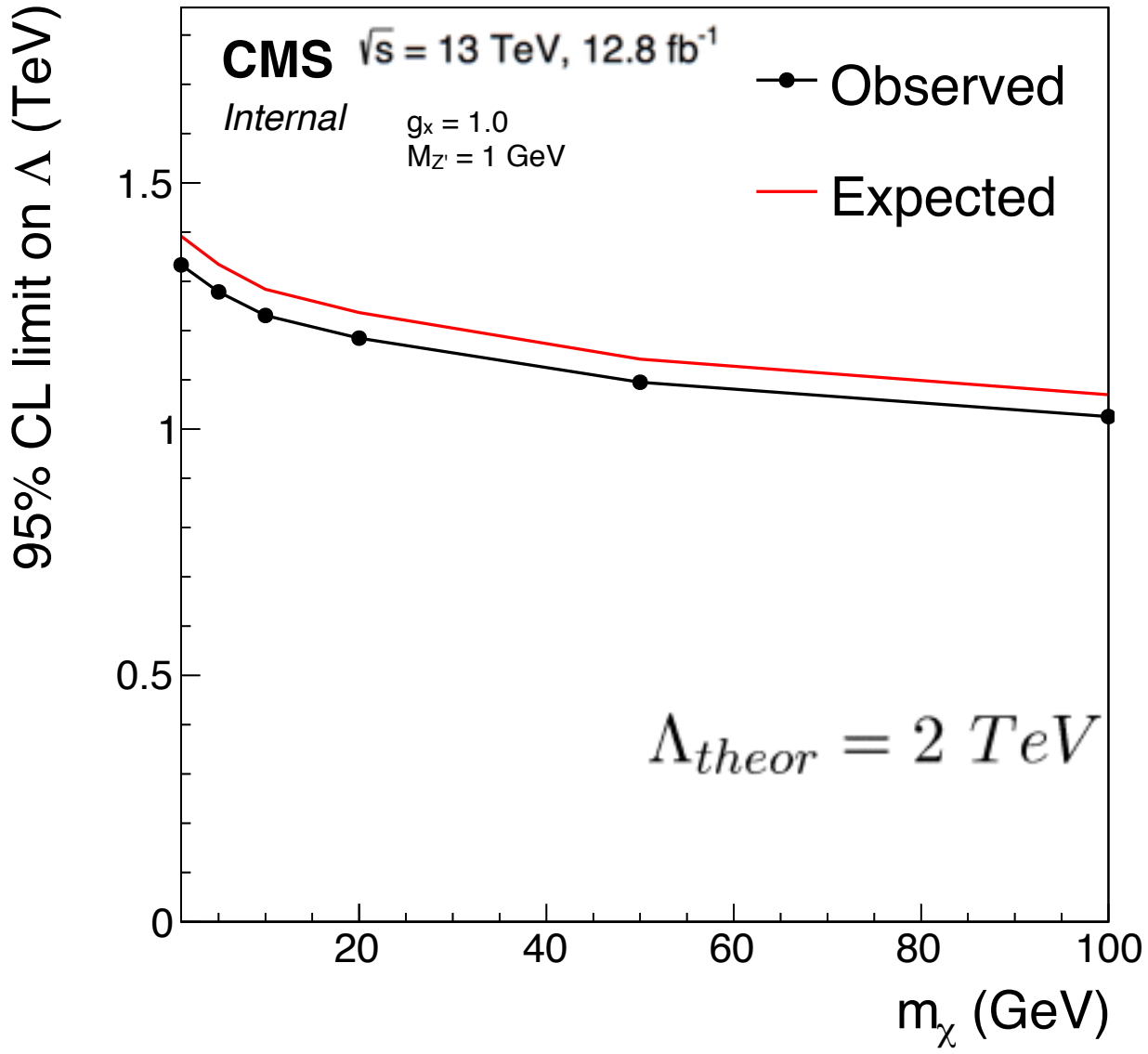

Bai et.al

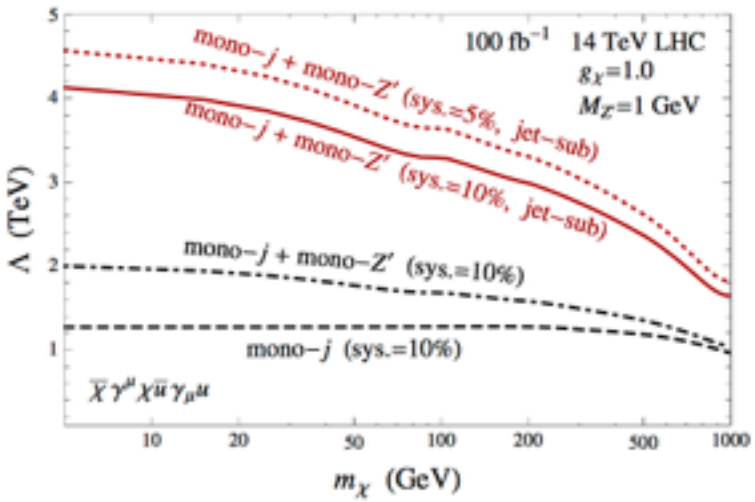

$$\Lambda = \Lambda_{theor} * \left(\frac{\sigma_{theor}}{\sigma}\right)^{1/4} TeV$$

- No previous experimental results with Mono-Z' FSR model
- Both ATLAS and CMS have results from ISR searches for dark matter
- Results are dependent on coupling values and choice of models.

Mon-Z' cross-section limit expectations

Spin-Independent **Spin-Dependent**

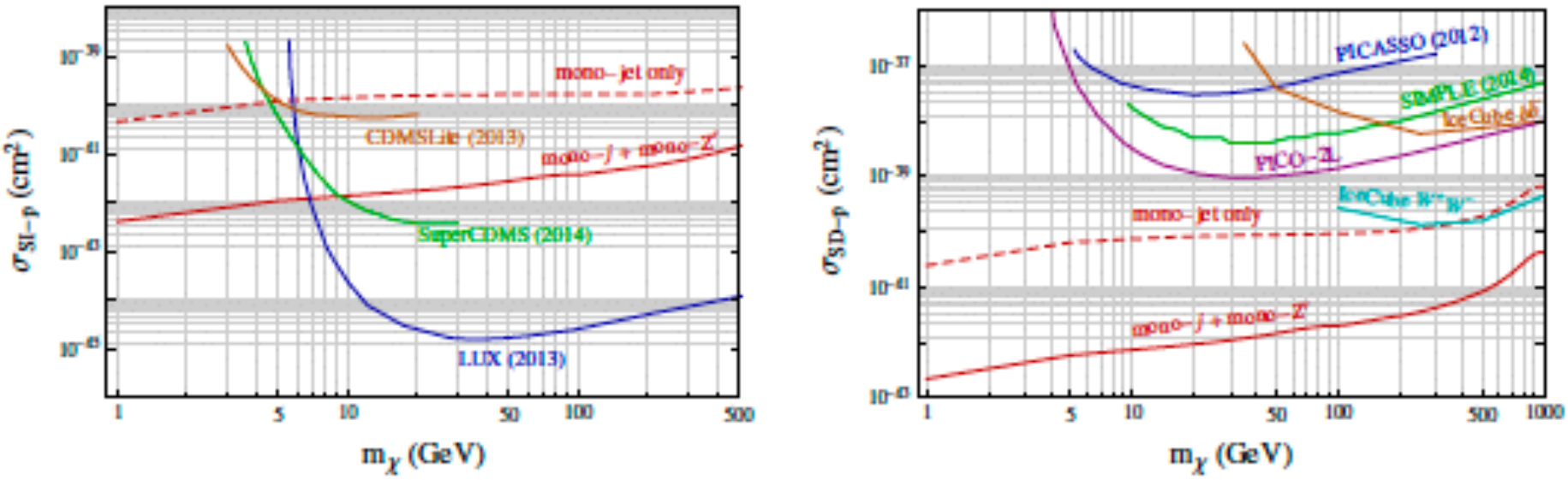

Figure 7: Left panel: projected constraints on dark matter-proton spin-independent scattering cross sections from the standard mono-jet analysis at the 14 TeV LHC with 100 fb^{-1} and the mono-Z' jet-substructure based analysis. The model parameters are $M_{Z'} = 1$ GeV and $g_\chi = 1.0$, and we take the limits on Λ assuming 10% systematic error. Also shown are the current constraints from direct detection experiments: LUX [69], SuperCDMS [70] and CDMSLite [71]. Right panel: similar to the left panel but for dark matter-proton spin-dependent scattering cross sections. The current experimental bounds are from: PICASSO [72], SIMPLE [73], PICO-2L [74] and IceCube [75].

source: arXiv:1504.01395v2

Signal Efficiency

Table 4.1: LHC design beam conditions and conditions in operation between 2010 and 2016.

Year	2010	2011	2012	2015	2016	2017	Design
Center of Mass Energy (TeV)	7	7	8	13	13		14
Energy per Beam (TeV)	3.5	3.5	4	6.5	6.5		7
Proton bunch spacing (ns)	150	50	50	50/25	25		25
N_b ($\times 10^{11}$)	1.2	1.5	1.7	1.15	1.25	1.25	1.15
n_b	348	1331	1368	2232	2208		2808
β^*	3.5	1.0	0.6	0.8	0.4	0.33	0.55
ϵ_n	2.2	2.3	2.5	3.5	3.0	2.3	3.75
Peak Instantaneous $\mathcal{L}$ 10^{34}	0.02	0.35	0.77	0.52	1.53 (above design)		1
Total Integrated $\mathcal{L}$ (fb^{-1})	0.04	6.1	23.3	4.2	41.1	1.9	-

Courtesy: L.Dodd

$L \sim f \cdot N_2 / (4\ \varepsilon \cdot \beta^*)$

Particle-Flow event Reconstruction

- To understand the basic principles of the particle-flow event reconstruction, an event display of a very simple hadronic jet with four particles (π+, π–, π0, K0L) and a pT of 65 GeV/c

- The K0L, the π– and the two photons from the π0 decay are detected as four well separated ECAL clusters (b). The π+ leaves no energy in the ECAL. The two charged pions are reconstructed as charged-particle tracks, appearing as vertical solid lines in the (η, ϕ) views and circular arcs in the (x, y) view. These tracks point towards two HCAL clusters (c). In all three views, the cluster positions are represented by dots, the simulated particles by dashed lines, and the position of their impact on the calorimeter surfaces by various open markers.

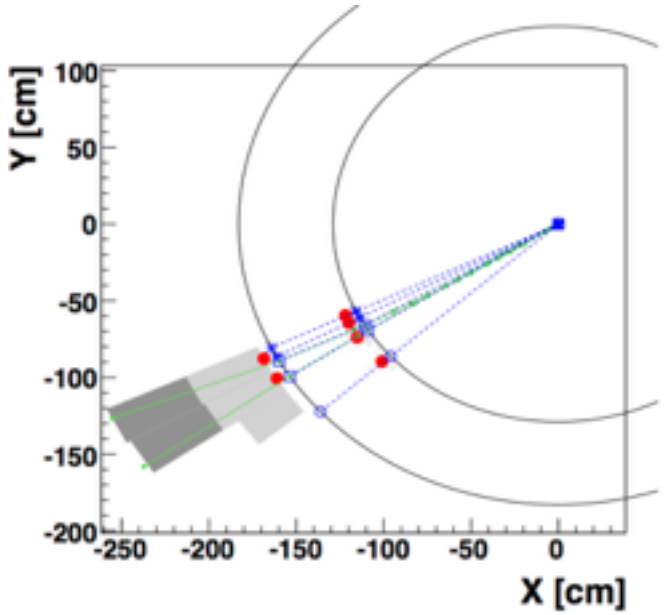

(a) The (x, y) view

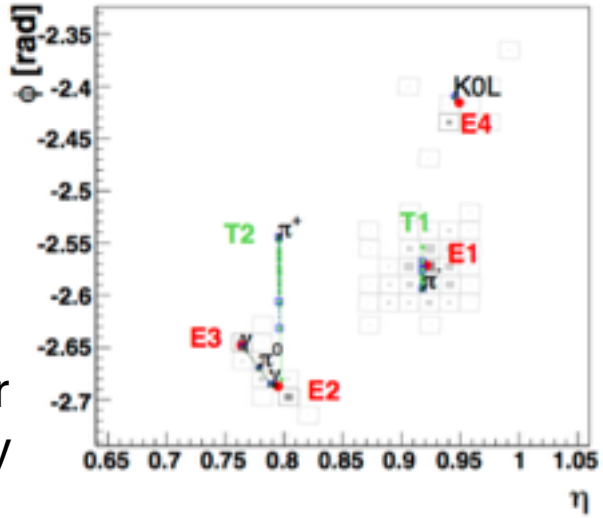

(b) The (η, φ) view on ECAL

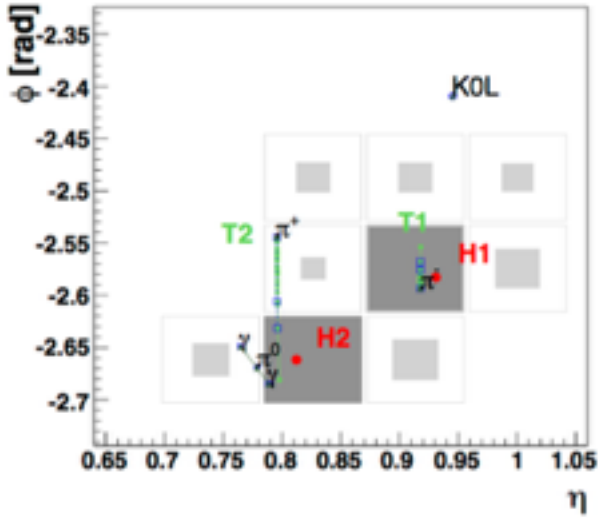

(c) The (η, φ) view on HCAL

Muon Reconstruction

Categories of reconstructed muons:

- **Tracker muons -** inner tracks matched with at least one segment in the muon system
  - High efficiency for low p_T muons
- **Standalone muons -** tracks from segments and hits in muon systems
- **Global muons -** match standalone muon tracks with silicon tracks

In the Mono-Z' analysis:

- Z' specifically decays to hadrons so lepton channel not being considered
- Muon Veto ensures muons ($p_T > 10$ GeV) do not overlap with Jet

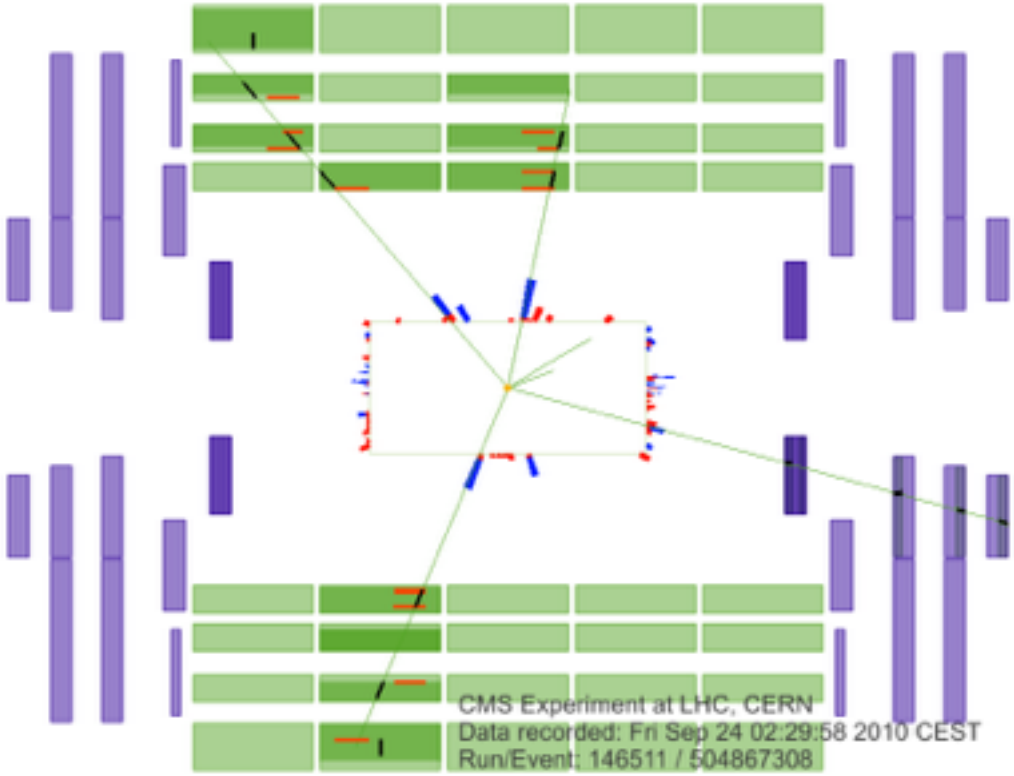

The longitudinal (r-z) view of a collision event in which four muons were reconstructed.

Electron Reconstruction

- Electron candidates identified by a combination of detectors
  - ECAL superclusters
  - Gaussian Sum Filter (GSF) track reconstruction

Electron candidates are found when a supercluster can be associated to a track reconstructed in the silicon tracker detector, and in particular its innermost layers.

- Track must be close to primary interaction vertex
- ECal supercluster includes elongated area in ϕ to contain bremsstrahlung photons radiated from electron

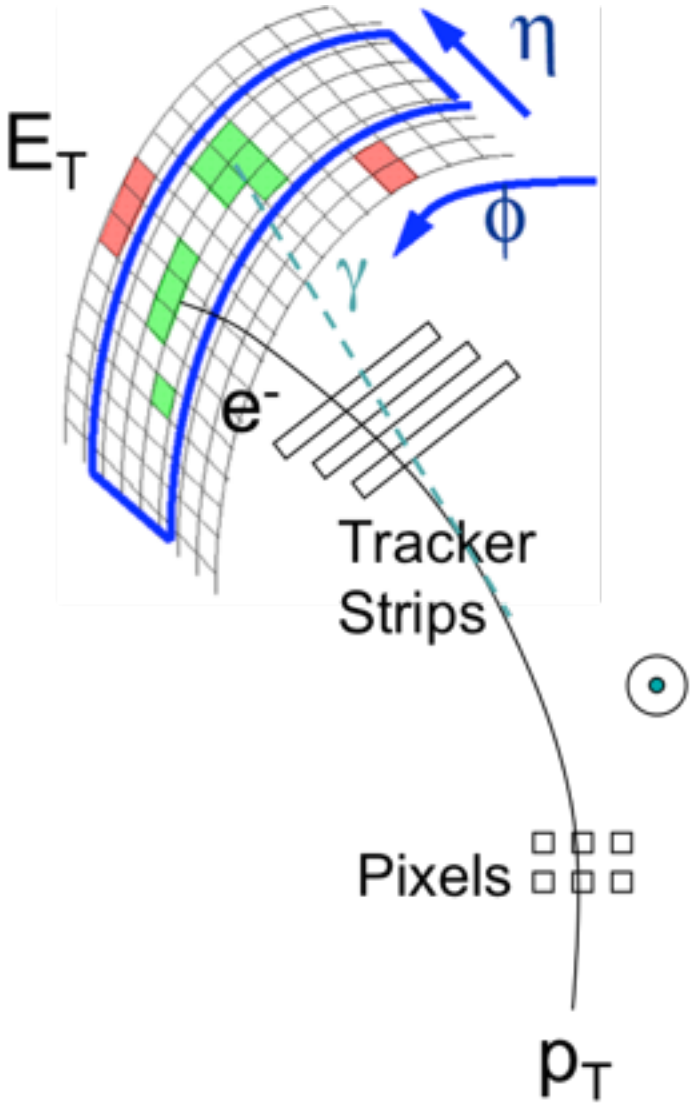

In the Mono-Z' analysis:

- Z' specifically decays to hadrons so lepton channel not being considered
- Electron Veto ensures electrons ($p_T > 10$ GeV) do not overlap with Jet

Dark Matter: Previous Results

- 95% CL exclusion regions in M_{med} – m_{DM} plane for di-jet searches and different E_T^{miss} based DM searches from CMS in the lepto-phobic Axial Vector model.
- Limits: **M_{med} ~ 2 TeV, m_{DM} ~ 600 GeV** Mono-jet most stringent - all channels contribute to interpretation

Source: CMS DP -2016/057

Summary of ISR searches

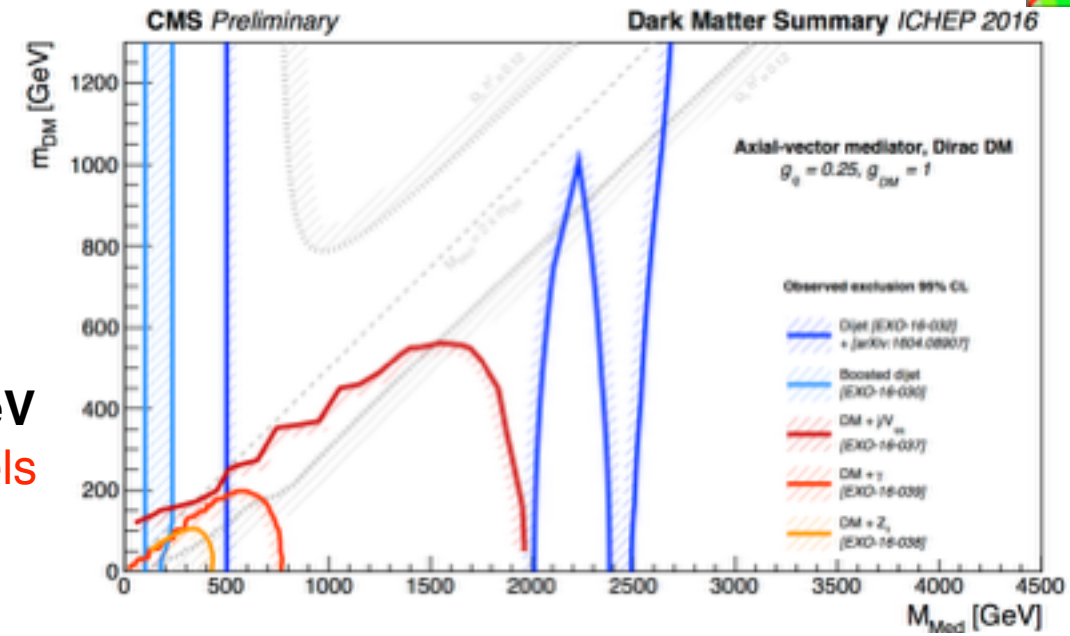

- A summary of ATLAS limits on the lepto-phobic axial vector mediators coupling to DM, with variable mediator and DM masses, from both the leading E_T^{miss}+X analyses and dark mediator searches.
- Limits: **M_{med} ~ 1 TeV, m_{DM} ~ 250 GeV**

Source: ATL-PHYS-PROC-2016-206

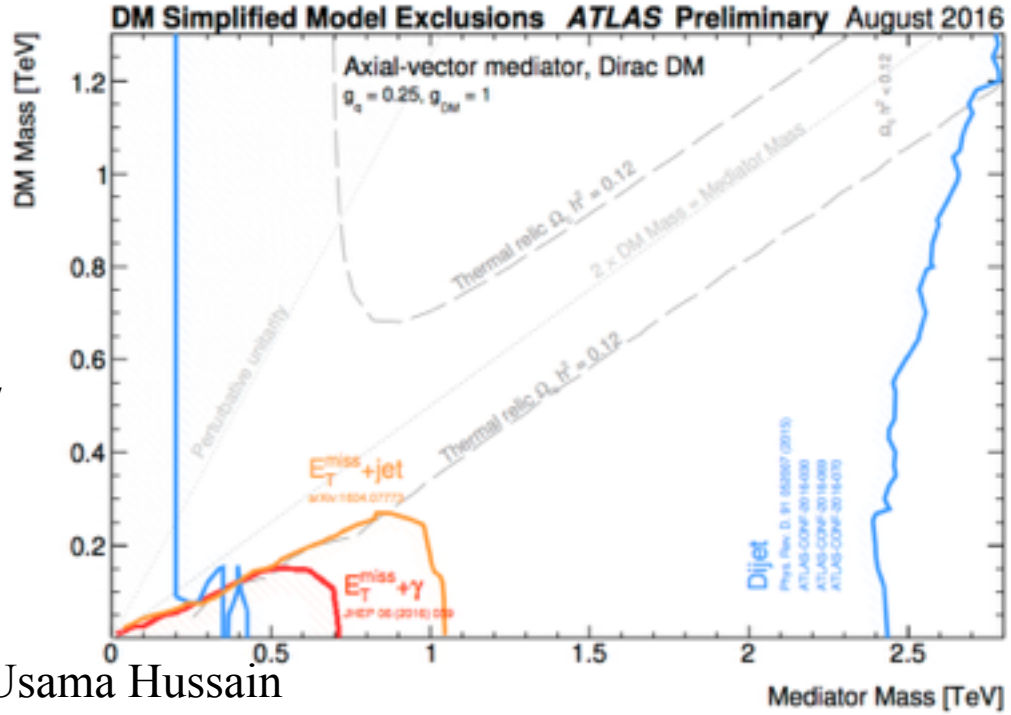

Dark Matter: CMS Results

- CMS searches for dark matter have been performed with various mono-X final states
  - 90% CL exclusion limits with 12.9 fb^{-1} of 2016 data from mono-jet/photon/Z
- Results were recast in terms of nucleon-DM scattering cross section for comparison to direct detection (DD) searches.
- No sign of excess yet
  - LHC especially competitive for **SD** (Pseudoscalar & Axial) and clearly better at low mass.
  - CMS results shown are dependent on coupling values and choice of models.

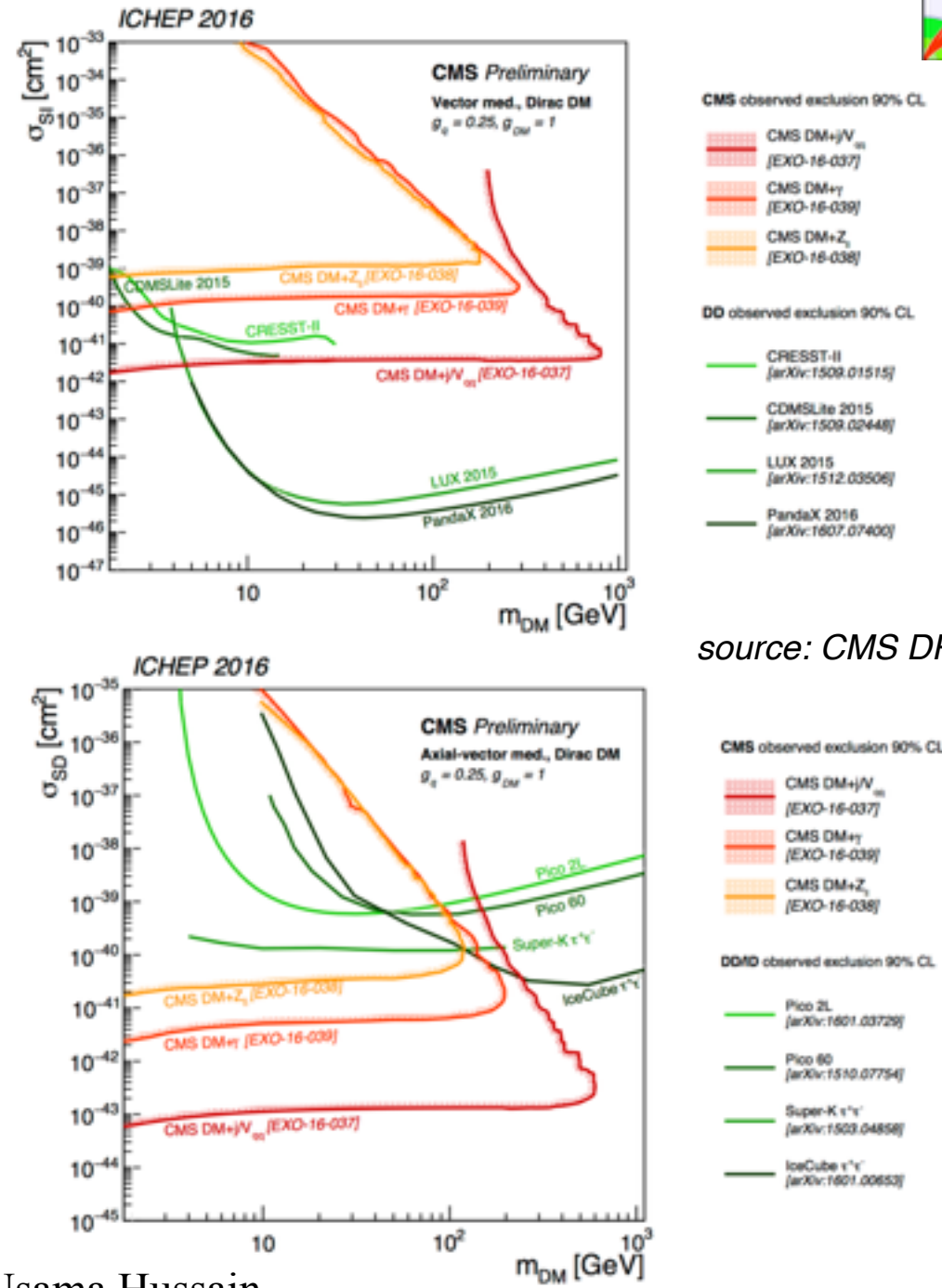

source: CMS DP -2016/057

Dark Matter EFT

- **Effective Field Theory (EFT)** with a contact interaction between DM and SM particles.
- EFT depends on two parameters:
  - DM mass: m_χ
  - Interaction scale: Λ
    - Cross section $\propto \Lambda^{-4}$
    - $\Lambda \approx \dfrac{M}{\sqrt{g_\chi g_q}}$ $\qquad \mu = \dfrac{m_\chi m_p}{m_\chi + m_p}$
    - Cross section $\propto \mu^2$ for both Spin-Independent (SI) and Spin-dependent (SD) cross-sections.
  - **Couplings:**
    - g_q : Mediator coupling to quarks
    - g_χ : Mediator coupling to dark matter

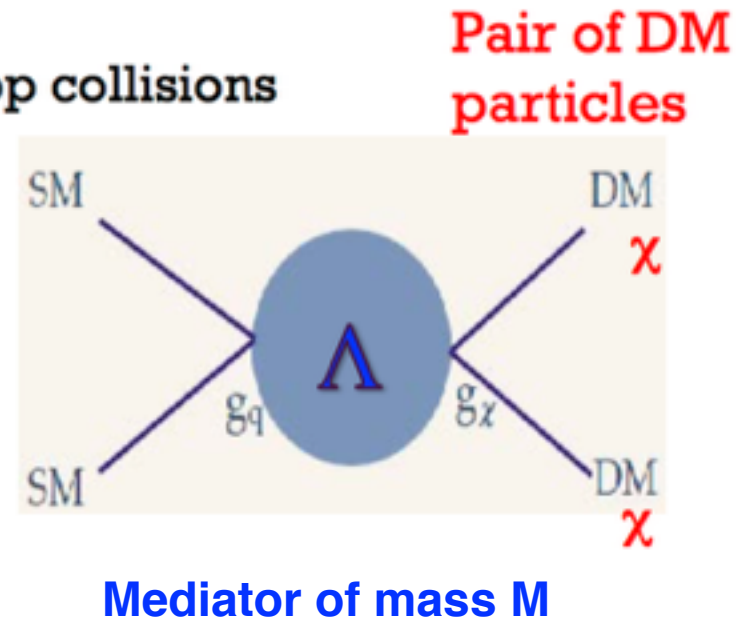

Direct and Indirect Detection Experiments

Direct detection: A number of experiments look for elastic scattering of ambient DM off target nuclei

- SuperCDMS: 10 kg Ge crystal
- CRESST-II: 5 kg $CaWO_4$ crystal
- LUX: 250 kg dual-phase Xe
- PandaX-II: 580 kg dual-phase Xe – PICO-2L: 2.9 kg liquid C_3F_8
- PICO-60: 36.8 kg liquid CF_3I

Indirect detection:

IceCube and Super-Kamiokande look for neutrinos produced by dark matter annihilating into $\tau^+\tau^-$, $b\bar{b}$, or W^+W^- in the sun

Dark Matter EFT

Pair production of χ can be characterized by a contact interaction with most prominent couplings

$$\sigma_{SI} = 9\frac{\mu^2}{\pi\Lambda^4}$$

$$\sigma_{SD} = 0.33\frac{\mu^2}{\pi\Lambda^4}$$

Two important couplings used by CMS are :

Vector coupling (V)

➡ Spin-independent (SI)

$$\mathcal{O}_V = \frac{(\bar{\chi}\gamma_\mu\chi)(\bar{q}\gamma^\mu q)}{\Lambda^2}$$

Axial-Vector coupling (AV)

➡ Spin-dependent (SD)

$$\mathcal{O}_{AV} = \frac{(\bar{\chi}\gamma_\mu\gamma_5\chi)(\bar{q}\gamma^\mu\gamma_5 q)}{\Lambda^2}$$

Source: DarkMatter_Seminar_SLAC.pdf (B.Gomber)

Type of PF Constituents of Leading Jet

- Signal Sample
  - m_chi = 5 GeV
- Sample of events
  - Total of 1205 events
  - Signal Efficiency = 1205/2133 = 0.565

PF Constituents of Leading Jet

TYPE OF CONSTITUENTS	TOTAL (1205 EVENTS)
Charged Pions	6,983
Photons	6,128
K^0_L mesons	2,885
Other particles	139

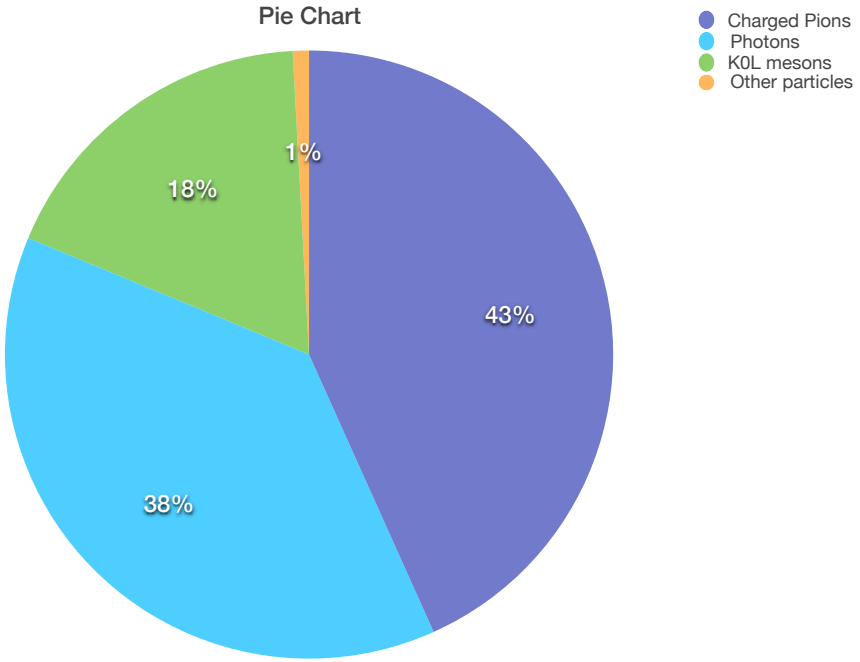

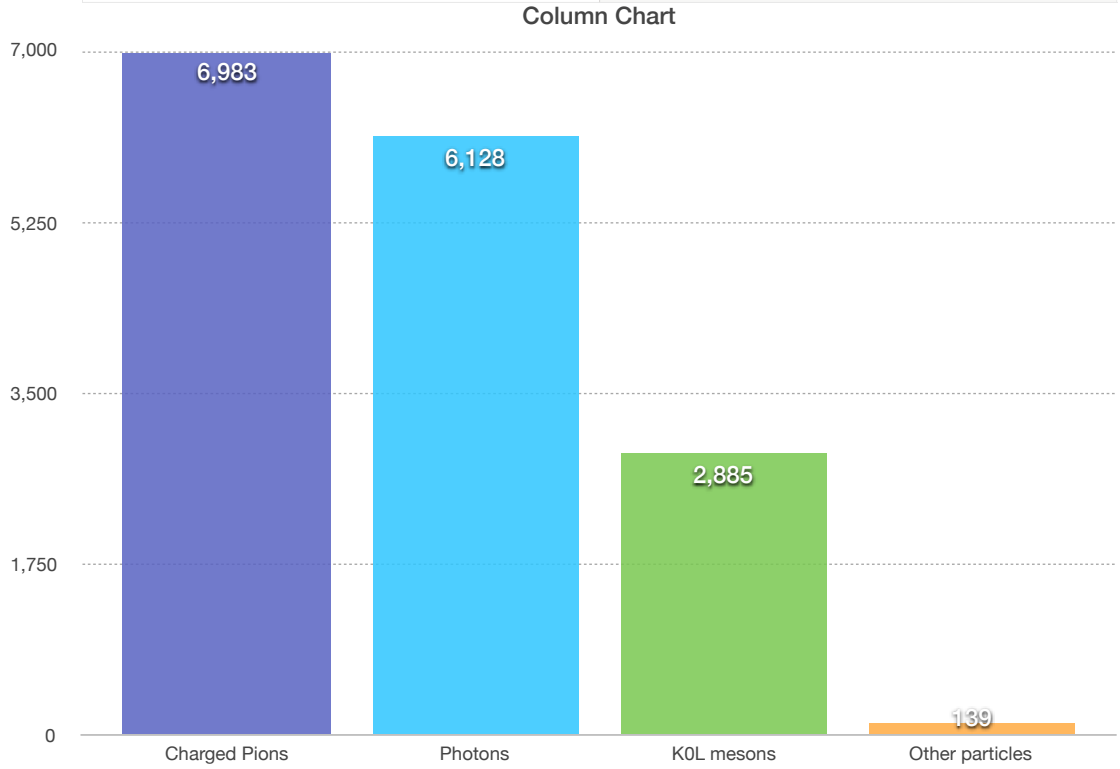

CMS Magnet

The CMS magnet is a central feature of the detector

- Huge – used for Silicon tracking, but placed outside of calorimeters to
  - not interfere with precision ***e*** and γ measurement,
  - give long "lever arm" for precision muon measurement at very high momentum
- 2.6GJ stored energy

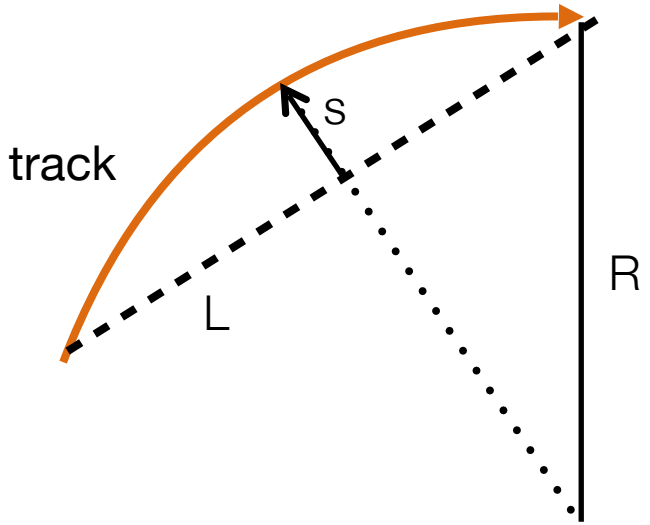

During Installation,

- Huge amount of superconducting wire
- Large and complex cryogenic infrastructure for liquid He

$$P_T \approx \frac{0.3L^2B}{8s}$$

The magnet bends charged particles, allowing the tracker to measure transverse momentum (p_T)

Evidence for DM

The main objective of Planck is to measure the spatial temperature and polarization anisotropies of the cosmic microwave background (CMB) radiation

- The CMB is a blackbody radiation with T=2.7 K extremely uniform across the whole sky; it is the relic radiation emitted at the time the nuclei and electrons recombined to form neutral hydrogen, when the Universe was ~ 400,000 years old.

Its tiny (~ 10^{-5}) temperature and polarization anisotropies encode a wealth of cosmological information.

TT refers to temperature angular power spectrum, to distinguish it from the temperature-polarization cross-power spectrum TE, as well as other possibilities such as EE, TB, EB, BB

Corrections

Jet Energy Corrections:

The detector response to particles is not linear and therefore it is not straightforward to translate the measured jet energy to the true particle or parton energy. The **jet corrections** are a set of tools that allows the proper mapping of the measured jet energy deposition to the particle-level jet energy.

L1 Pile Up: remove energy coming from pile-up events

L2L3 MC-truth: The simulated jet response corrections are determined on a QCD dijet sample, by comparing the reconstructed pT to the particle-level one (i.e. particle-level jets do not include energy from neutrino contributions).

L2L3Residuals: The L2 and L3 residuals are meant to correct for remaining small differences (of the order of %) within jet response in data and MC.

Monte Carlo : L1 + L2L3 MC-truth

Data : L1 + L2L3 MC-truth + L2L3Residuals

Backgrounds Cross-Sections

Dataset Name	Cross-section (pb)	Cross-section Order in QCD
/ZJetsToNuNu_HT-100To200_13TeV-madgraph	280.5	LO
/ZJetsToNuNu_HT-200To400_13TeV-madgraph	77.7	LO
/ZJetsToNuNu_HT-400To600_13TeV-madgraph	10.71	LO
/ZJetsToNuNu_HT-600ToInf_13TeV-madgraph	4.098	LO
/WJetsToLNu_TuneCUETP8M1_13TeV-amcatnloFXFX-pythia8	61527	NNLO
/WJetsToLNu_HT-100To200_TuneCUETP8M1_13TeV-madgraphMLM-pythia8	1343	LO
/WJetsToLNu_HT-200To400_TuneCUETP8M1_13TeV-madgraphMLM-pythia8	359.6	LO
/WJetsToLNu_HT-400To600_TuneCUETP8M1_13TeV-madgraphMLM-pythia8	48.85	LO
/WJetsToLNu_HT-600To800_TuneCUETP8M1_13TeV-madgraphMLM-pythia8	12.05	LO
/WJetsToLNu_HT-800To1200_TuneCUETP8M1_13TeV-madgraphMLM-pythia8	5.501	LO
/WJetsToLNu_HT-1200To2500_TuneCUETP8M1_13TeV-madgraphMLM-pythia8	1.329	LO
/WJetsToLNu_HT-2500ToInf_TuneCUETP8M1_13TeV-madgraphMLM-pythia8	0.03216	LO
/DYJetsToLL_M-50_TuneCUETP8M1_13TeV-amcatnloFXFX-pythia8	6025.2	NNLO
/DYJetsToLL_M-50_HT-100to200_TuneCUETP8M1_13TeV-madgraphMLM-pythia8	148	LO
/DYJetsToLL_M-50_HT-200to400_TuneCUETP8M1_13TeV-madgraphMLM-pythia8	40.94	LO
/DYJetsToLL_M-50_HT-400to600_TuneCUETP8M1_13TeV-madgraphMLM-pythia8	5.497	LO
/DYJetsToLL_M-50_HT-600toInf_TuneCUETP8M1_13TeV-madgraphMLM-pythia8	2.193	LO
/GJets_HT-100To200_TuneCUETP8M1_13TeV-madgraphMLM-pythia8	9235	LO
/GJets_HT-200To400_TuneCUETP8M1_13TeV-madgraphMLM-pythia8	2298	LO
/GJets_HT-400To600_TuneCUETP8M1_13TeV-madgraphMLM-pythia8	277.6	LO
/GJets_HT-600ToInf_TuneCUETP8M1_13TeV-madgraphMLM-pythia8	93.47	LO
/TTJets_TuneCUETP8M1_13TeV-amcatnloFXFX-pythia8	831.76	NNLO+NNLL
/TT_TuneCUETP8M1_13TeV-powheg-pythia8	831.76	NNLO+NNLL
/ST_s-channel_4f_leptonDecays_13TeV-amcatnlo-pythia8_TuneCUETP8M1	3.4	NLO
/ST_t-channel_top_4f_leptonDecays_13TeV-powheg-pythia8_TuneCUETP8M1	44.1	NLO
/ST_t-channel_antitop_4f_leptonDecays_13TeV-powheg-pythia8_TuneCUETP8M1	26.2	NLO
/ST_tW_top_5f_inclusiveDecays_13TeV-powheg-pythia8_TuneCUETP8M1	35.6	NNLO
/ST_tW_antitop_5f_inclusiveDecays_13TeV-powheg-pythia8_TuneCUETP8M1	35.6	NNLO
/WW_TuneCUETP8M1_13TeV-pythia8	118.7	NNLO
/WZ_TuneCUETP8M1_13TeV-pythia8	47.2	NLO
/ZZ_TuneCUETP8M1_13TeV-pythia8	16.6	NLO
/QCD_HT100to200_TuneCUETP8M1_13TeV-madgraphMLM-pythia8	2.75×10^7	LO
/QCD_HT200to300_TuneCUETP8M1_13TeV-madgraphMLM-pythia8	1.735×10^6	LO
/QCD_HT300to500_TuneCUETP8M1_13TeV-madgraphMLM-pythia8	3.67×10^5	LO
/QCD_HT500to700_TuneCUETP8M1_13TeV-madgraphMLM-pythia8	2.937×10^4	LO
/QCD_HT700to1000_TuneCUETP8M1_13TeV-madgraphMLM-pythia8	6524	LO
/QCD_HT1000to1500_TuneCUETP8M1_13TeV-madgraphMLM-pythia8	1064	LO
/QCD_HT1500to2000_TuneCUETP8M1_13TeV-madgraphMLM-pythia8	121.5	LO
/QCD_HT2000toInf_TuneCUETP8M1_13TeV-madgraphMLM-pythia8	25.42	LO

Table 3: Background Monte Carlo datasets produced in the Spring16 campaign.

Leading Jet phi Width (N-1 Plots)

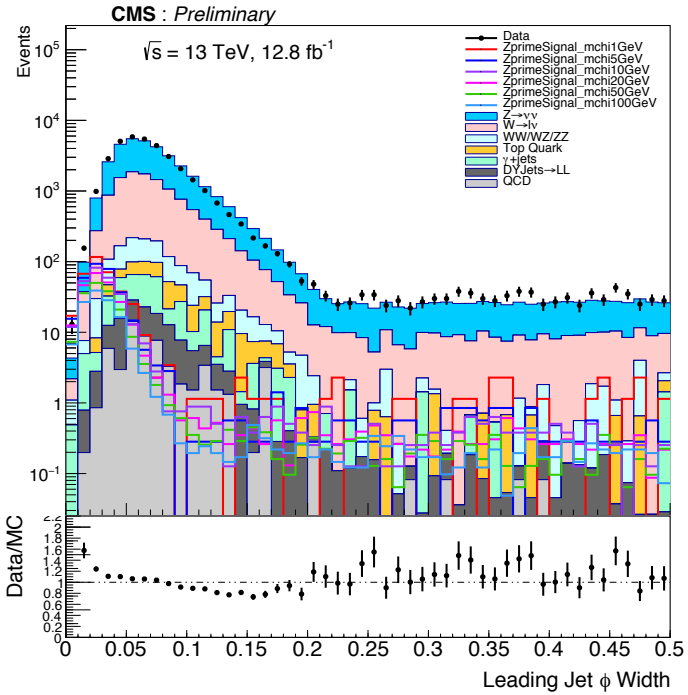

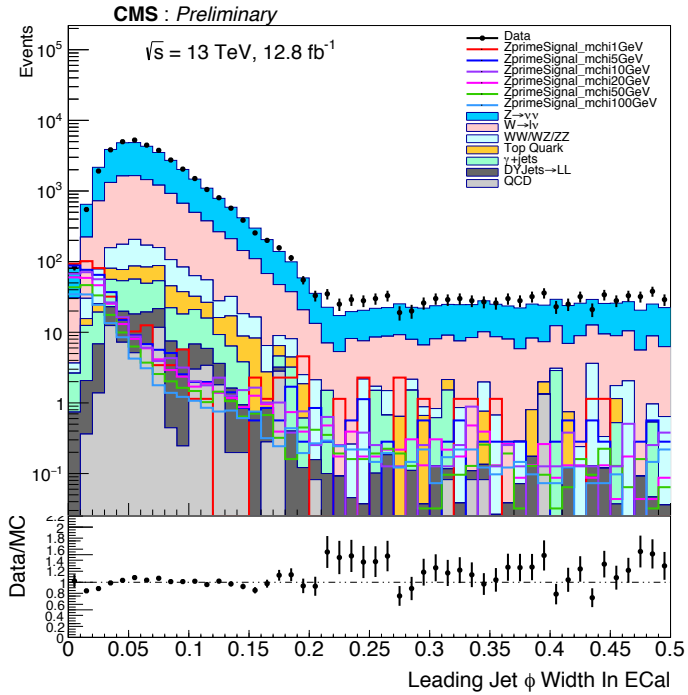

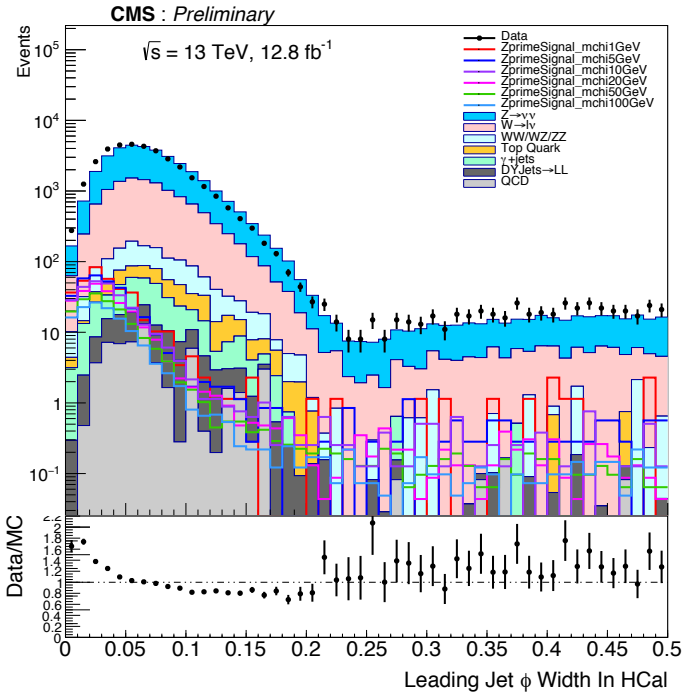

- Jet phi Width is not a good variable for this analysis which is confirmed by this plots and some other studies that we have done.
- phiWidth = $$\sqrt{\frac{\sum(\phi_i^2 E_i)}{\sum E_i} - \left(\frac{\sum(\phi_i E_i)}{\sum E_i}\right)^2}$$

Some more Jet substructure variables (N-1 Plots)

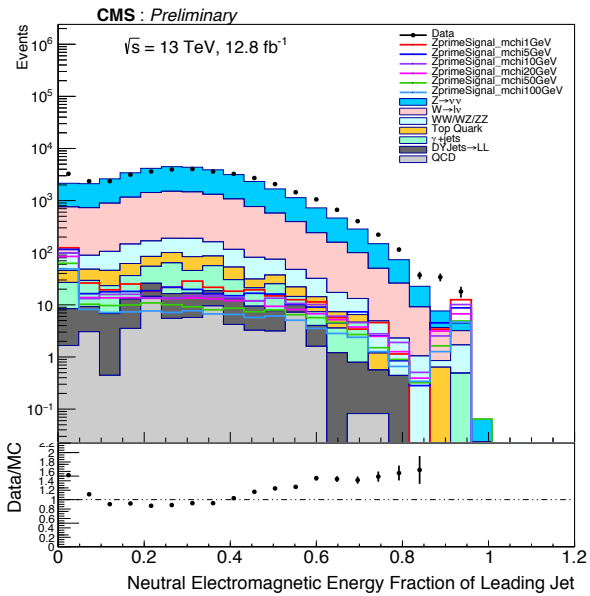

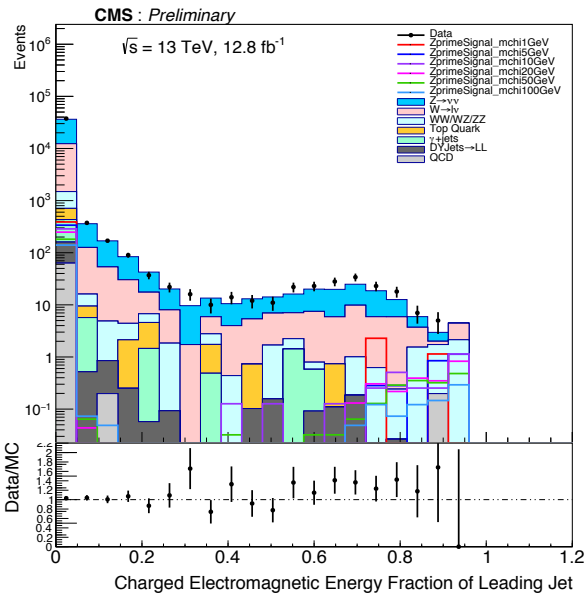

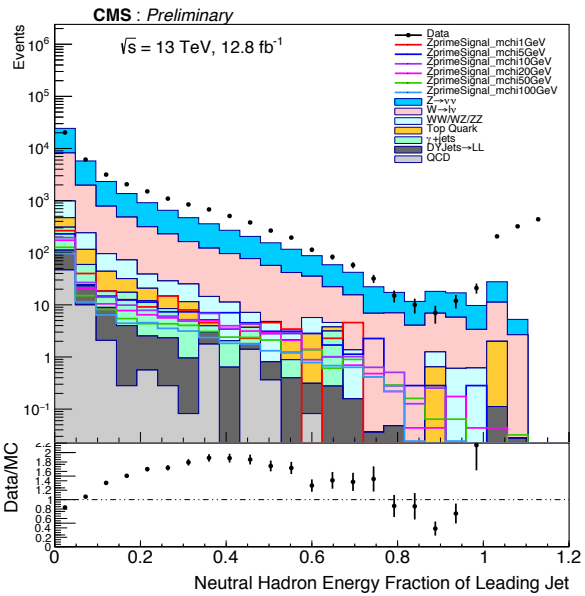

- Unfortunately, these jet variables do not show good data/mc agreement and so we have not used them in the analysis so far. In most cases we think things can be improved when we shift to data-driven backgrounds, add systematic uncertainties etc. However, it might also be interesting to study how MC samples from different generators will behave in the context of this analysis.

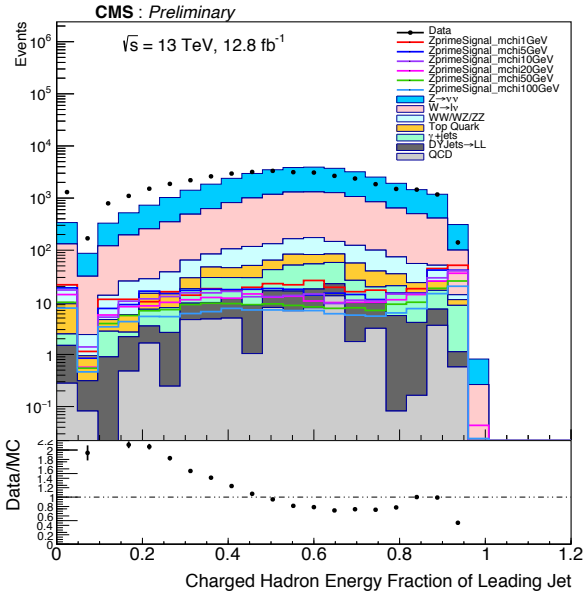

Limit Plots

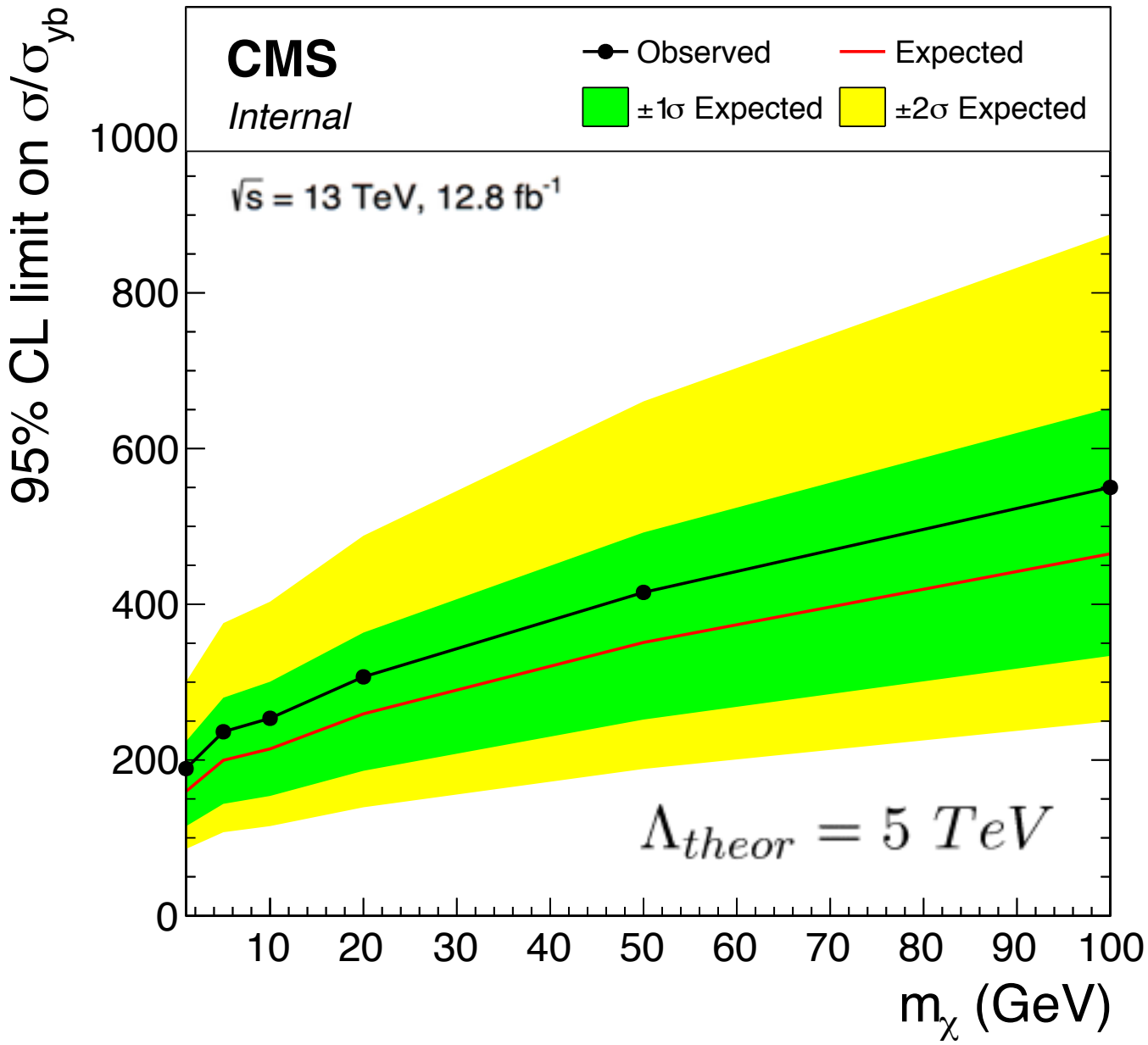
CMS
Internal
Observed
Expected
±1σ Expected
±2σ Expected
√s = 13 TeV, 12.8 fb-1
95% CL limit on σ/σyb
1000
800
600
400
200
0
10
20
30
40
50
60
70
80
90
100
mχ (GeV)
$\Lambda_{theor} = 5\ TeV$

Limit Plots

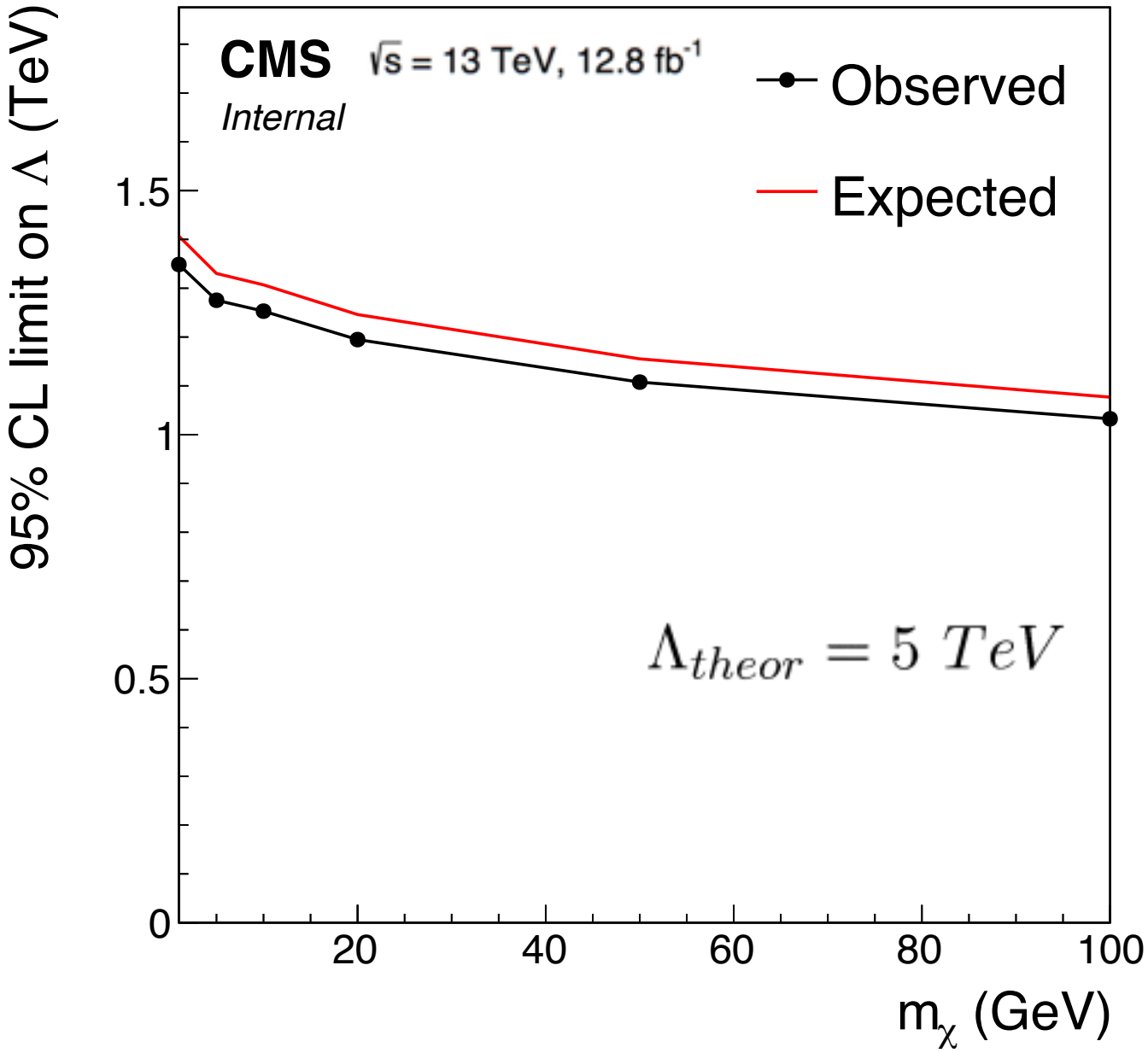
CMS
Internal
√s = 13 TeV, 12.8 fb-1
Observed
Expected
95% CL limit on Λ (TeV)
1.5
1
0.5
0
20
40
60
80
100
mχ (GeV)
$\Lambda_{theor} = 5\ TeV$